

LASER ABLATION INDUCTIVELY COUPLED PLASMA MASS SPECTROMETRY – PRINCIPLES AND APPLICATIONS IN THE ANALYSIS OF ENVIRONMENTAL GEOLOGICAL, ARCHAEOLOGICAL AND TECHNOLOGICAL MATERIALS



Viktor Kanický

Laboratory of Atomic Spectrochemistry,
Division of Analytical Chemistry,
Department of Chemistry,
Faculty of Science
Masaryk University, Brno, Czech Republic

OUTLINE

- Principles and instrumentation of laser assisted plasma spectrometry
- Applications
 - Imaging of 2D-distribution of elements
 1. examples from literature;
 2. research at the Department of Chemistry MU:
 - i. technological materials;
 - ii. geology;
 - iii. archaeology;
 - iv. environmental.
 - Provenance study in archaeology

What is laser assisted plasma spectrometry?

Laser ablation processes

- Interaction of pulsed (nanosecond, fs) laser focused beam with solids at high laser power density ($\sim 10^9$ W/cm²) causes rapid release of material from the surface and near-surface layer – laser ablation
- Laser ablation results from rapid heating of sub-surface volume \Rightarrow high pressure of vaporized sub-surface material brings about surface layer explosion. Besides, melting occurs.
- Released matter consists of aerosol, vapour, atoms&ions.

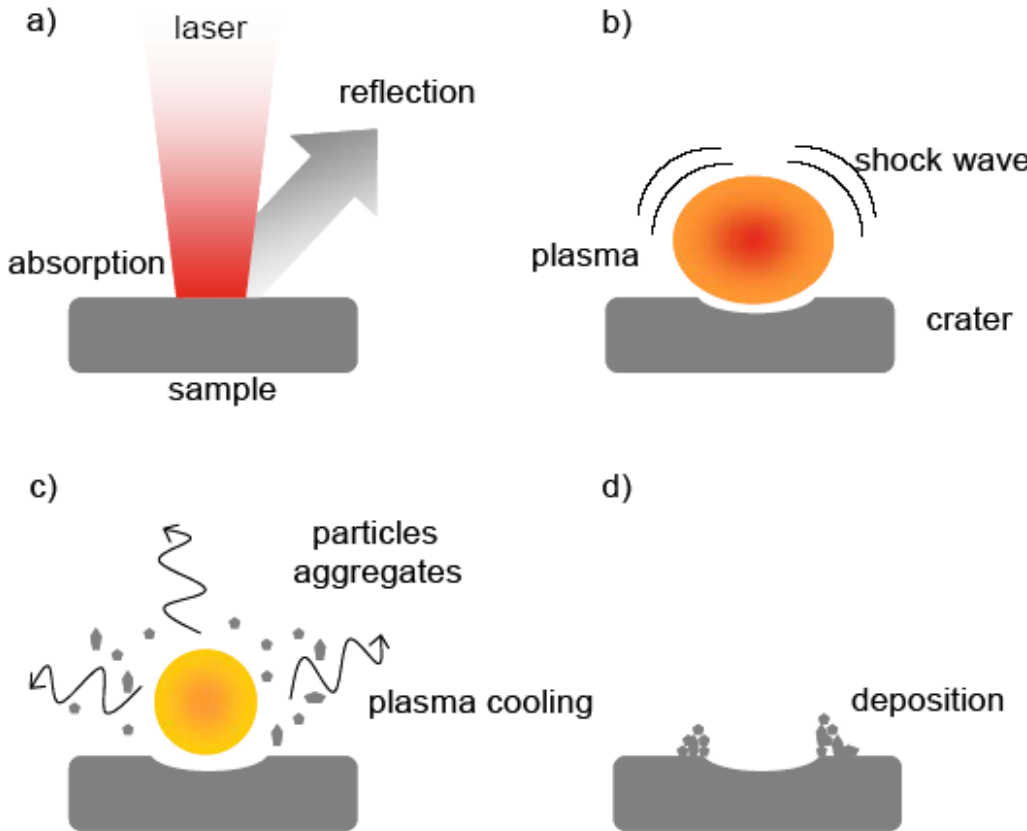
Laser ablation processes

- Besides, ambient gas is ionized and forms together with ionized sample microplasma
- Laser radiation is partly absorbed in microplasma ⇒ energy transfer to atoms and ions occurs
- Absorbing microplasma existing for μ -seconds shields sample surface – attenuation of laser beam power applied to a sample – efficiency decreases ⇒ contribution of thermal effects ⇒ undesired melting ⇒ fractionation of elements (boiling temperatures)
- Microplasma existing for μ -seconds in contact with sample heats surface ⇒ undesired melting ⇒ fractionation of elements (boiling temperatures).

Laser ablation processes

- Heating of gas induces shock wave (pressure, acoustic effect), microplasma expands and extinguishes
- Cooling of microplasma causes condensation of vapours into fine aerosol droplets and solidification of liquid droplets into coarse particles ⇒ different composition ⇒ fractionation of elements
- Some particles (coarse, liquid droplets) fall around crater „ejecta“
- Aerosol is possible to transport with carrier gas into ICP with detection either radiation (LA-ICP-OES) or ions (LA-ICP-MS)
- Radiation of analytes in microplasma is measured (LIBS)

Laser ablation



Laser ablation process: a) laser – sample interaction; b) plasma and sample creation; c) plasma cooling effect; d) rim deposition

T. Čtvrtníčková: PhD Dissertation, Masaryk University, 2008

- Laser assisted plasma spectrometry
 - **Laser Ablation Inductively Coupled Plasma Mass Spectrometry: LA-ICP-MS**
 - **Laser Ablation Inductively Coupled Plasma Optical Emission Spectrometry: LA-ICP-OES**
 - **Laser Induced Breakdown Spectrometry: LIBS**

Laser Ablation

ICP-OES
ICP-MS

Aerosol

Atoms, ions,
clusters, aerosol

Laser beam

Microplasma

Absorption of
radiation in plasma

Vaporisation
Atomisation
Excitation
Ionisation

Emission $h\nu$

LM-OES, LIBS

Deposited material

Cracking of material

Solid sample

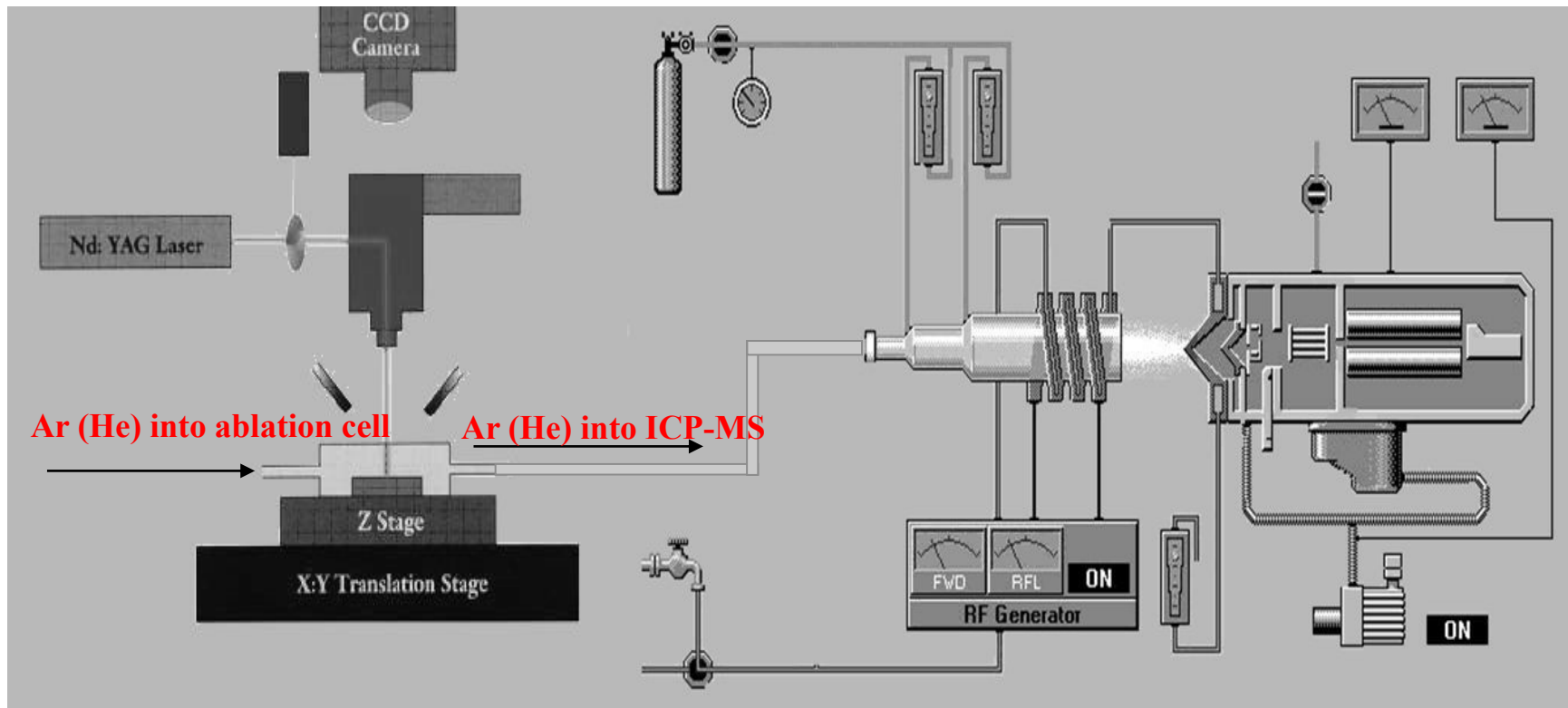
Shock wave

Heating, melting,
vaporisation, explosion

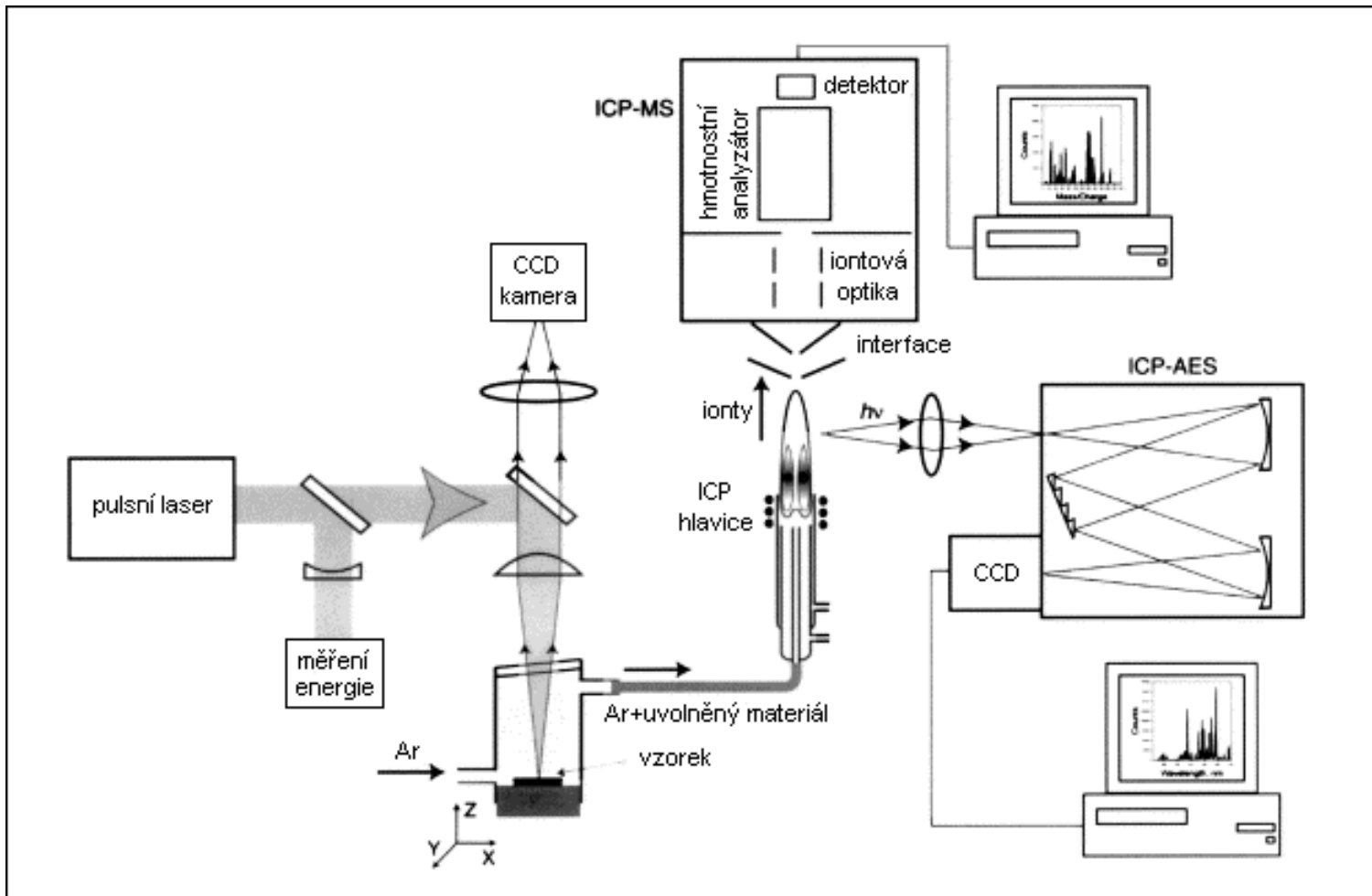
LA-ICP-MS/OES

Laser – assisted plasma spectrometry: instrumentation

- Laser ablation inductively coupled plasma mass spectrometry (LA-ICP-MS)

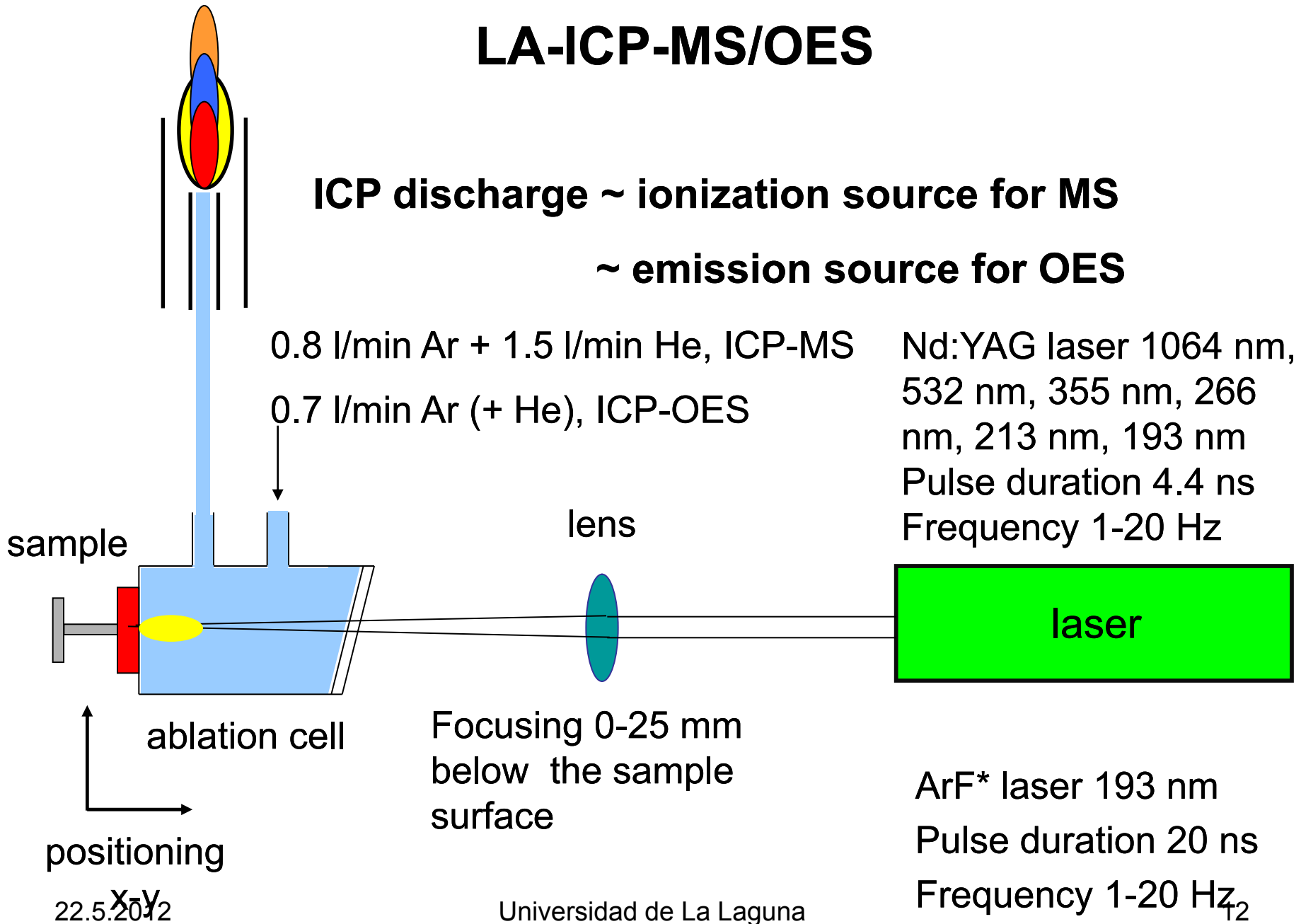


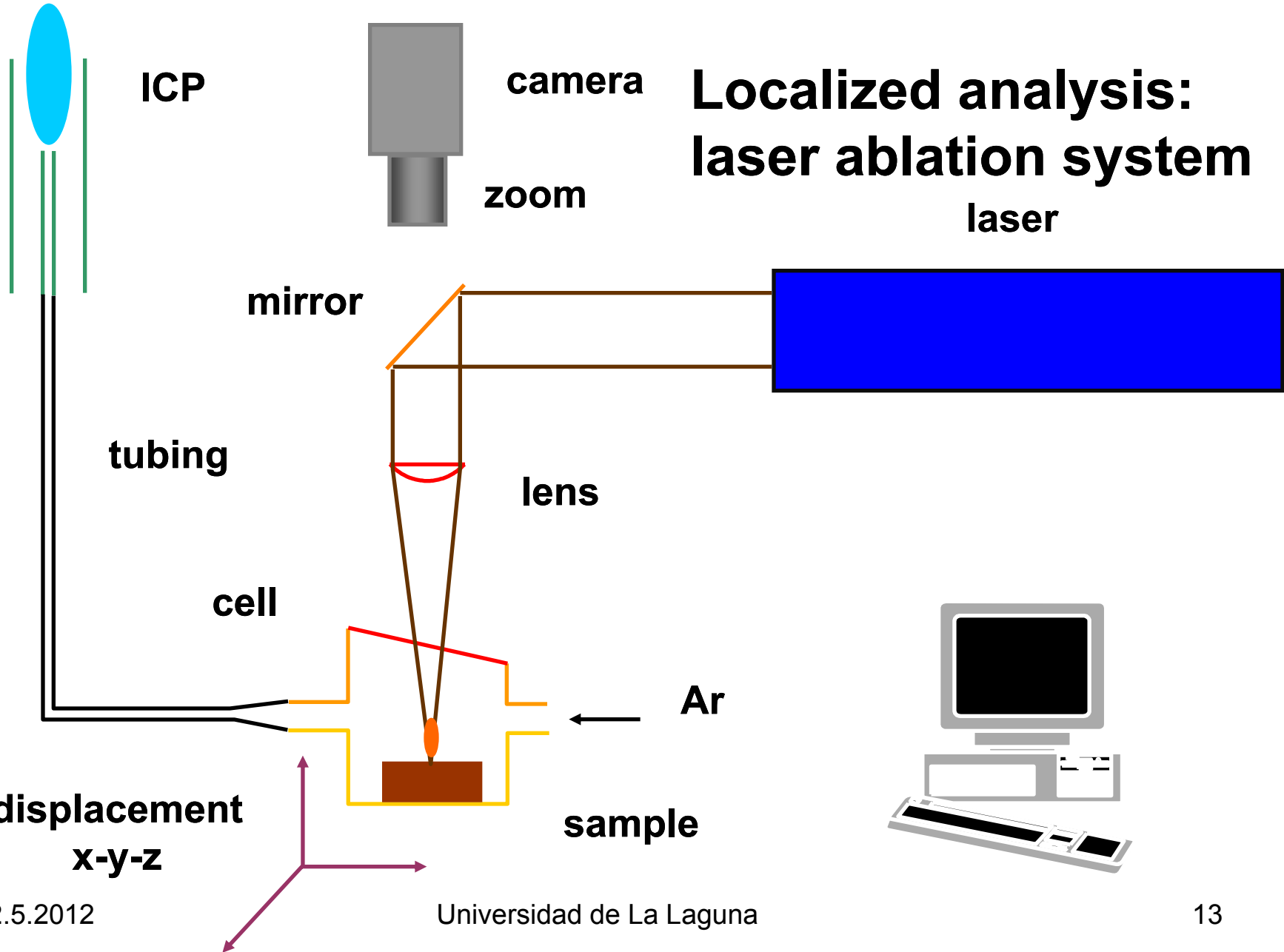
LA-ICP-MS/OES



[R.E. Russo, X. Mao, H. Liu, J. Gonzalez, S.S. Mao, Review, Talanta 57 (2002) 425–451]

LA-ICP-MS/OES





LA-ICP-MS instrumentation LAS, Masaryk University, Brno



**Nd:YAG laser UP-213
(New Wave Research)**

213 nm

frequency: 1-20 Hz

pulse: 4.2 ns

spot size 4-300 µm

ICP-MS Agilent 7500ce

generator 27.12 MHz

collision cell

quadrupole mass filter

electron multiplier

Laser – assisted plasma spectrometry: instrumentation

- LA-ICP-(Q)MS at Masaryk University



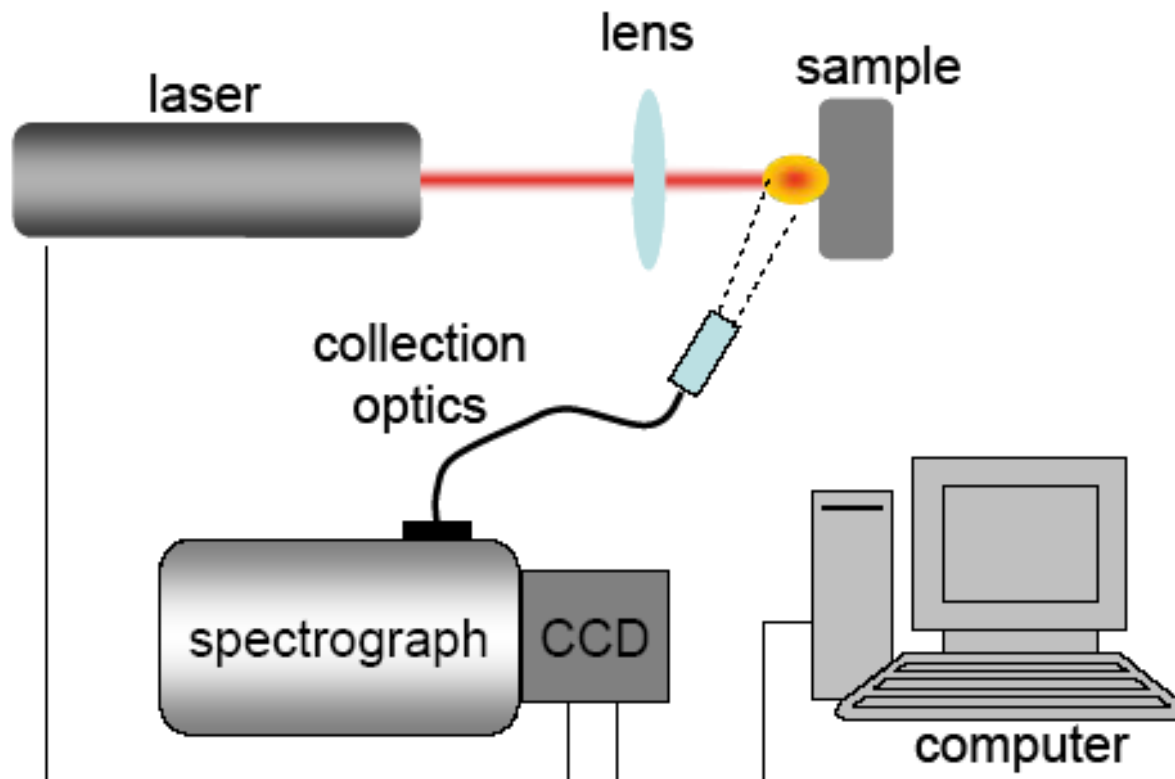
Ablation system – UP213
(New Wave, USA)



ICP-(Q)MS
Agilent 7500 CE (Agilent, Japan)

LIBS

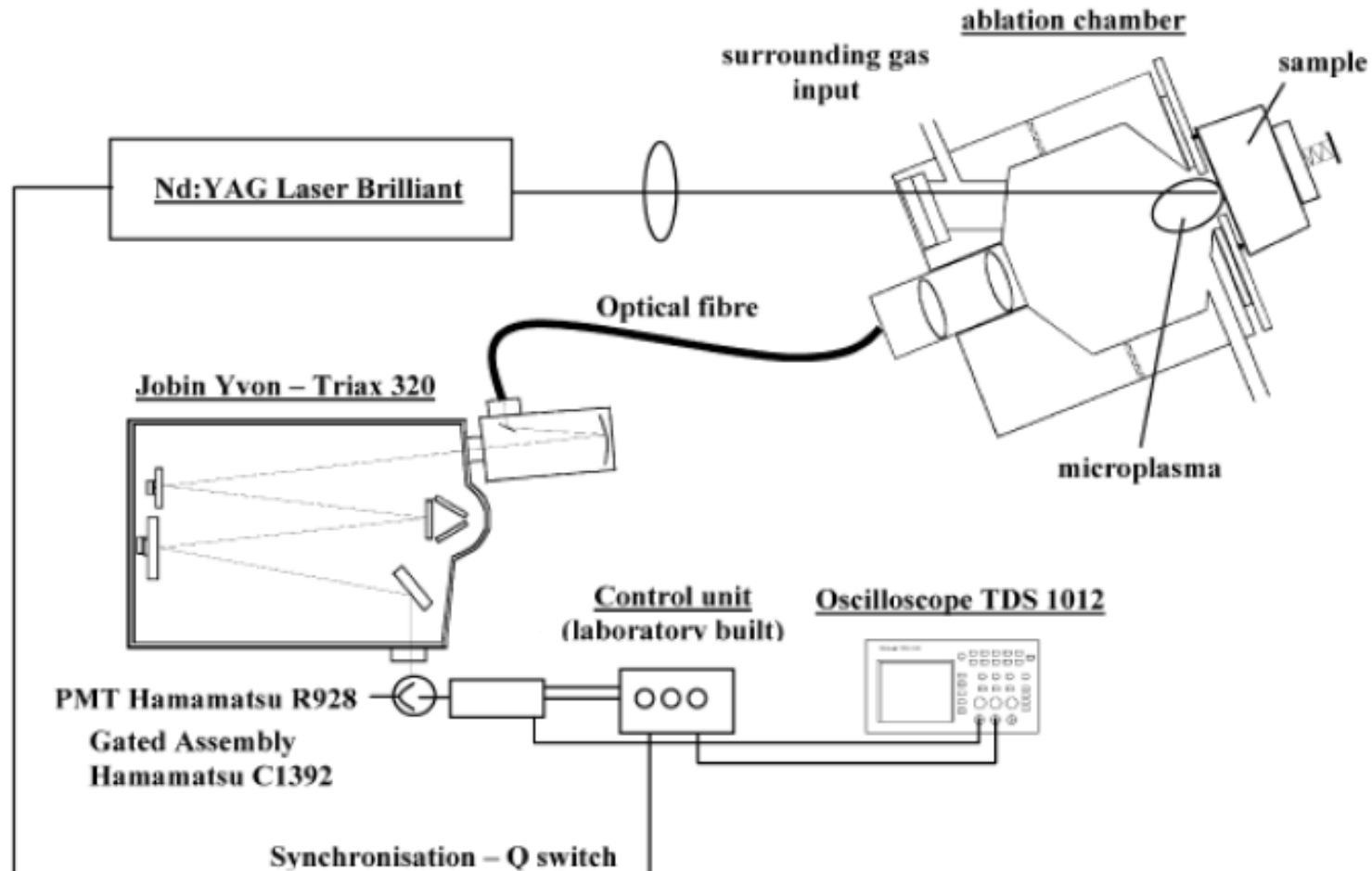
LIBS



The scheme of LIBS instrumentation

T. Čtvrtníčková: PhD Dissertation, Masaryk University, 2008

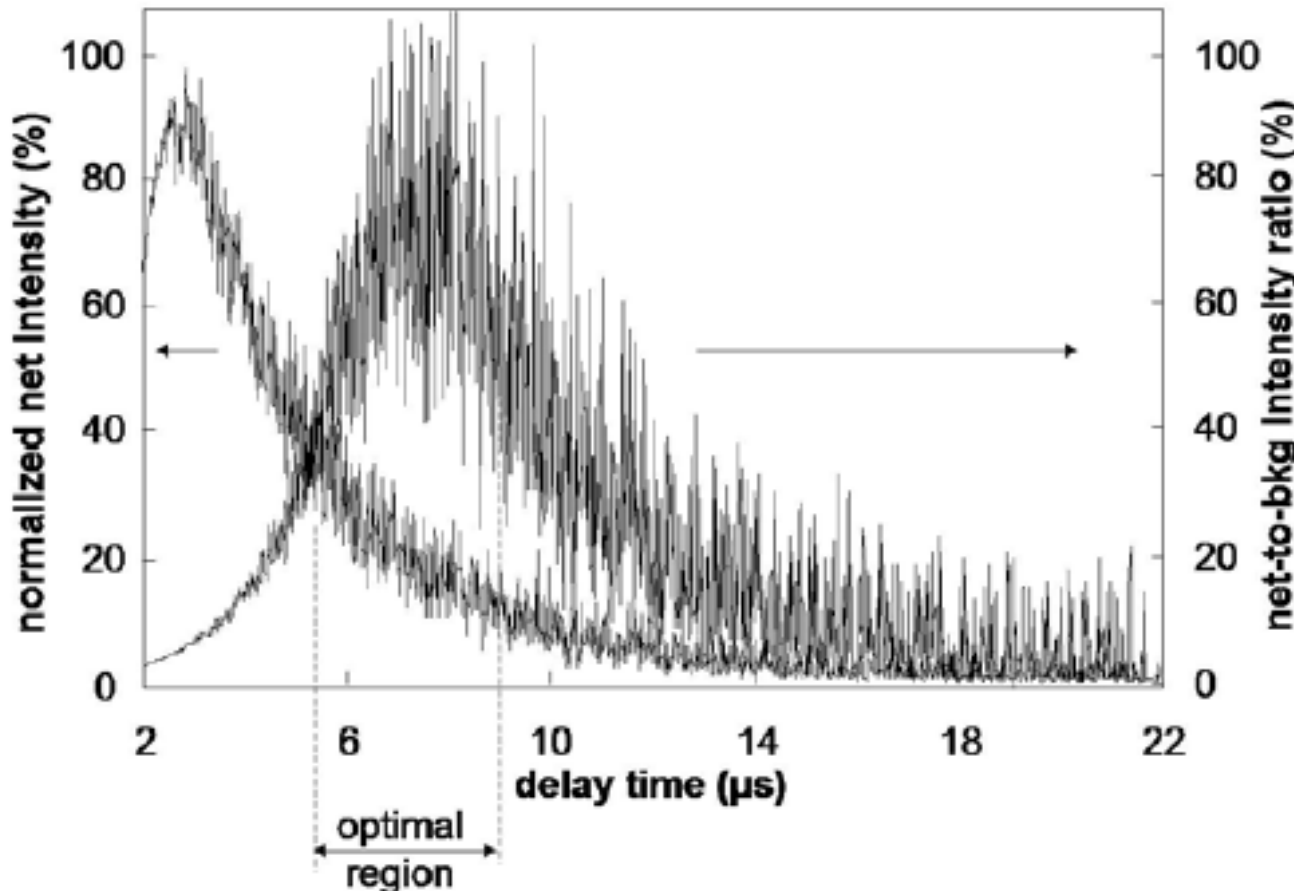
LIBS arrangement



K. Novotný, Masaryk University

LIBS – optimum delay time

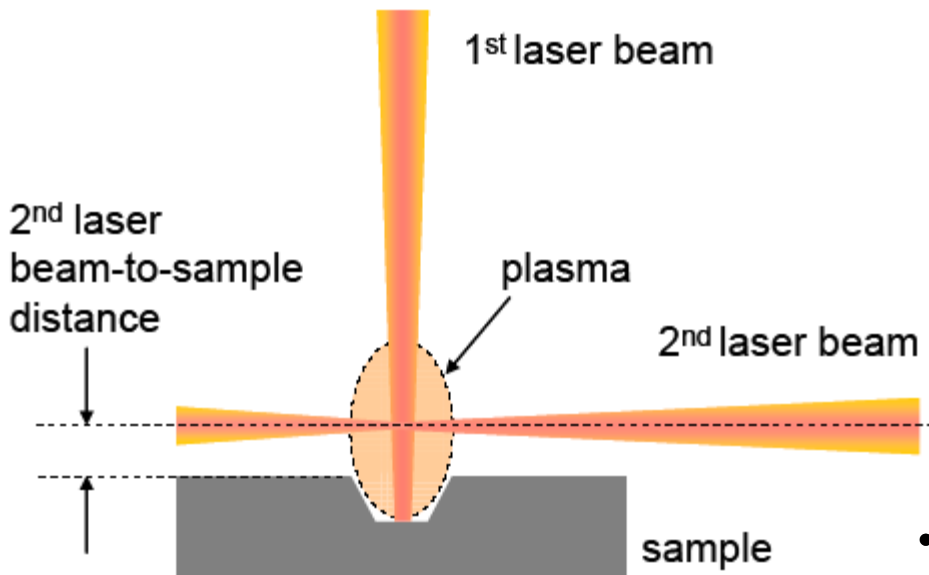
Optimum delay time selection from signal and background intensity dependence on delay time, Al (I) 396.152 nm, background 397.5 nm; 266 nm laser (4th harmonics)



T. Čtvrtníčková: PhD Dissertation, Masaryk University, 2008

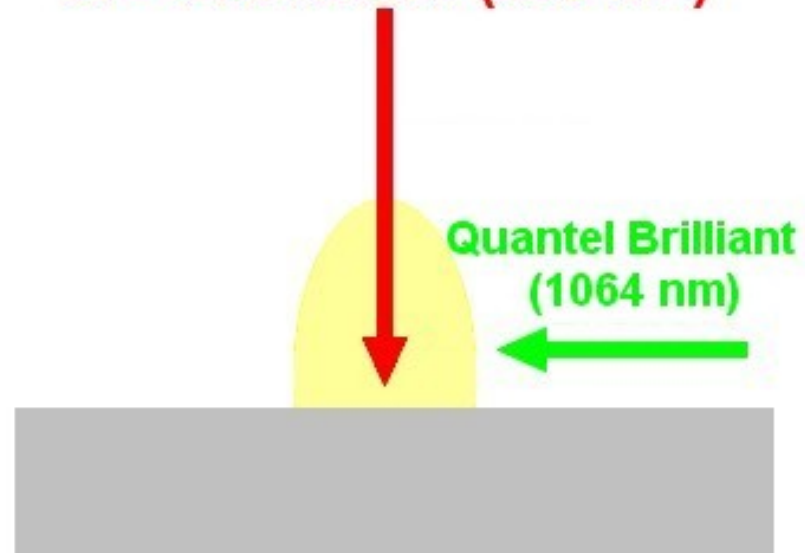
Double-pulse LIBS

orthogonal, re-heating mode



T. Čtvrtníčková: PhD Dissertation,
Masaryk University, 2008

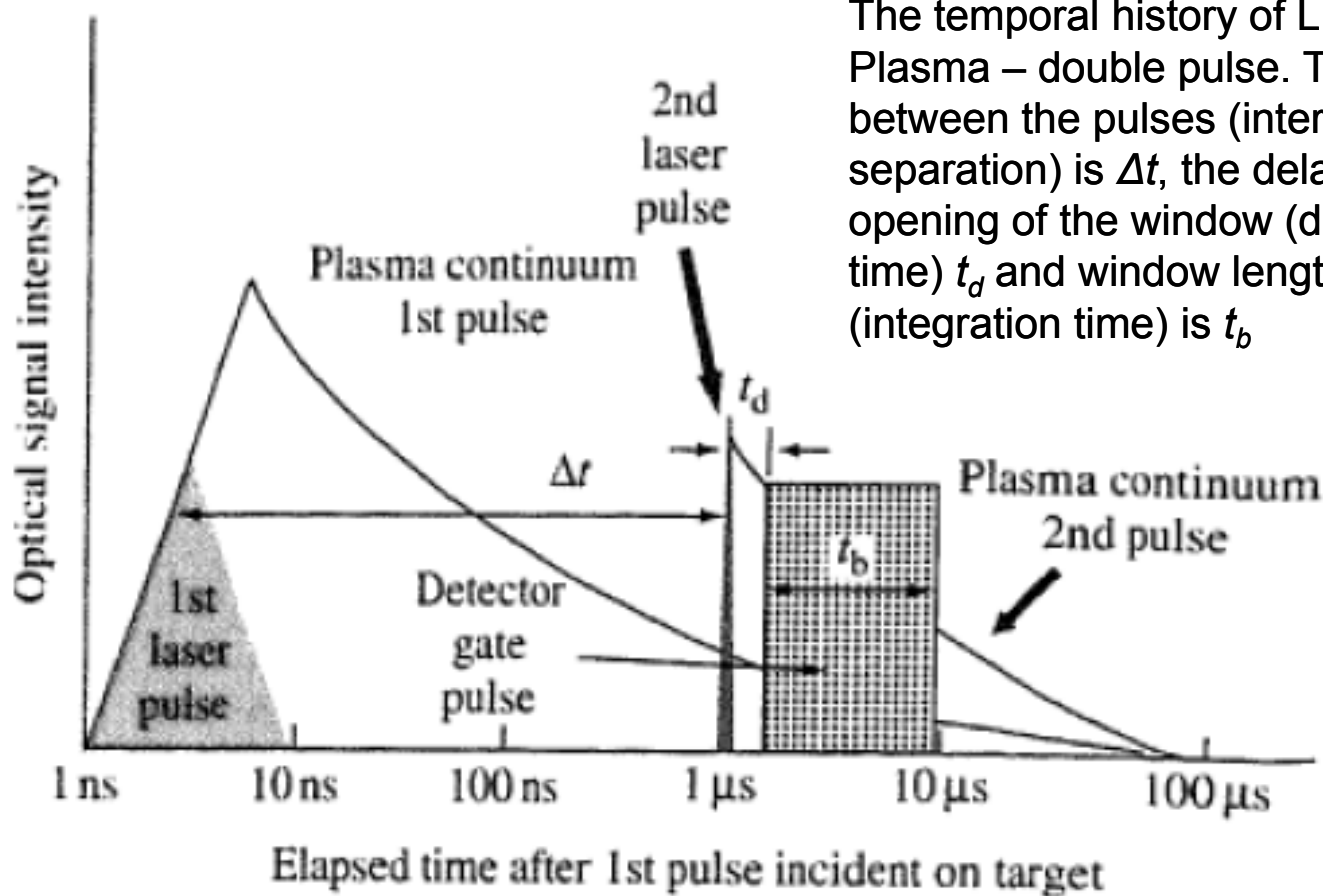
UP - 266 Macro (266 nm)



K. Novotný: Masaryk University

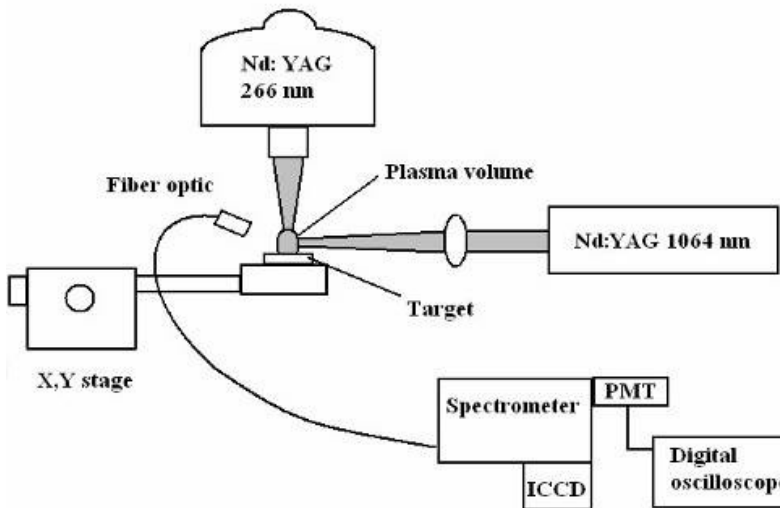
- monochromator Jobin - Yvon TRIAX, optical fiber,
- CCD Jobin Yvon Horiba,
- gated photomultiplier Hamamatsu

Double pulse LIBS



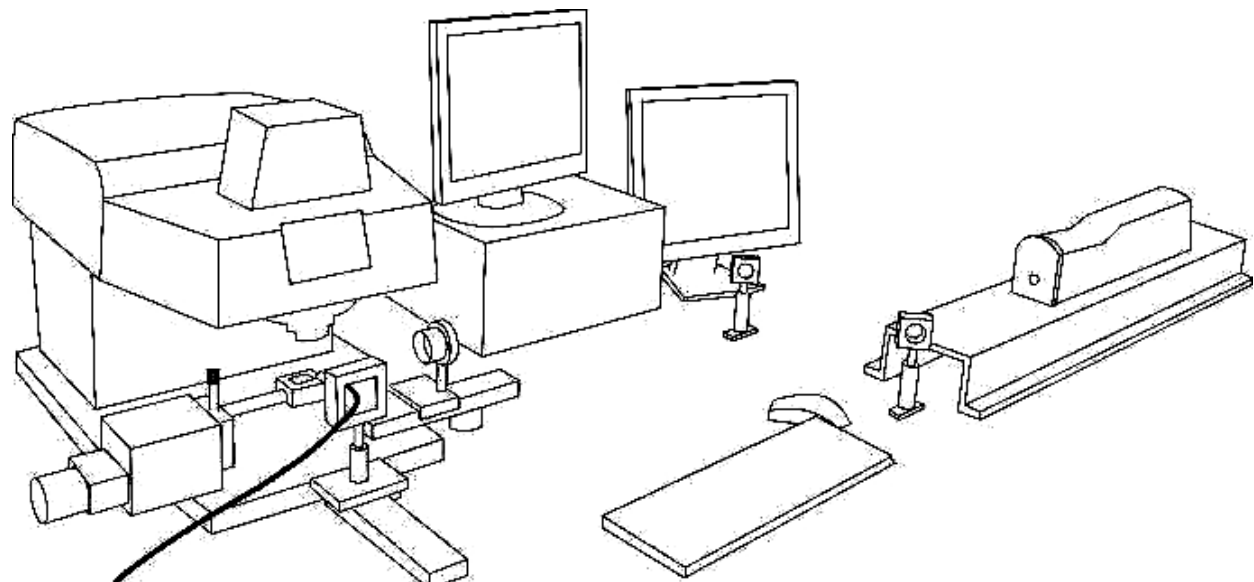
The temporal history of LIBS
Plasma – double pulse. The delay between the pulses (interpulse separation) is Δt , the delay to the opening of the window (delay time) t_d and window length (integration time) is t_b

D. Cremers, L.J. Radziemski, Handbook of laser-induced breakdown spectroscopy,
John Wiley & Sons, London, 2006.



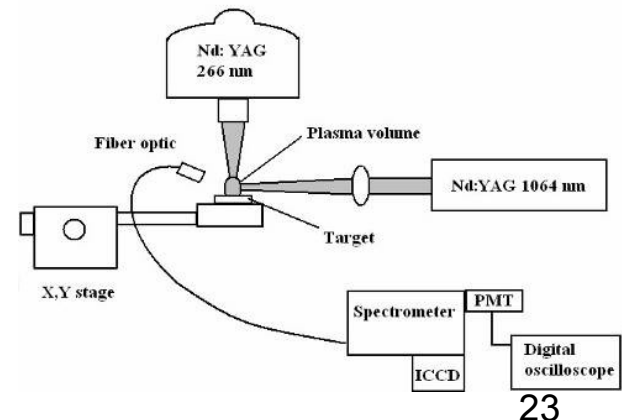
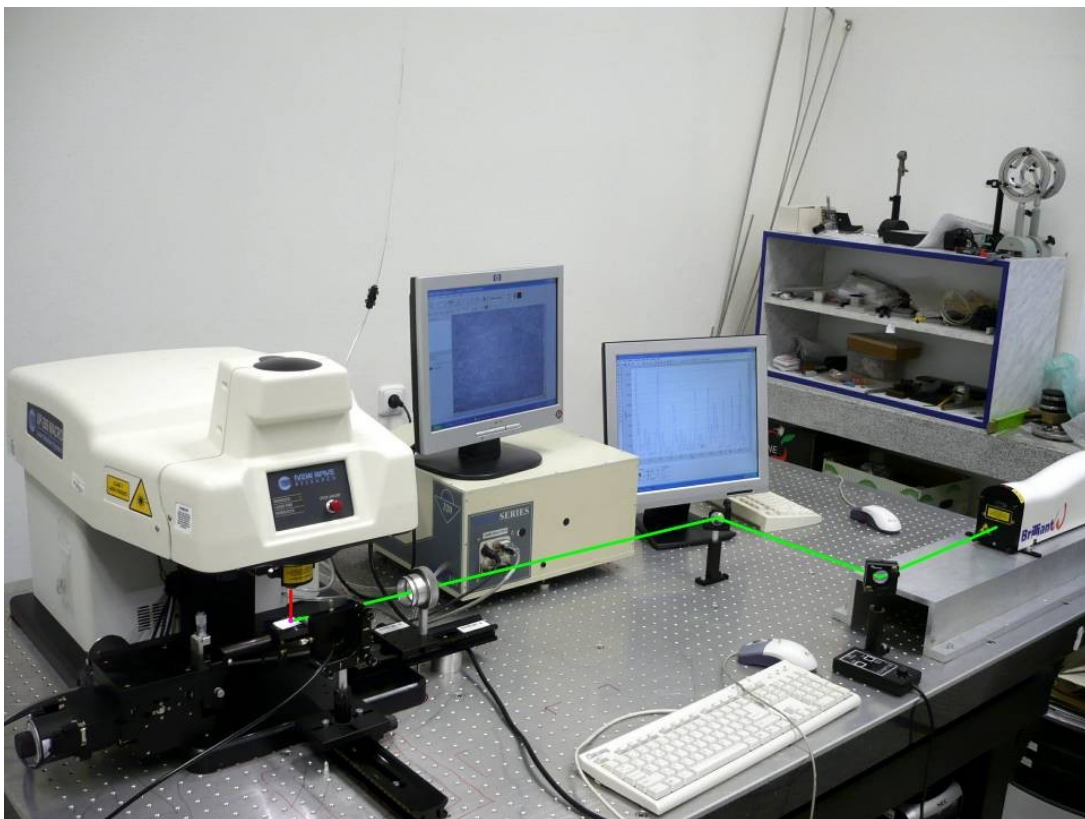
Double-pulse orthogonal configuration in reheating mode

K. Novotný, Masaryk University



Laser – assisted plasma spectrometry: instrumentation

- LIBS Double – pulse setup (DP), orthogonal configuration, reheating arrangement (Masaryk University)



Laser – assisted plasma spectrometry: instrumentation

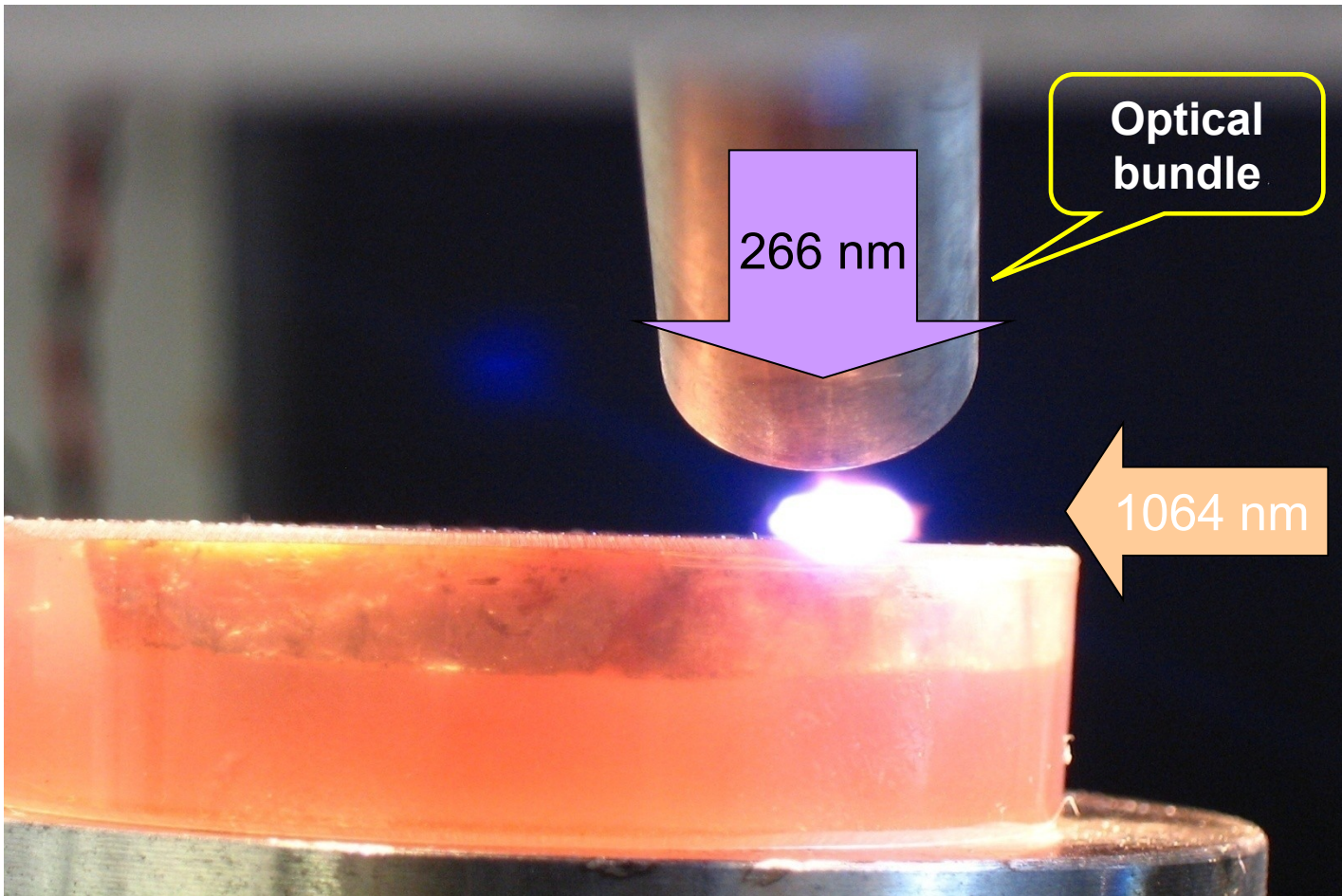
- LIBS Double – pulse setup (DP), orthogonal configuration, reheating arrangement (Masaryk University)



1 – Ablation laser (New Wave, MACRO 266 nm),
2 – Reheating laser (Quantel Brilliant, 1064 nm),
3 – Sample holder and precision movements,
4 – Delay Generators (Stanford RS)
5 – Spectrometer and ICCD camera (Jobin Yvon, Triax).



Double pulse LIBS



A. Hrdlička, L. Prokeš, V. Konečná,
K. Novotný, V. Kanický, V. Otruba

K. Novotný, J. Novotný, J. Kaizer, R.
Malina, M. Galiová, V. Otruba, V.K.

Why and for what do we use laser – assisted plasma spectroscopy?

Laser-assisted analysis of solids

- Features of laser ablation based techniques
 - Elimination of decomposition for solution analysis
 - Elimination of water, O, N, S, Cl from acids; resulting species cause spectral interferences in ICP-MS
 - Universal: electric conductors, non(semi)conductors
 - Non-destructive: material removing from the area $10 \mu\text{m}^2$ to 1mm^2 to the depth cca $0.01\text{-}0.1\mu\text{m}$ /laser pulse
 - 2D-3D „speciation”: preserves information on spatial distribution of elements

Priorities of laser-assisted plasma spectroscopy

- 1) Analysis of surfaces and coatings: xy - local analysis, microanalysis, areal mapping (mineralogical sections, inhomogeneities in steel)
- 2) Depth profiling of multi-layer advanced materials or natural structured objects (xyz resolution)
- 3) Bulk analysis:
 - Compact samples (steel, alloys, glass, ceramics)
 - Powdered samples:
 - ❖ pressed pellets with or without a binder,
 - ❖ cast pellets with e.g. epoxy resin, polyurethane ... ,
 - ❖ melted with fusing agents for XRF ⇒ cast pearls

Influencing parameters

- Laser wavelength.
- Pulse energy.
- Focus position relative to surface.
- Laser repetition rate.
- Crater diameter/depth (aspect ratio).

Critical parameters of LA

- **Wavelength (UV×IR) vs fractionation**
- **Pulse duration (fs×ns) vs fractionation**

Features important for particular tasks

- Depth profiling, mapping, local analysis:
 - Laser beam profile, spot size, aspect ratio,
- Bulk analysis:
 - Powders: pellet preparation, cohesion and homogeneity, easy calibration
 - Compacts: no preparation, homogeneity, lack of calibration samples

Effect of laser wavelength

- ✓ Infrared laser: Nd:YAG 1064 nm
 - ✓ Strongly absorbing microplasma, long interaction
⇒ thermal effects ⇒ selective volatilisation,
fractionation
- ✓ Ultraviolet laser: ArF* 193 nm, Nd:YAG 266 nm, 213 nm or 193 nm.
 - ✓ Short interaction, minimum thermal effects,
minimum fractionation.

Fractionation

- 1) different particle size;
- 2) size-dependent composition

- ✓ Fractionation I: during ablation (*in situ* fractionation)
thermal effects ⇒ selective volatilisation, smaller particles enriched with more volatile elements as they are formed by condensation of vapours; coalescence of small particles, bigger particles by explosion of material.
- ✓ Fractionation II: during particle transport bigger particles are preferentially lost;
- ✓ Fractionation III: in the ICP discharge smaller particles are completely evaporated contrary to bigger ones

Applications

Imaging of 2D distributions of elements

Why elemental mapping by laser - assisted plasma spectrometry ?

There already exist advanced methods for mapping (SEM, EMPA, SIMS, PIXE, ...), however,

Laser - assisted plasma spectrometry:

- does not need vacuum environment in a sample compartment, and therefore allows:
 - faster sample exchange/manipulation in a sample cell
 - analysis of porous or wet samples;
- does not need any surface treatment prior to analysis;
- involves greater thickness of probed layer and yields more representative composition in some cases
- provides efficient detection of light elements (Li, Be, B...).

Limitations of laser-assisted plasma spectrometry

- Spatial variability of composition to be mapped is associated obviously with variability of sample physical properties in space \Rightarrow variability of ablation rate and therefore amount of ablated material \Rightarrow matrix effect;
- Consequently, calibration is not mostly feasible even using reliable homogeneous standard samples or CRM;
- Rather qualitative results are obtained instead of quantitative, especially in case of complex structured samples of biological origin (biominerals, bones, plant or animal tissues)
- Spatial resolution is poorer in comparison to particle beam based techniques ($X - XX \mu\text{m}$ for laser techniques vs. nanometers for particle beams).

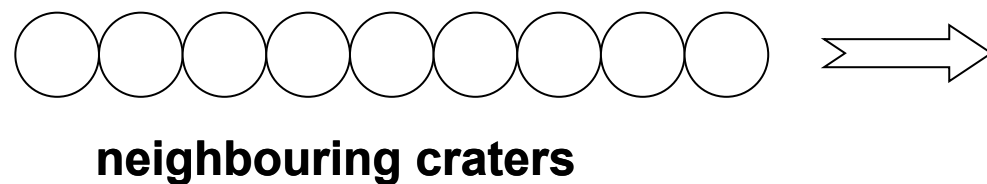
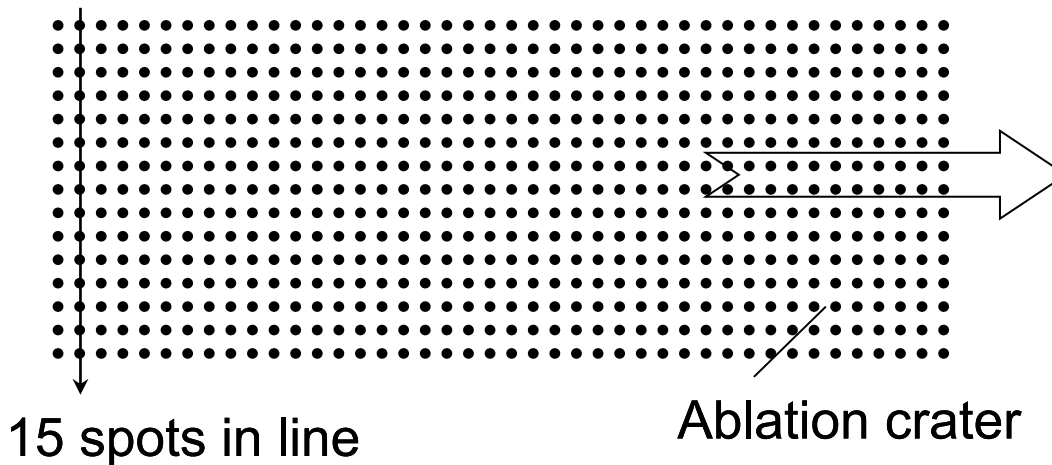
Mapping of surfaces

- Techniques
 - Grid of isolated craters – discrete points obtained at intermittent ablation:
 - ablation chamber dead volume and consequent signal tailing is not critical at LA-ICP-MS
 - time consuming process
 - Raster of parallel line scans – continuous ablation:
 - requires fast rise and decay of signal in time – small volume of ablation cell and tubing
 - requires fast and simultaneous data acquisition – TOF-MS or simultaneous sector analyzers
 - faster analysis

Mapping of surfaces

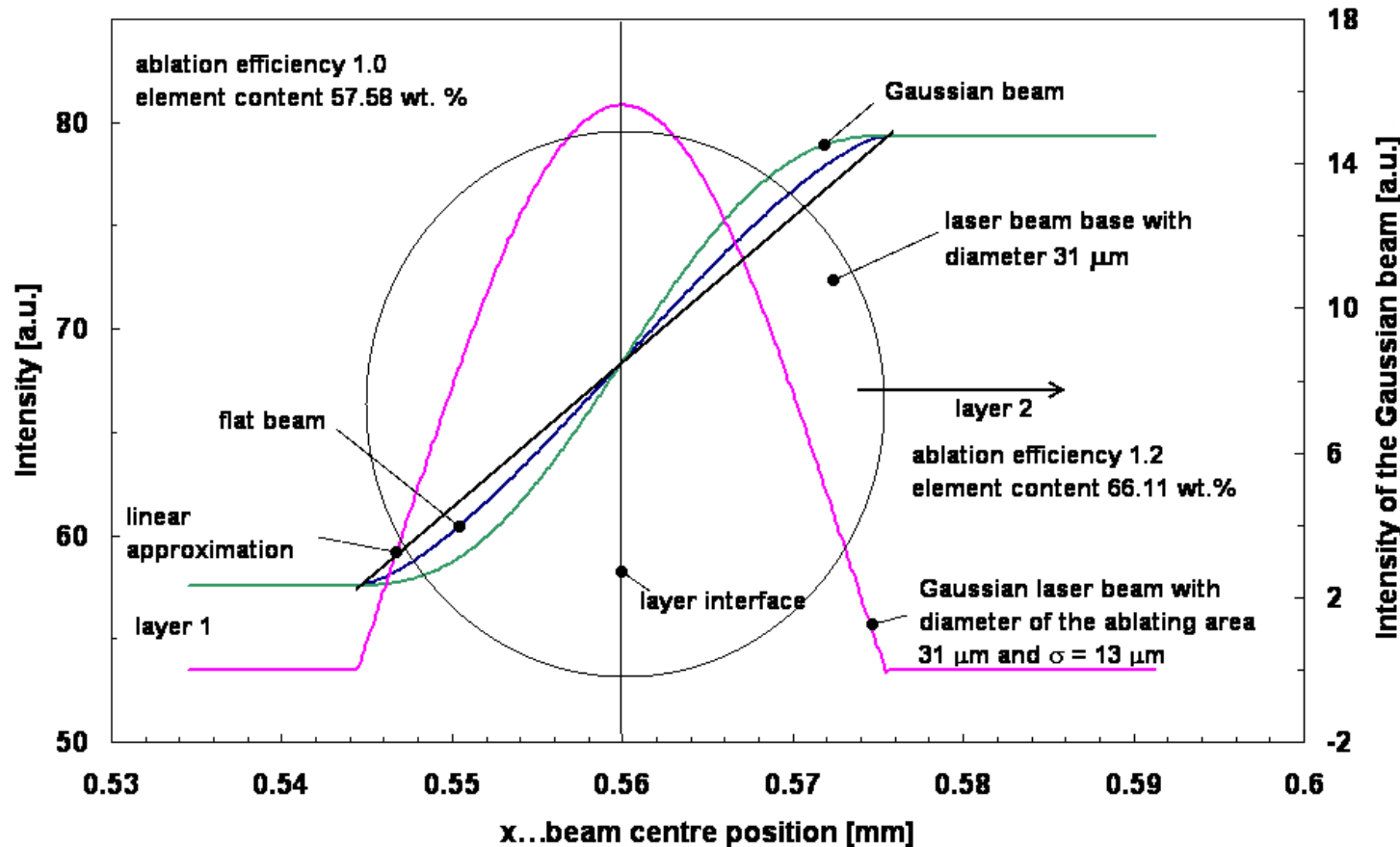
- Techniques

Matrix of discrete points: non-overlapping ablation spots



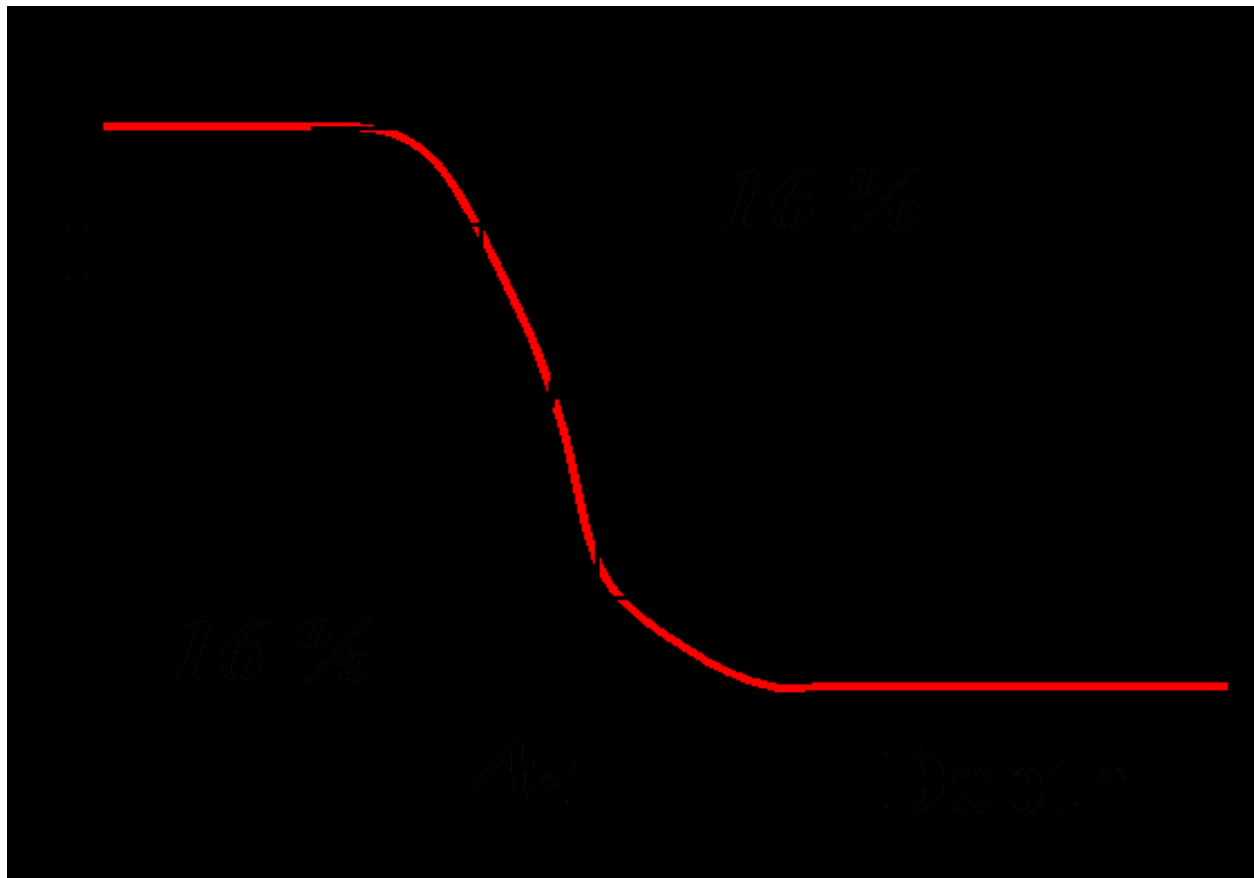
Mapping of surfaces

- Spatial resolution A. Hrdlička, Ph.D. Thesis 2006
 - Influence of laser beam energy profile



Mapping of surfaces

- Spatial resolution A. Hrdlička, Ph.D. Thesis 2006
 - Definition (lateral or depth resolution)

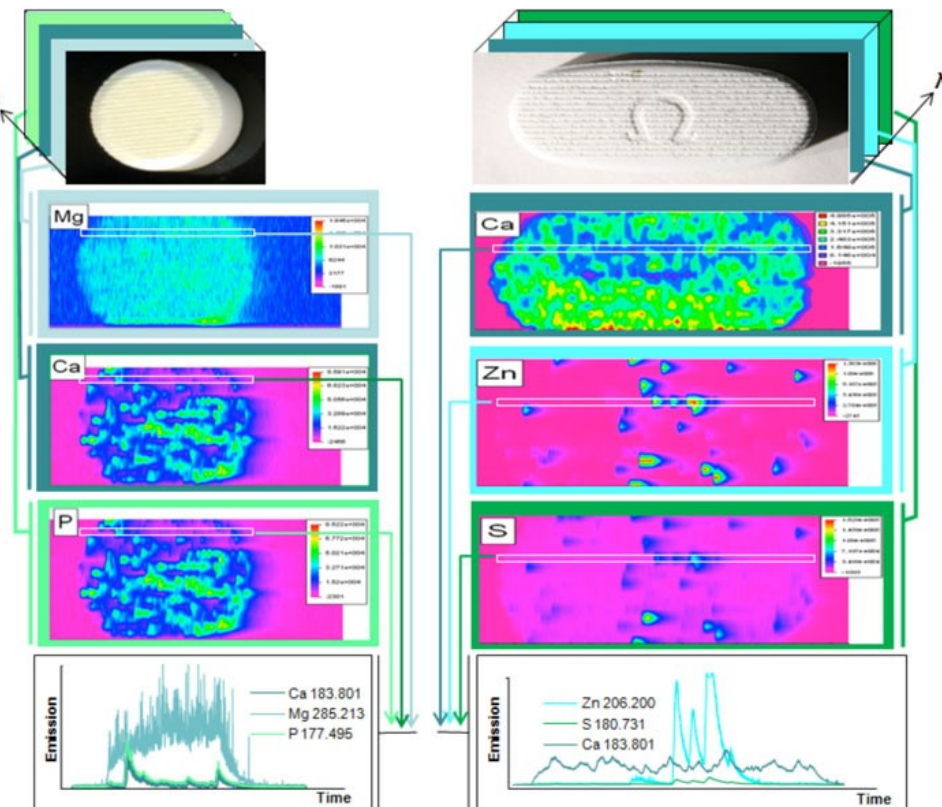


Mapping of surfaces

- Examples from literature: www.analyticalsciences.group.shef.ac.uk/
 - Compact homogenized sample
- LA-ICP-OES mapping of pharmaceutical tablets

Distribution of drugs and matrix

- repetition rate 10Hz,
- beam diameter 100 and 240 μm ,
- scan speed 60 $\mu\text{m}/\text{s}$,
- integration time 100 ms,
- element and wavelength, (nm)
Ca 183.801, Mg 285.21,
Zn 206.200, P 177.495,
S 180.731.



Copyright © 2010, The University
of Sheffield

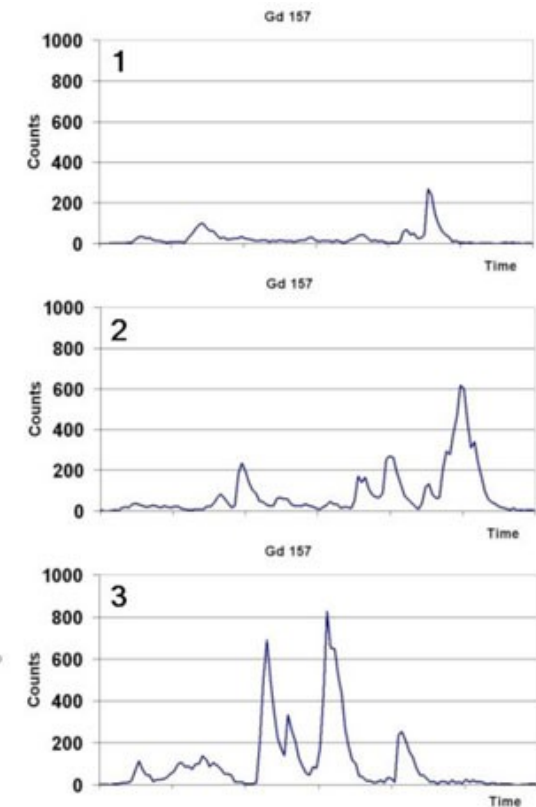
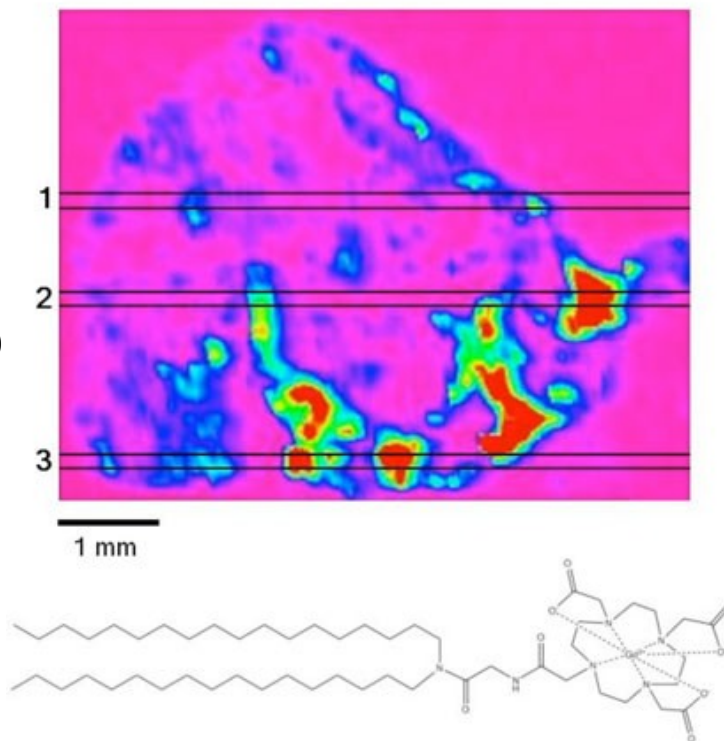
Mapping of surfaces

- Examples from literature:
 - Distribution of contrast agent (MRI) in tumor tissue

LA-ICP-MS ^{157}Gd image distribution from thin-section of treated tumour - distribution in vascular and necrotic areas

- histology section and structure of novel Gd contrast agent (bottom),
- Laser line-raster data (1-3) shows Gd signal strength.

MRI research group at Hammersmith Hospital (Prof. J. Bell);
<http://www.imperial.nhs.uk/hammersmith/index.htm>

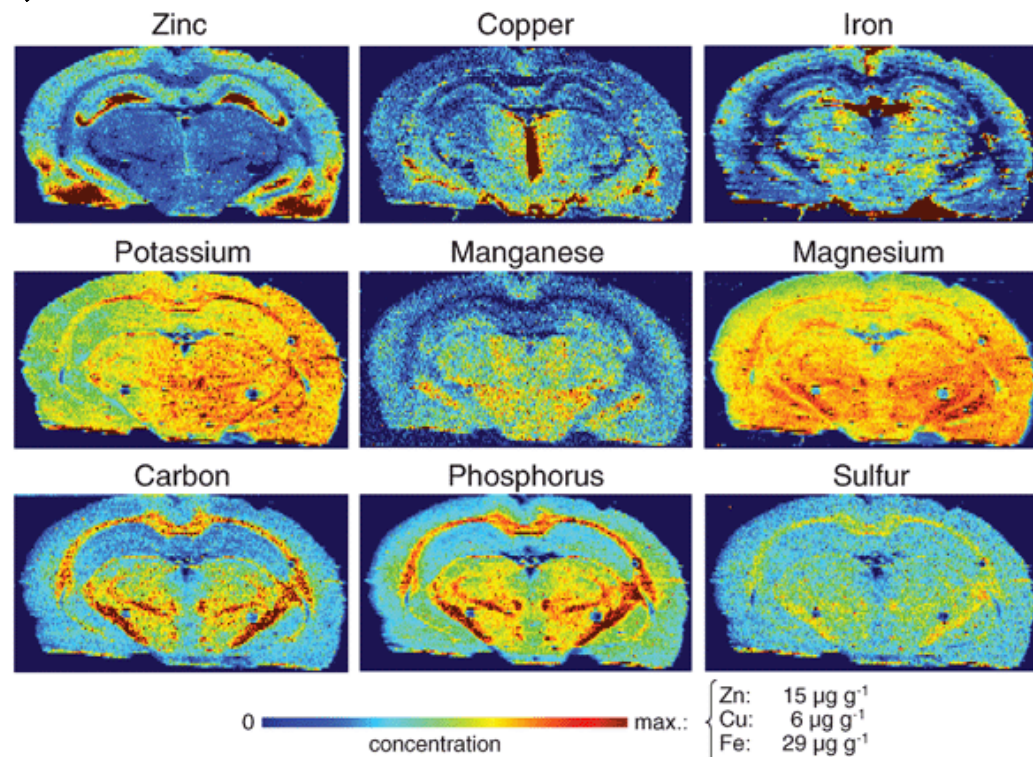


Mapping of surfaces

- Examples from literature:
 - LA-ICP-MS images of quantitative distribution of Zn, Cu, Fe, K, Mn, Mg, C, P and S in a rat brain section

Quantitation is based on calibration with standards prepared from homogenized rat brain tissue with added standard solutions of elements

For Zn, Cu and Fe the maximum of the concentration scale bar is indicated, the minimum being zero.



J. Sab. Becker et al., Metallomics, 2010, 2, 104-111.

Applications Experimental results Masaryk University

Technological samples

- Analysis of technological materials for nuclear power plants
 - Study of corrosion of structural materials for cooling circuits of nuclear reactors by cooling media - molten fluoride salts

CORROSION OF COOLING CIRCUIT STRUCTURAL MATERIALS OF NUCLEAR REACTORS BY COOLING MEDIA - MOLTEN FLUORIDE SALTS



**Nuclear power station Temelín
Czech Republic**

**Nuclear power station Dukovany
Czech Republic**



Molten fluoride salts

Development of new types of reactors:

- **Transmutor** – reactor exploiting a substantial part of the long-term nuclear wastes for transfer into useful power; cooling medium – molten fluoride mixture (LiF-NaF) attacks a surface of piping and heat exchanger parts => corrosion processes study of sample surface by means of LA-ICP-MS
- 3 structural materials for piping and heat exchangers parts are examined:
 - ✓ pure Ni,
 - ✓ Ni-based alloy,
 - ✓ pure Fe with Ni-coating

LA-ICP-MS mapping with quantitation – corrosion layers on alloys

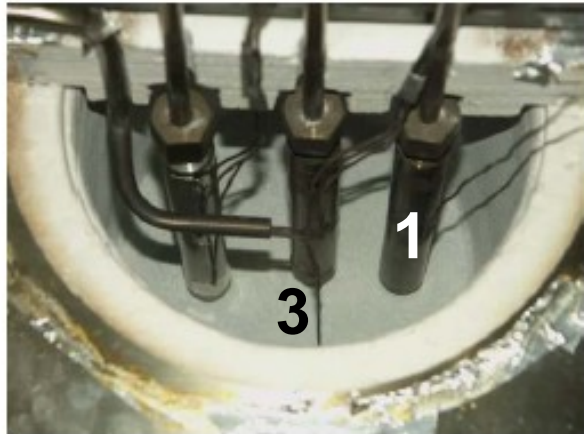
Molten Salts Reactors (MSR) – thermal reactor with neutron moderator, coolant – molten fluoride salt, working temp. 700 C, nuclear fuel – UF_4 or ThF_4 dissolved in MFS

- Candidate structural materials were exposed to effect of mixture of molten fluoride salts (composition in mol.%) :
- 60 LiF - 40 NaF or 42 LiF - 29 NaF – 29 ZrF_4
- for 112, 350 and 1000 hours
- at temperatures 680, 720 and 740 C.

T. Vaculovic, P. Sulovsky, J. Machat, V. Otruba, O. Matal, T. Simo, Ch. Latkoczy, D. Günther and V. Kanicky, The EPMA, LA-ICP-MS and ICP-OES study of corrosion of structural materials for a nuclear reactor cooling circuit by molten fluoride salts treatment, *J. Anal. Atom. Spectrom.* 24, 649-654 (2009).

Molten fluoride salts

1. Ampoules with samples of structural material and salt

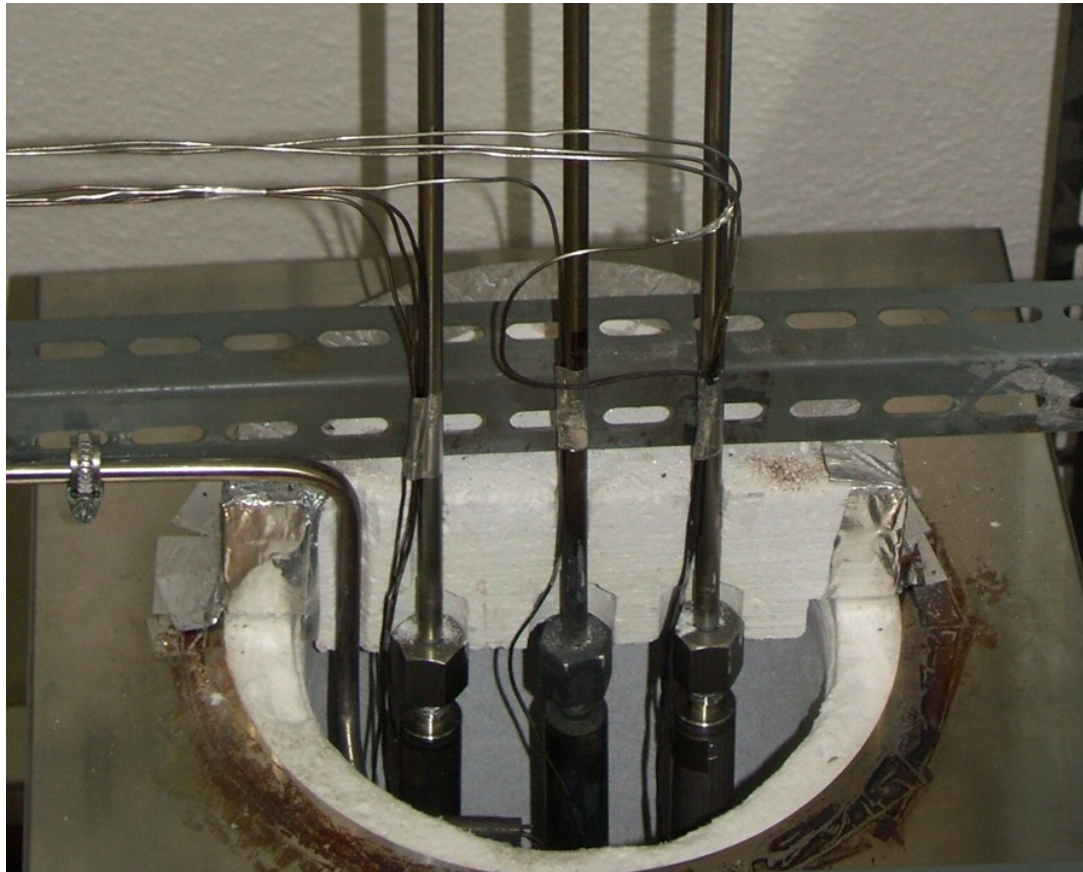


2. Pressure and vacuum system
3. Oven for heating of ampoules
4. Measuring & control system

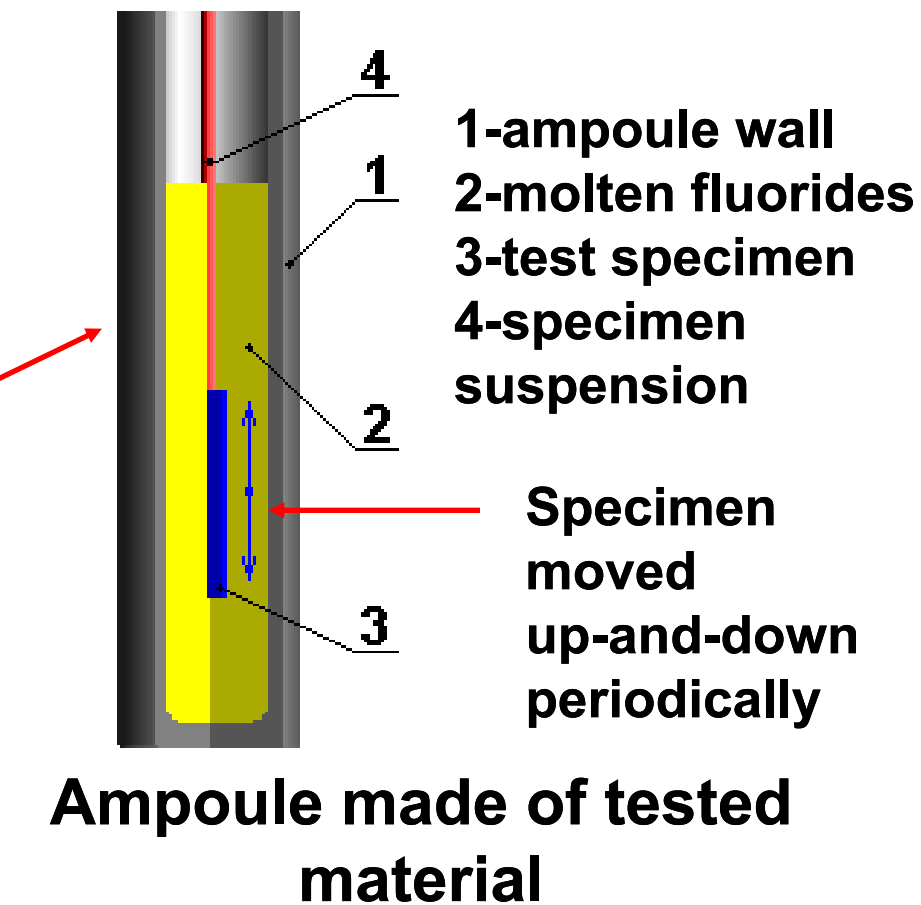
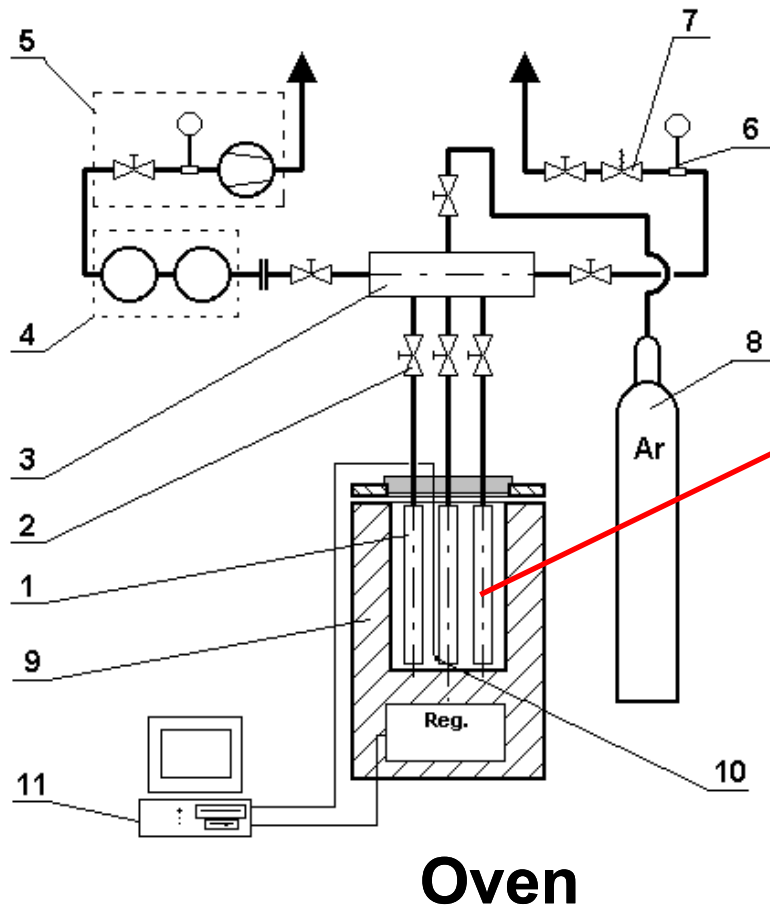


Molten fluoride salts

Sample is placed into ampoule which is filled with molten fluoride salts for the duration of 112 and 351 hours, respectively



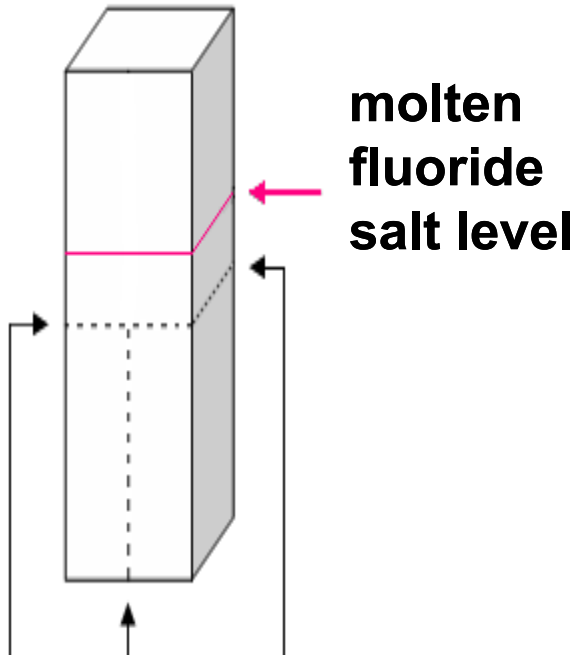
Corrosion experiment



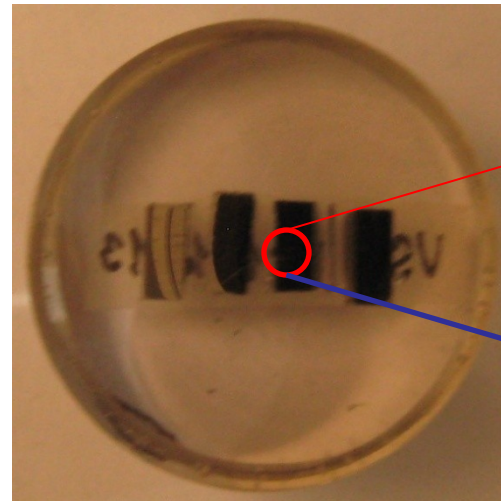
O. Matal, T. Šimo, L. Nesvadba, V. Dvořák, V. Kanický, P. Sulovský, J. Machát, Interaction of pipeline materials with molten fluoride salts. *Zeitschrift für Naturforschung: Teil a*, 62a, 12, 769-774 (2007).

Sample preparation

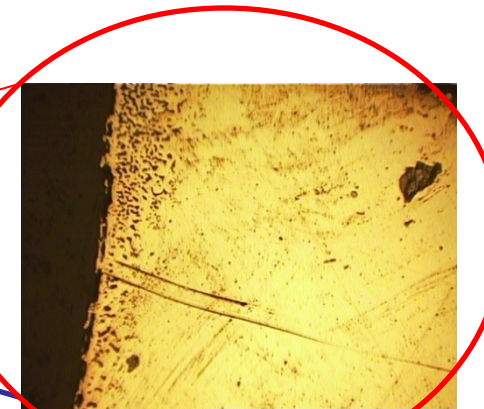
Test specimen
exposed in ampoule



Section of
specimen
embedded
in Araldite



Section with
corroded
surface



cut of the specimen

Electron probe microanalysis of sections and surfaces of ampules

SX100 microprobe (CAMECA, France)

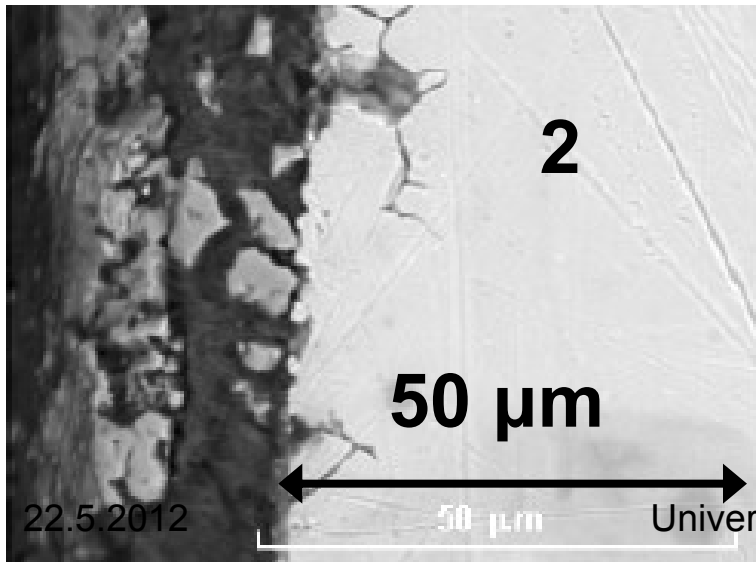
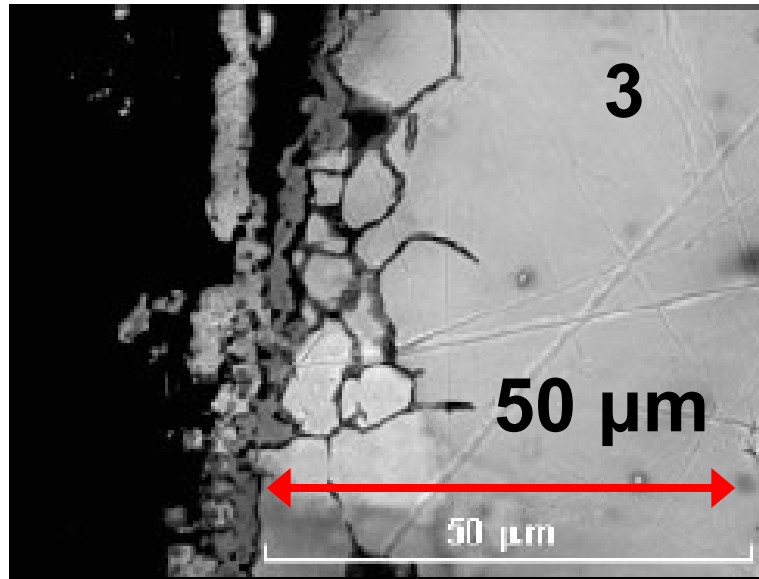
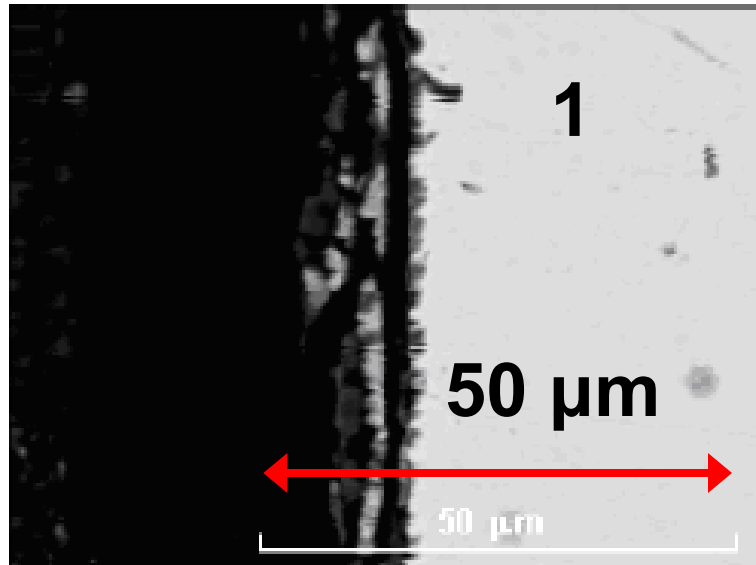
Polished sections and relief specimens (inner wall of the ampule, test body surface) were imaged:

- **Morphology-** Images in secondary electrons – SE
- **Material contrast-**Images in backscattered electrons – BSE

In order to reveal the compositional changes at the alloy/fluoride melt interface, polished sections of ampule walls and solidified melts were investigated by EPMA, the limits of determination being about 2 – 3x10-2 %:

- **Linear concentration profiles-** X-ray analysis
- **2D elemental concentration maps-** X-ray analysis

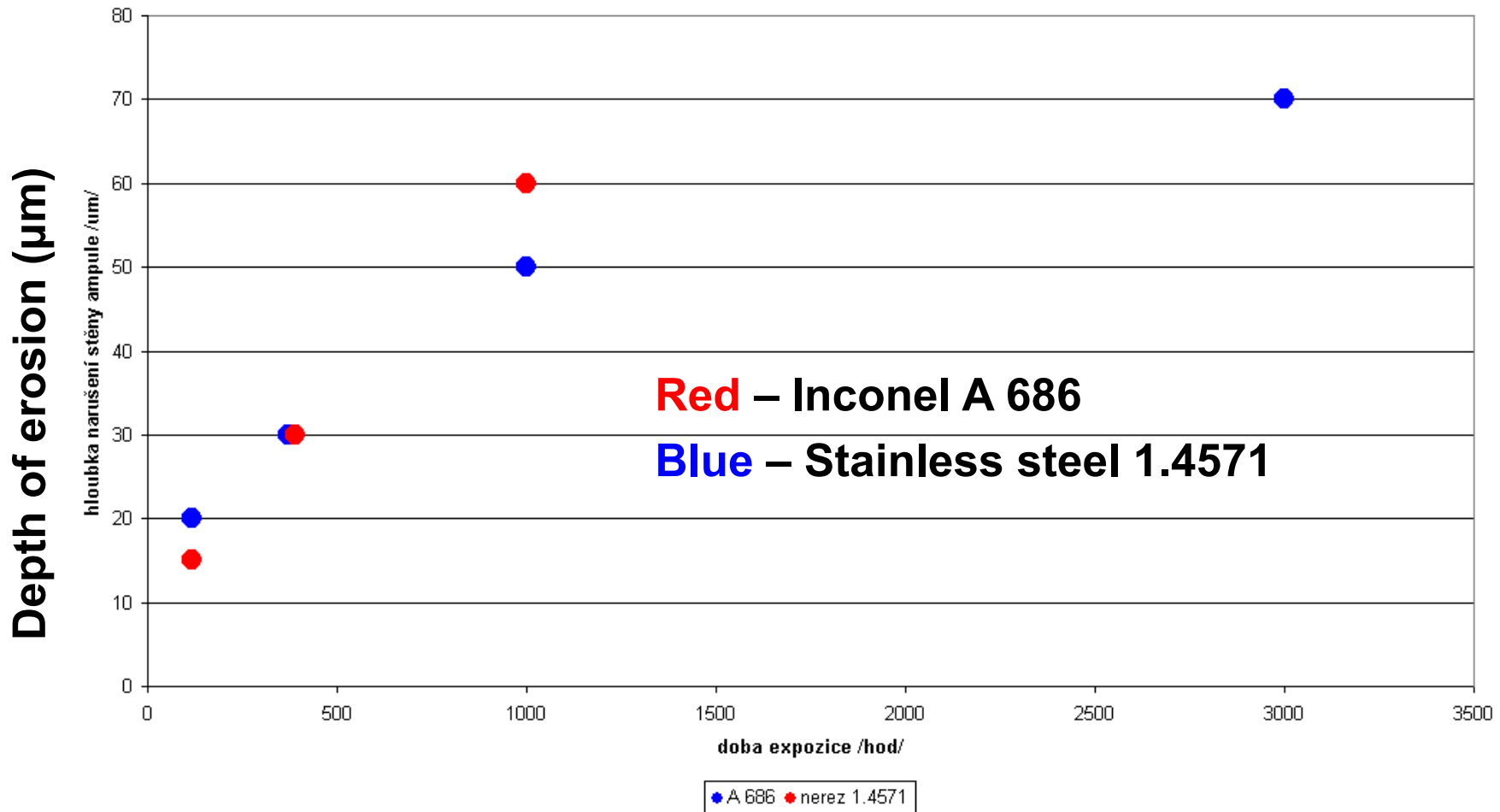
Damage of ampule wall by NaF/LiF melt



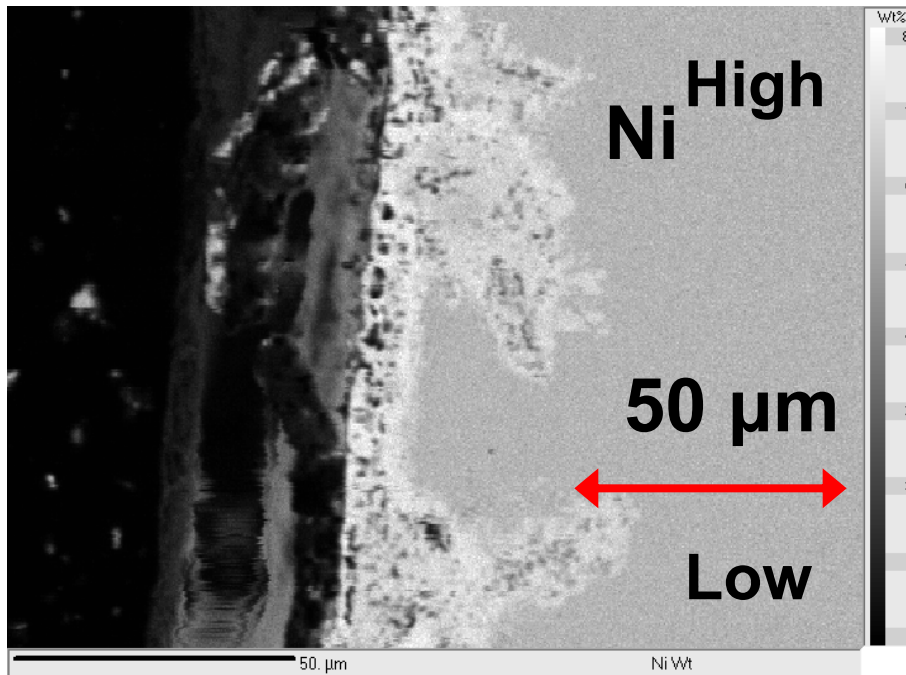
1. Ampule wall section 100 h exposure
2. Ampule wall section 300 h exposure
3. Ampule wall section 1000 h exposure

**1.4571 STAINLESS STEEL
Images BSE**

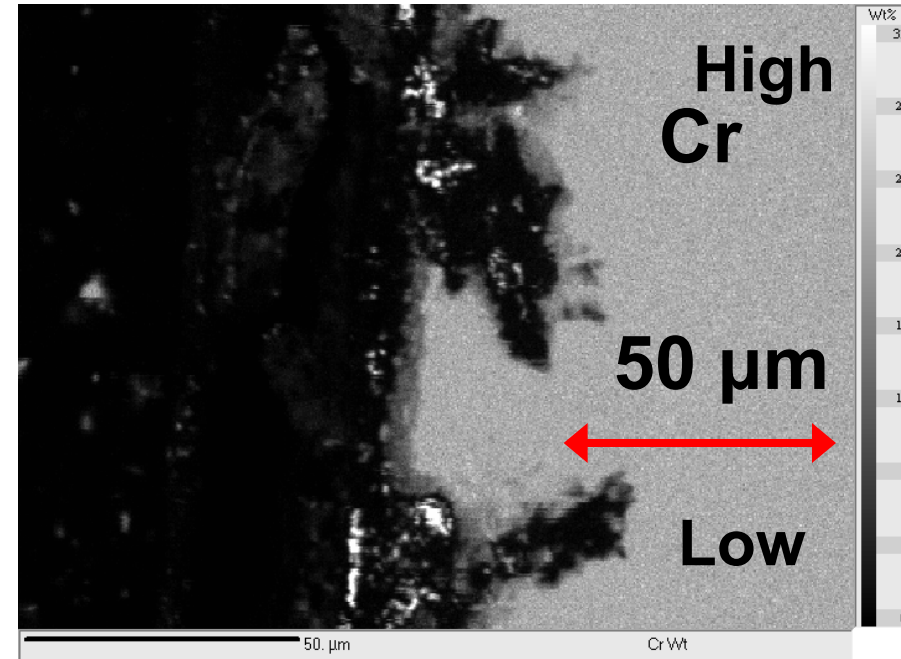
Depth of erosion of ampule wall



X-ray maps of Inconel by EPMA

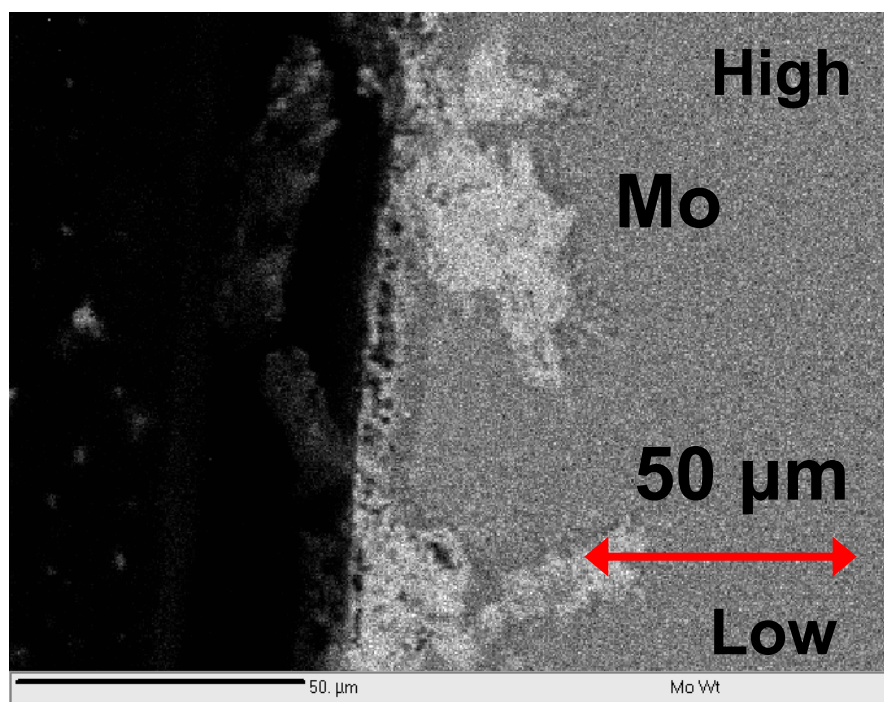


**X-ray map of Ni – Inconel 686,
exposed to 60% LiF – 40%
NaF melt for 117 hours**

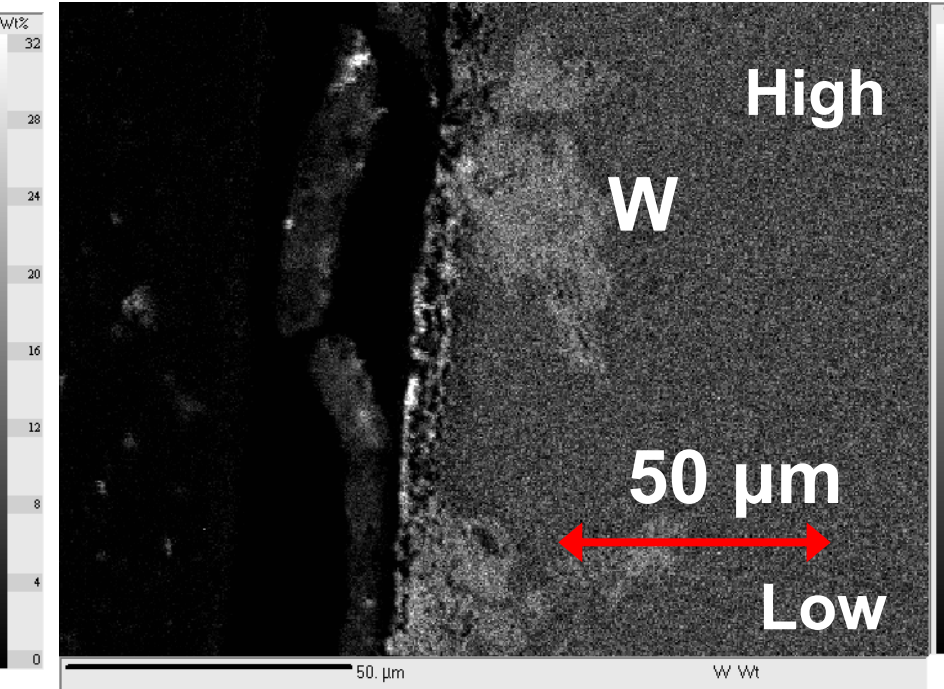


**X-ray map of Cr – Inconel 686,
exposed to 60% LiF – 40%
NaF melt for 117 hours**

X-ray maps of Inconel by EPMA

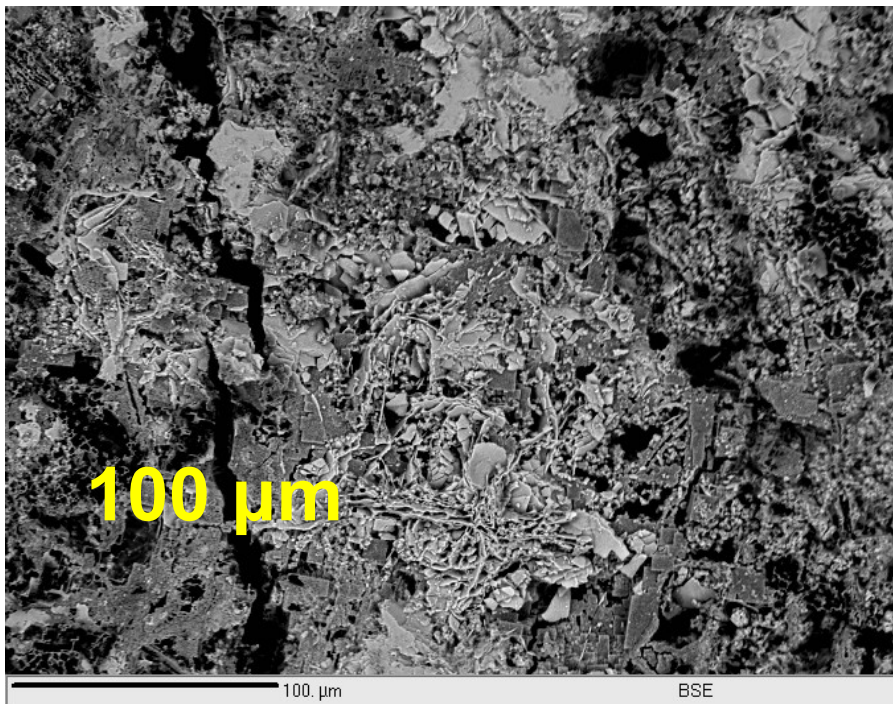


**X-ray map of Mo – Inconel 686,
exposed to 60% LiF – 40% NaF
melt for 117 hours**

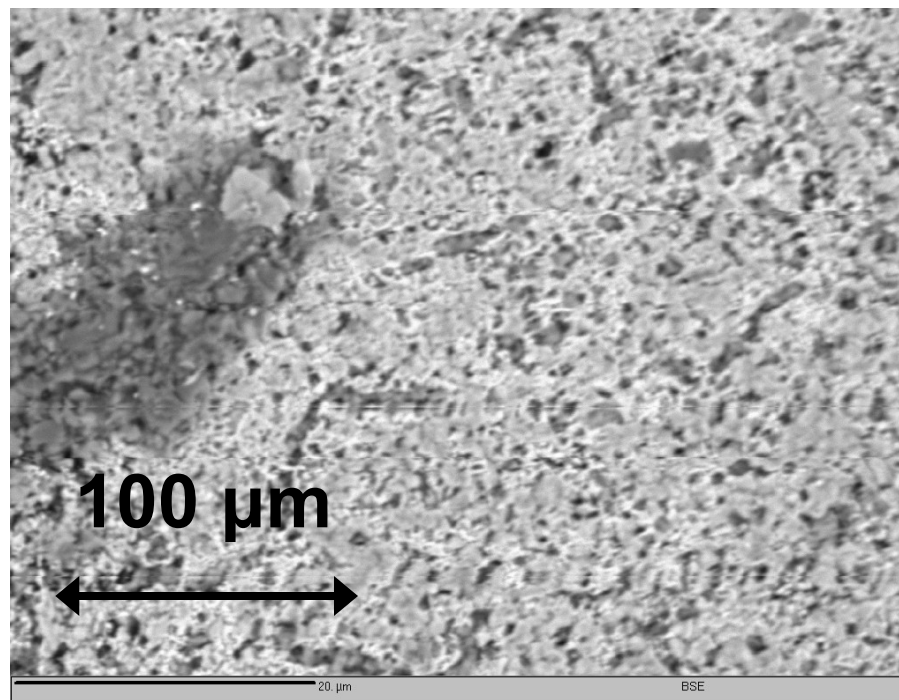


**X-ray map of W – Inconel
686, exposed to 60% LiF –
40% NaF melt for 117 hours**

SE images of Inconel sample surface



Crystalline crust of chromium trioxide (bright grey platelets) on the surface of Inconel A686 exposed to 60% LiF – 40% NaF melt for 1000 hours



Another part of the surface of Inconel 686 test body exposed to 60% LiF – 40% NaF melt for 1000 hours - area without Cr₂O₃ crust.

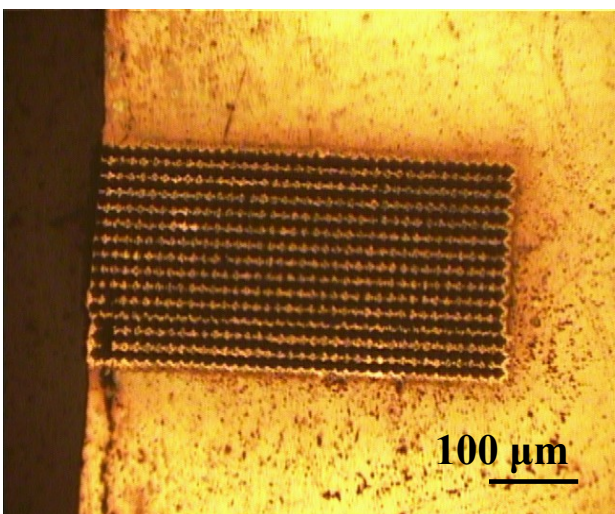
Results EPMA

- The Inconel 686, exposed to 60% LiF – 40 % NaF melt (1000 h, dynamic test) shows significant compositional changes at the interface with melt. The depth to which these changes affected the composition of the tested material, however, does not exceed 20 – 25 µm.
- The corrosion of Inconel by LiF/NaF is characterized by two processes:
 - diffusion and dissolution of the alloy,
 - oxidation of released Cr by traces of O₂ in the Ar filling the space above the melt level.
- Fe content is homogeneously increased in the subsurface 20 – 25 µm thick layer by max. 10%
- Cr is depleted in this layer, while Ni and Mo are distinctly enriched in it.

Ablation mapping

Laser ablation conditions :

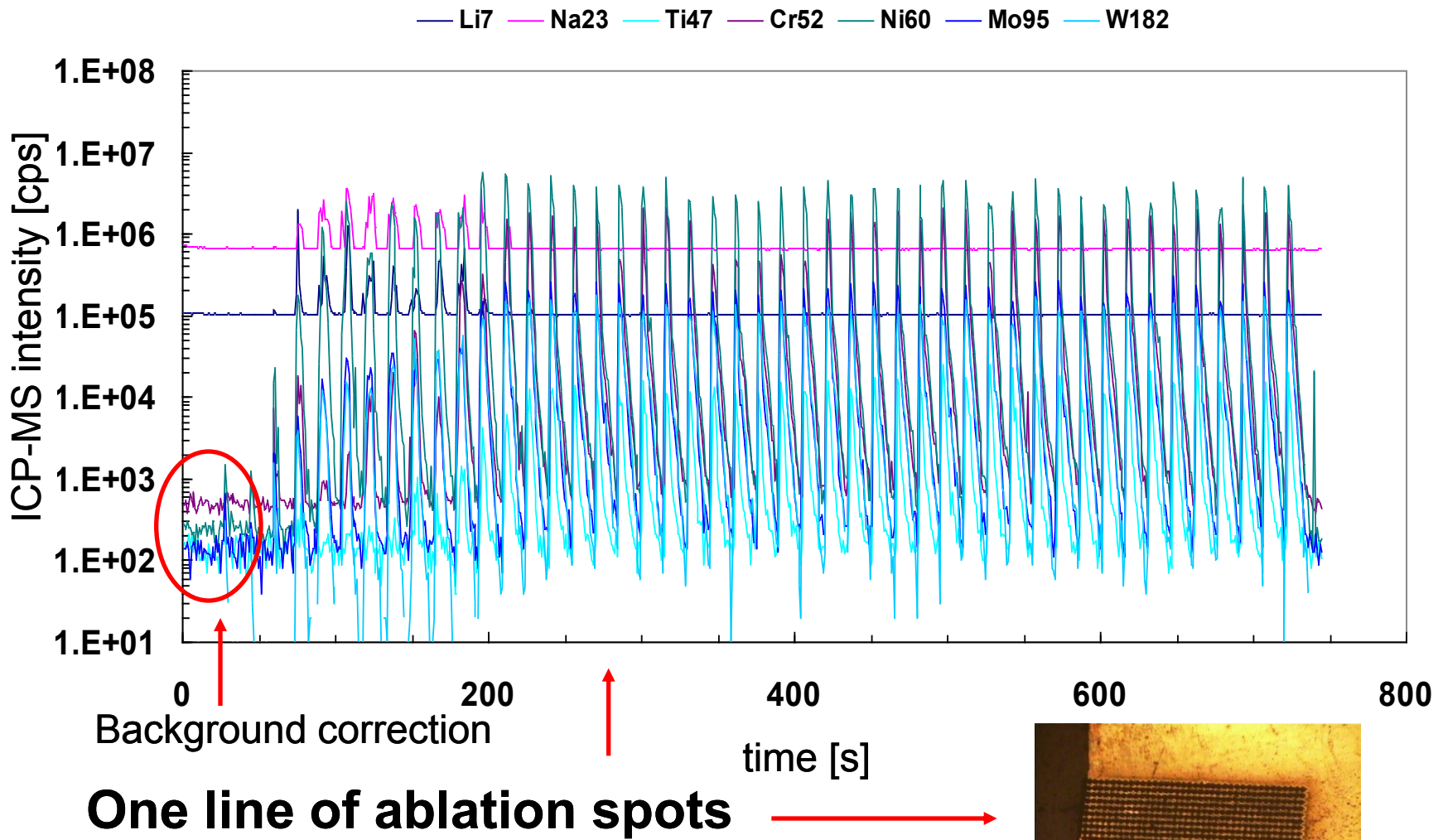
laser beam fluency:	25.5 J cm ⁻²
laser beam spot diameter:	12 µm
repetition rate:	20 Hz
ablation mode:	hole drilling
distance between spots:	12 µm
Laser beam dwell time:	5 s



**ICP-MS
Agilent 7500 ce**



Signal measurement



Quantitation

Isotope signals total sum normalization
– abundance corrected intensity

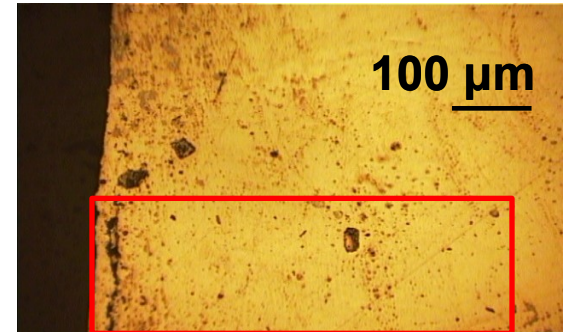
$$I(Mn)_{\text{abund}} = I(^{55}\text{Mn})_{\text{corr}} / \text{abundance}(^{55}\text{Mn})$$

$$I(Li)_{\text{abund}}, I(Na)_{\text{abund}}, I(Ni)_{\text{abund}}, I(Cr)_{\text{abund}}, \dots \Rightarrow \sum I_{\text{abund}}$$

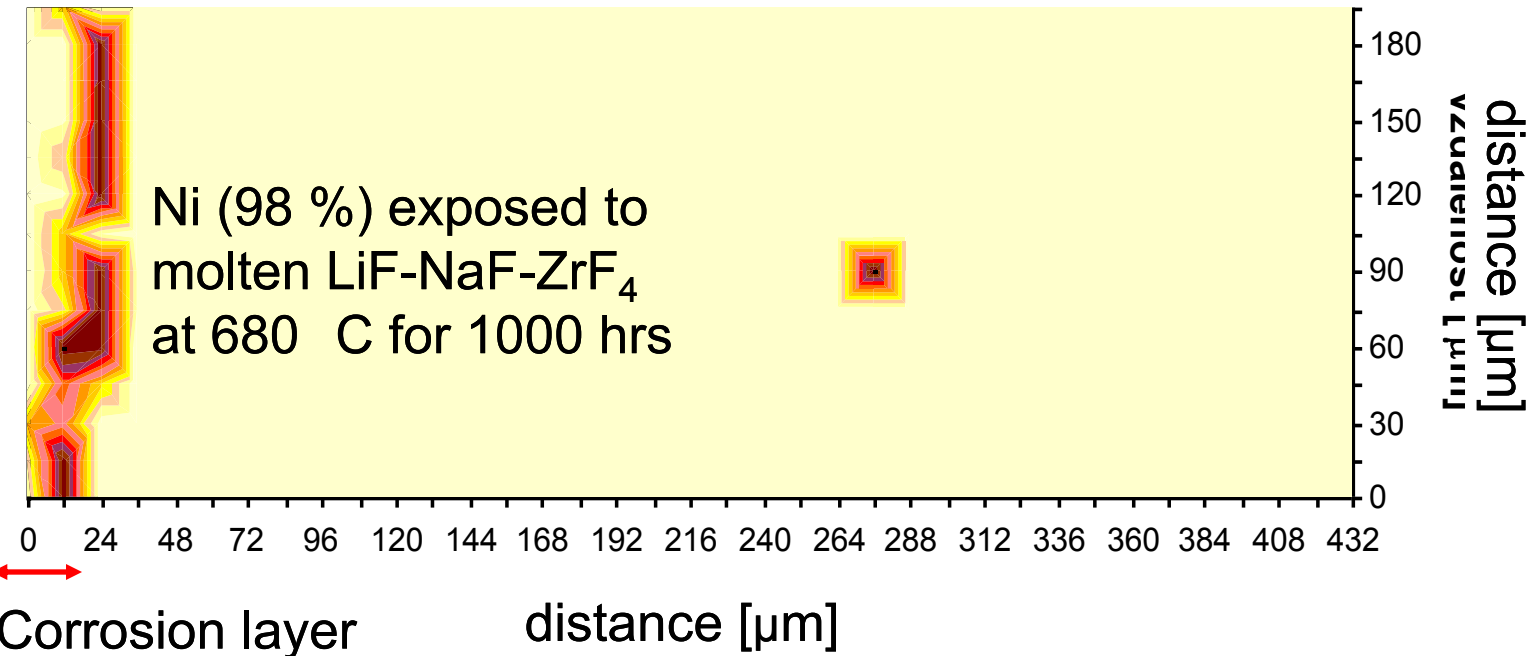
Fluoride ion counts were calculated from stoichiometry of fluoride salts and Na, Li, Zr counts

$$\text{content Mn} = [I(Mn)_{\text{abund}} / \sum I_{\text{abund}}] * 100 (\%)$$

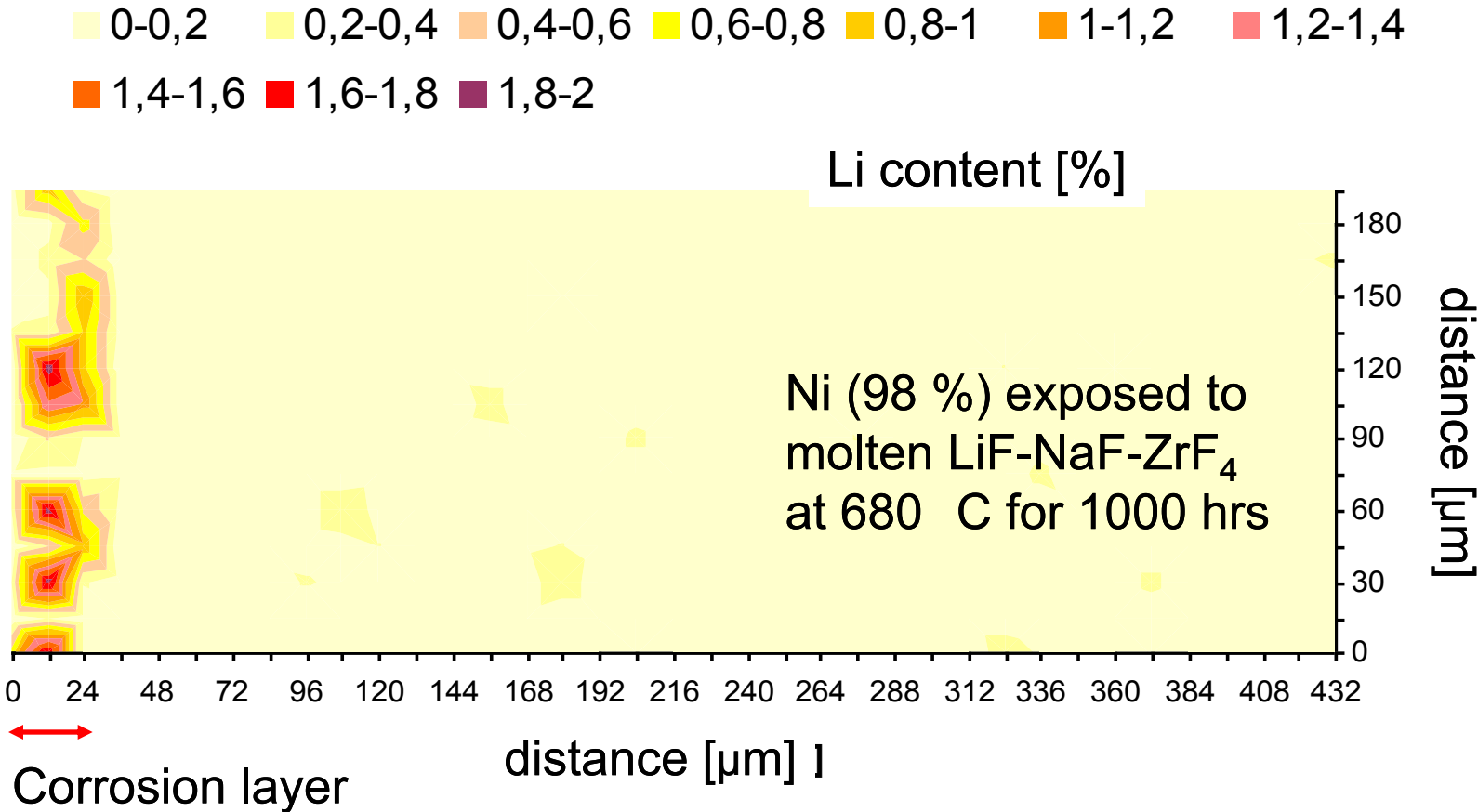
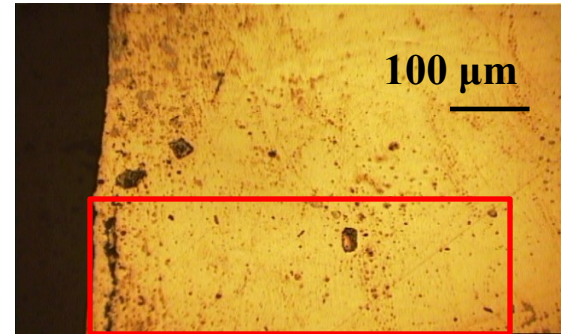
Zr map of „Nickel“ sample corroded surface



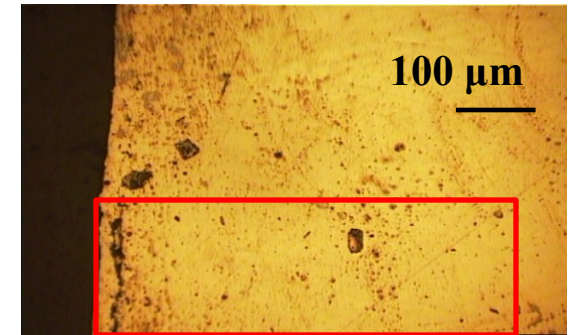
Zr content [%]



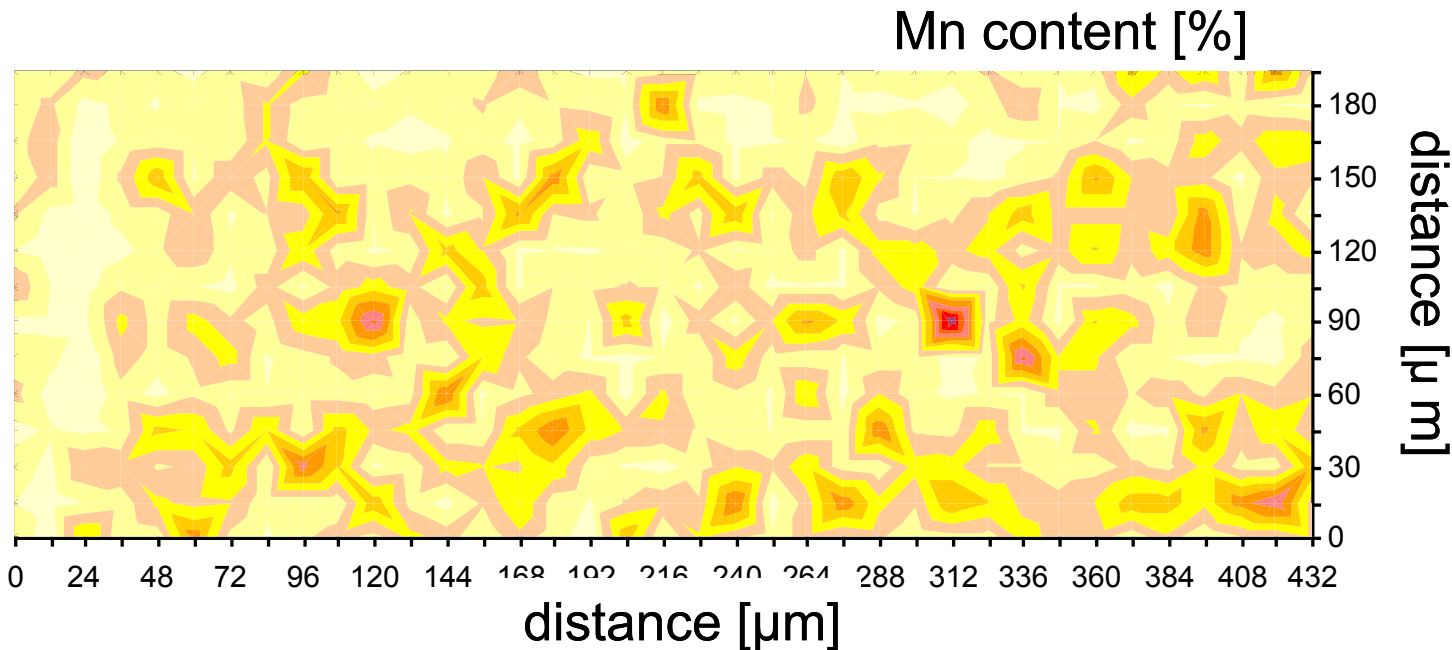
Li map of „Nickel“ sample corroded surface



Mn map of „Nickel“ sample corroded surface



Ni (98 %) exposed to molten LiF-NaF-ZrF₄ at 680 °C for 1000 hrs



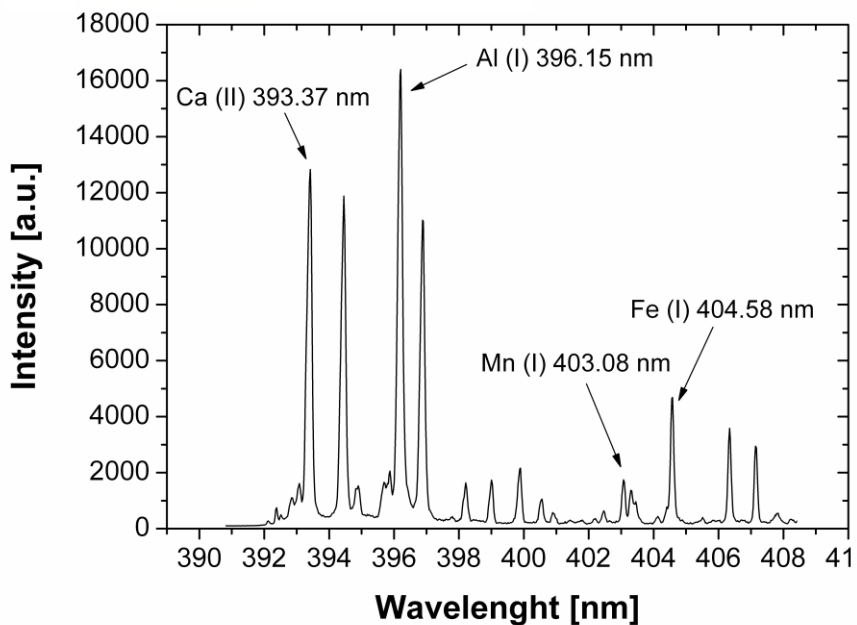
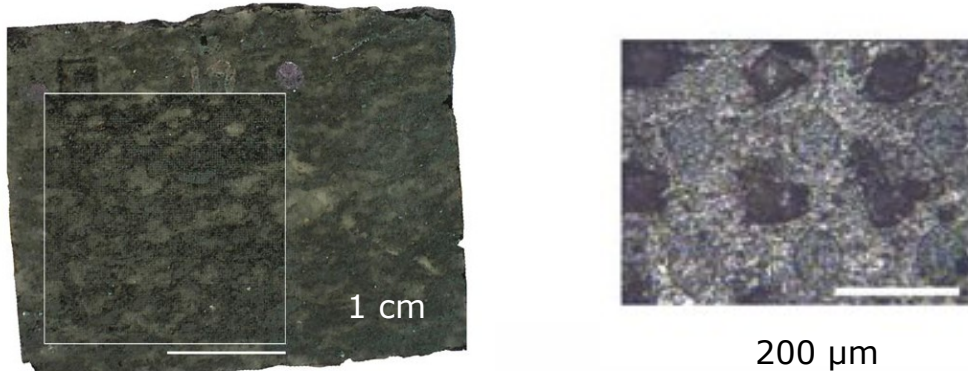
Conclusion I

- Penetration of molten salts into specimen material was proved (signals Zr, Li, Na).
- Corrosion depth was determined from elemental maps (Zr, Li, Na)... 30 µm.
- Quantitation of elemental mapping is possible by normalization to total sum of signals for „easy“ matrix (alloys,metals, ceramics).

Geology

- 2D-mapping of granite by LIBS and LA-ICP-MS

Exploratory study - granite

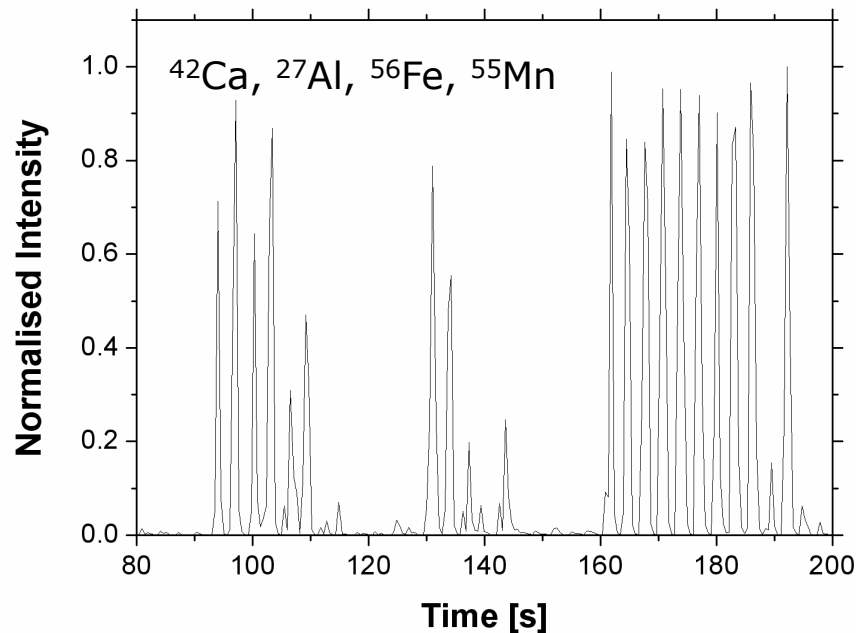


LIBS

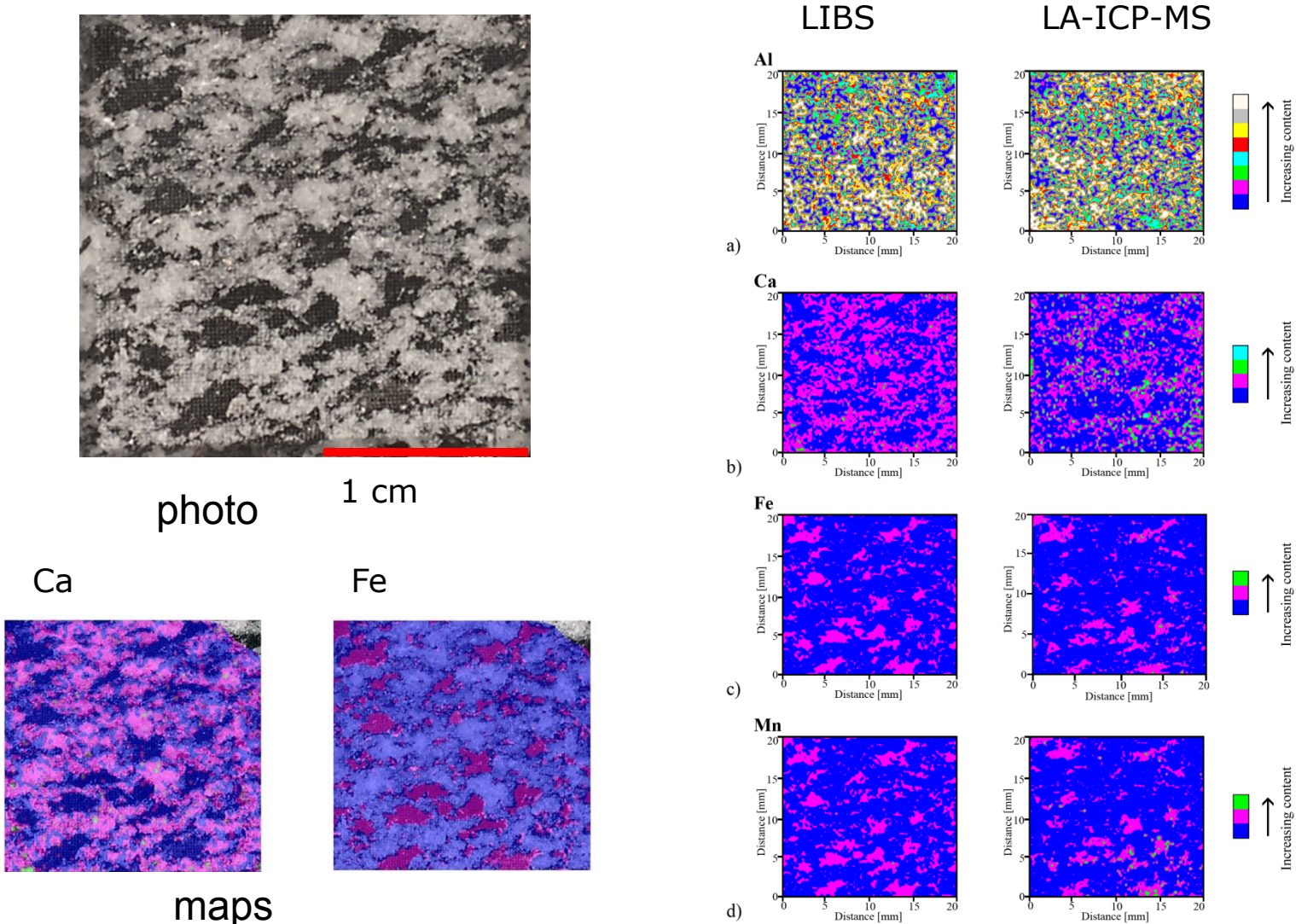
120 μm laser spot diameter, 2 laser pulses per sample point

LA-ICP-MS

hole drilling mode, 110 μm laser spot diameter, 20 laser pulses per sample point, distance between individual laser spots was 200 μm



K. Novotný, J. Kaiser, M. Galiová, et al.: Mapping of different structures on large area of granite sample using laser-ablation based analytical techniques, an exploratory study, Spectrochimica Acta Part B 63 (2008) 1139–1144.



Archaeology

Study of prehistoric bear tooth for acquiring knowledge about diet

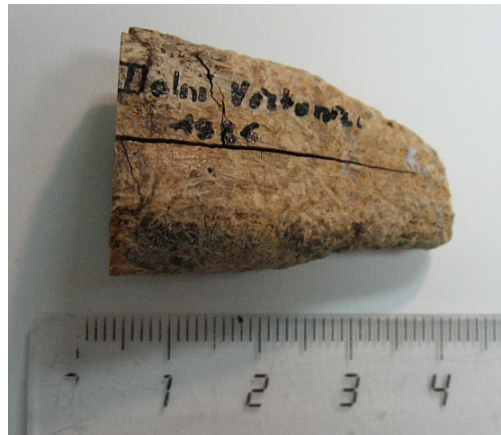
Known facts

- Ratio $^{87}\text{Sr}/^{86}\text{Sr}$ depends on the geological substrate and Sr enters to the food chain *via rock decay*. *The sequence is as follows: rocks → water → plants → herbivores.*
- Strontium and calcium metabolism are similar and strontium can substitute calcium in hydroxyapatite matrix.
- The fluctuation of Sr/Ca ratio enables to reconstruct the migration of an animal or human due to environment change of ratio. Both elements have nutrition character and they are used for the determination of diet.
- Content of Sr [mg/kg] in teeth and bones ($\text{Ca}_{10}(\text{PO}_4)_6(\text{OH})_2$) in the order
- carnivores → omnivore → herbivores → marine foodstuff is
- 100-300 → 150-400 → 400-500 → >500

Known facts

- Similar properties can be observed from Sr/Ba ratio. This fluctuation is more sensitive in comparison with Sr/Ca due to the presence of barium. However, higher content of Ba on the surface can indicate contamination.
- Opposite behavior was observed for zinc in comparison with Sr content. Content of Zn increases as follows:
 - herbivores → omnivore → carnivores
 - 90-150 mg /kg1 → 120-220 mg/kg1 → 175-250 mg/kg.
- Higher concentration of the element is typical for meat, nuts or mollusks. On the other side, it can be caused by inflammation.

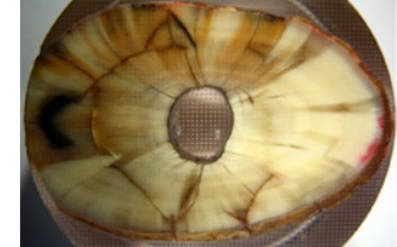
Bear tooth



root section



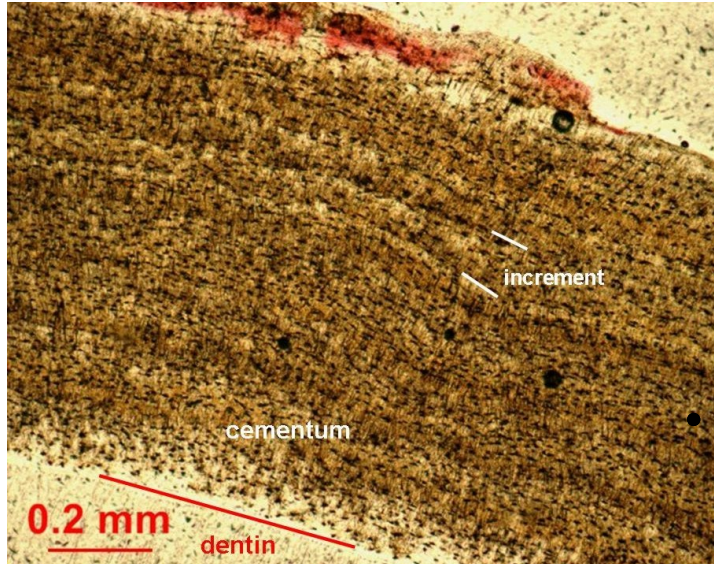
crown section



- The investigated tooth (canine-C1) of fossil brown bear (*Ursus arctos*) was excavated at Dolní Věstonice II-Western Slope, South Moravia, Czech Republic.
- The locality is dated to 26 640 – 110 BP (uncalibrated 14C data) and belongs to Gravettien.

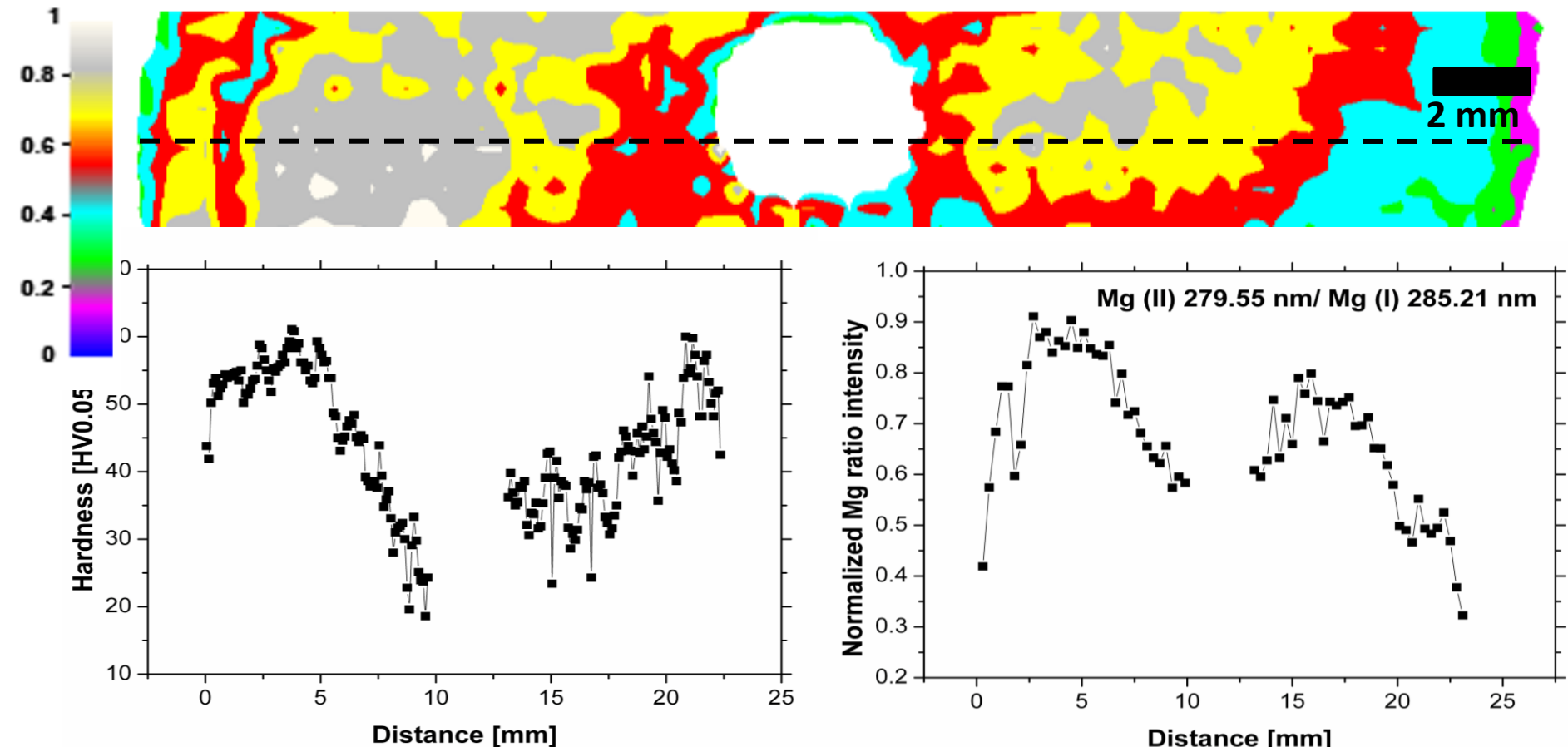


Bear tooth



- Abrasion of tooth's occlusal area and increments of cementum of tooth's root were studied in order to determine the age and seasonality.
- This bear died at the age of 14 years and it is possible to appoint the term of death from unfinished summer increment and absence of winter increment in between summer and autumn season (August to October).

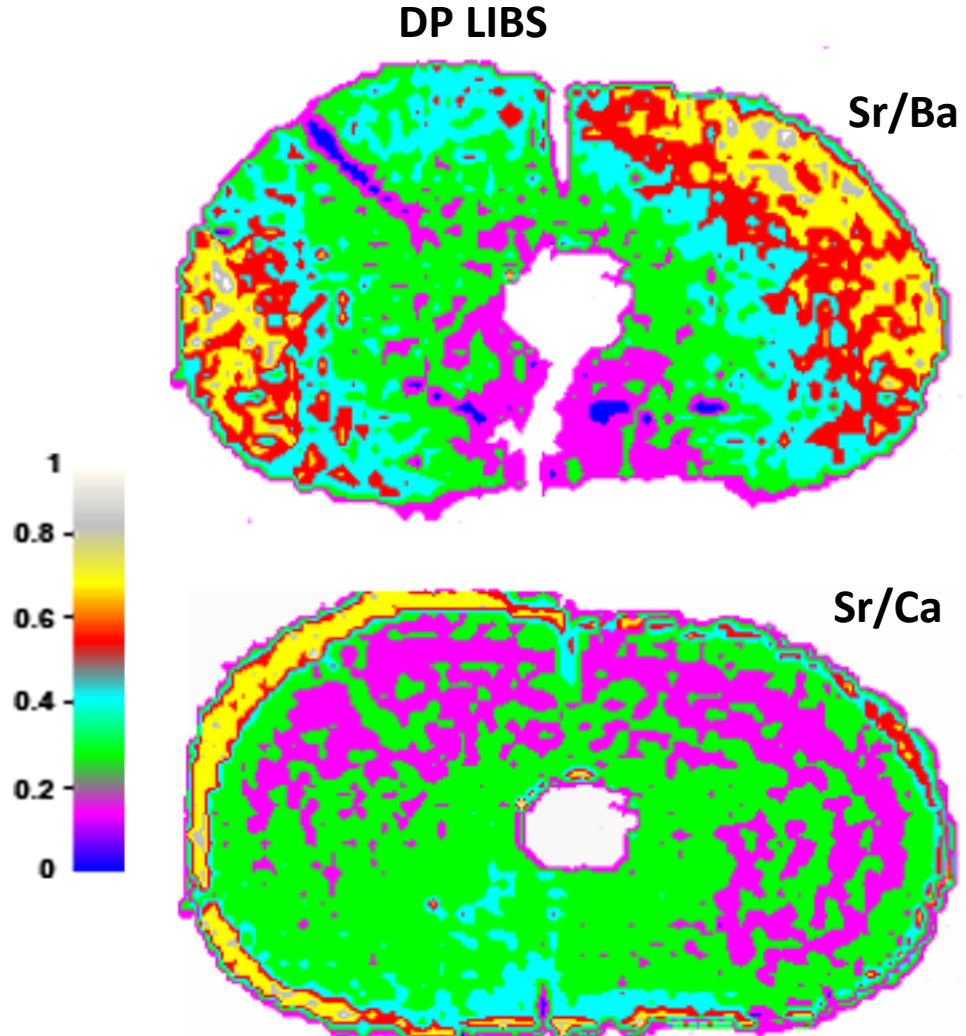
Hardness of the sample (canine tooth root)



- The estimation of the *sample hardness* via Mg II/Mg I intensity ratios is shown.
- The estimated hardness characteristic was proved by microhardness measurements.
- The Vickers test pattern was placed nearby the LIBS ablation craters for Mg detection.

Ethology of the studied fossil brown bear

SP and DP LIBS and LA-ICP-MS

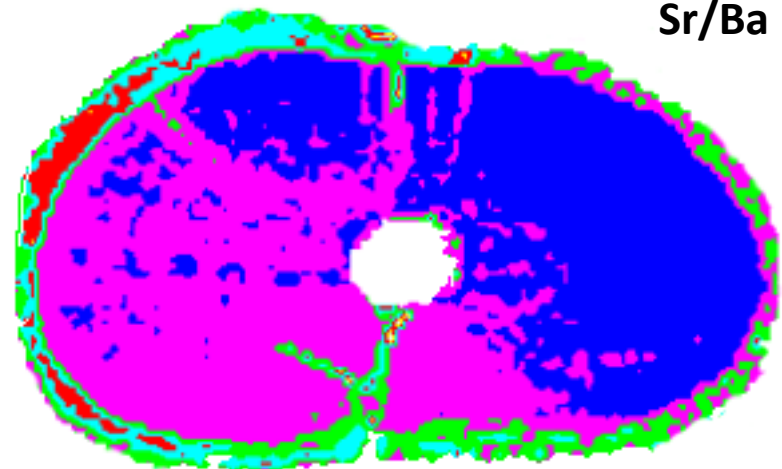
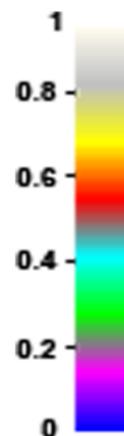


The dark areas on the sample are well correlated with the lower Sr/Ba Sr/Ca ratio in the map. They are rather related to the narrow winter strips.

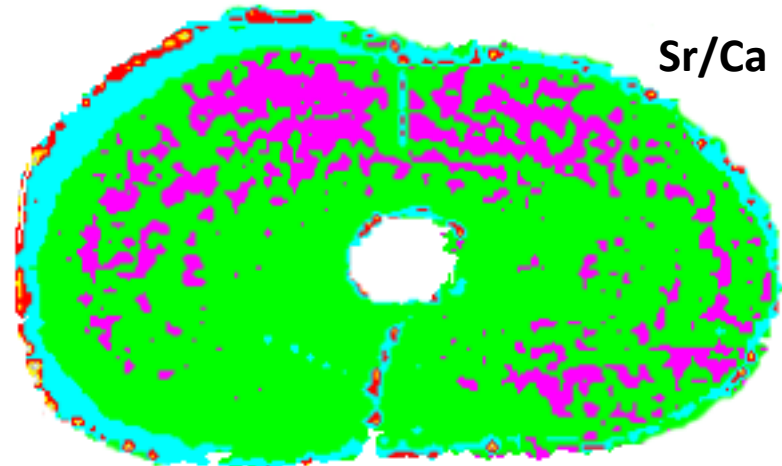
Ethology of the studied fossil brown bear

SP and DP LIBS and LA-ICP-MS

SP LIBS



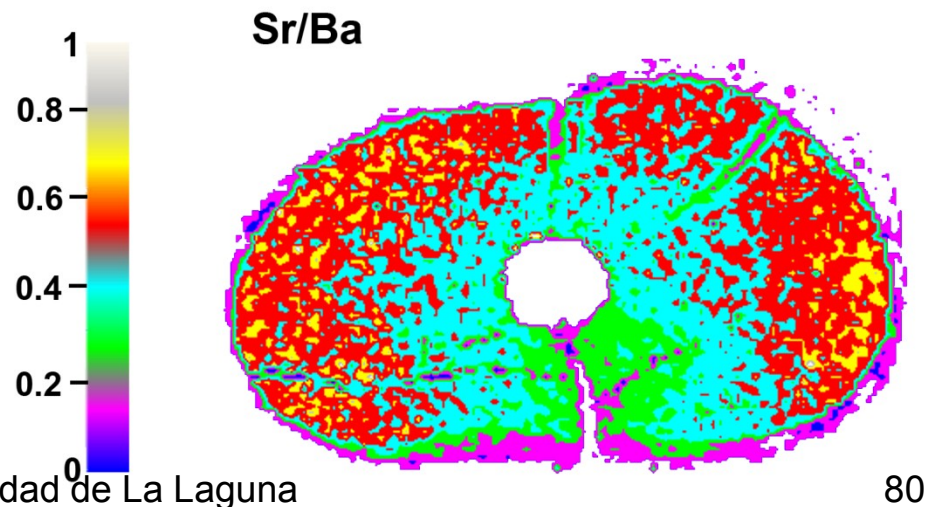
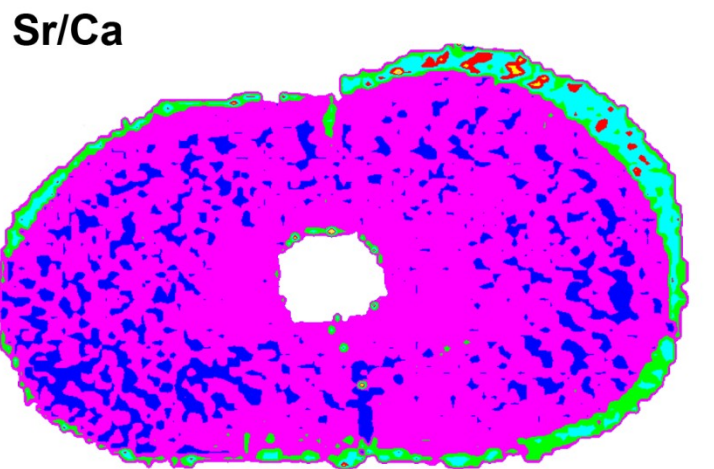
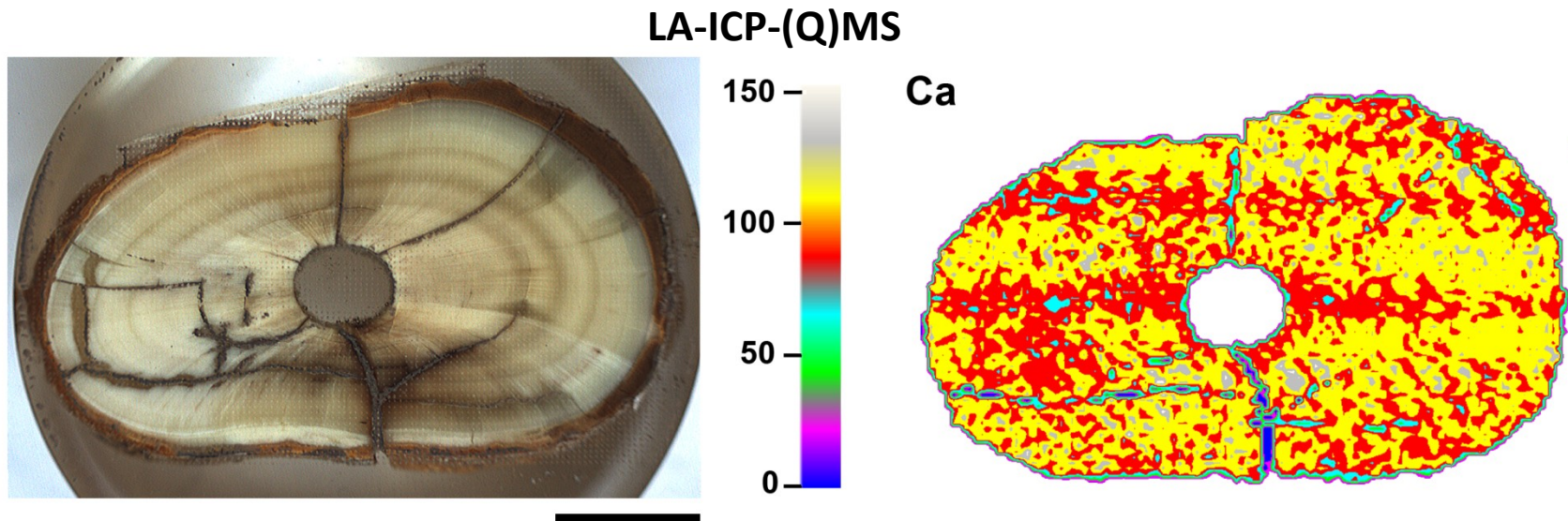
Sr/Ba

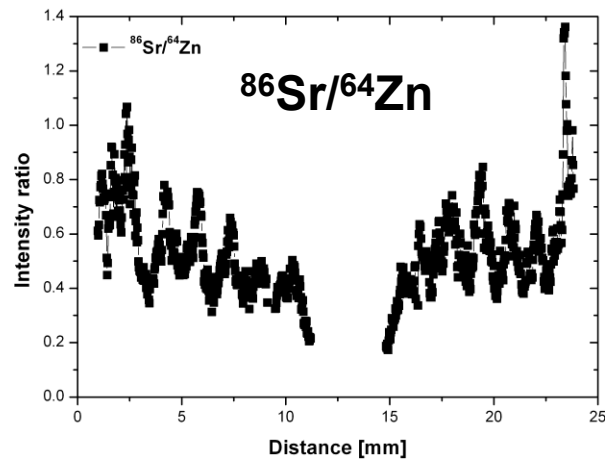


Sr/Ca

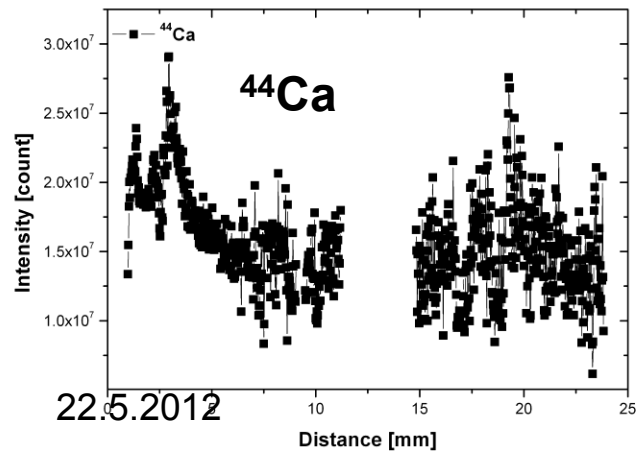
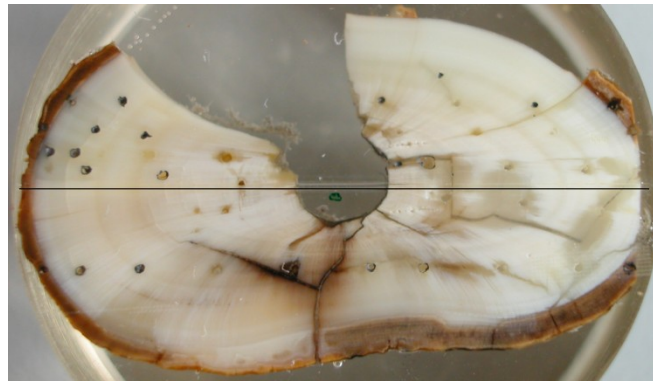
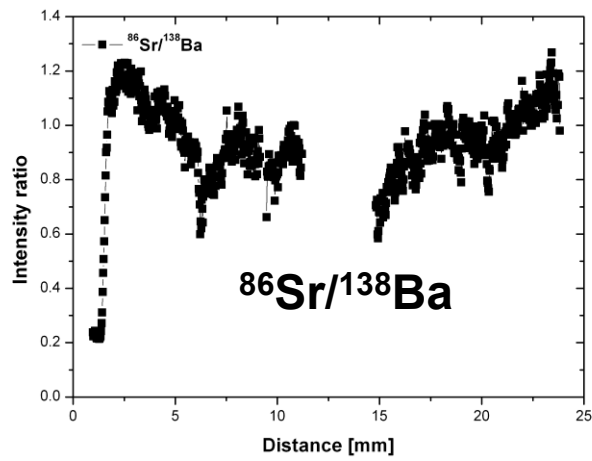
The seasonal fluctuations of the Sr/Ca and Sr/Ba detected by laser-ablation based techniques (SP and DP LIBS and LA-ICP-MS) evidenced the migration of this bear between his hibernaculum's location and the place where the fossils were found.

Ethology of the studied fossil brown bear

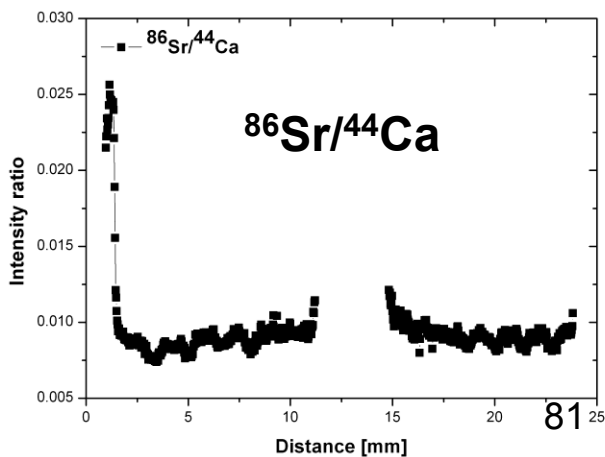




LA-ICP-(TOF)MS



Universidad de La Laguna



Environmental

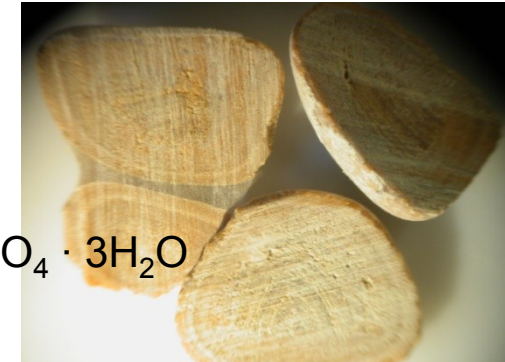
Uroliths – renal calculi

UROLITH LOCAL ANALYSIS

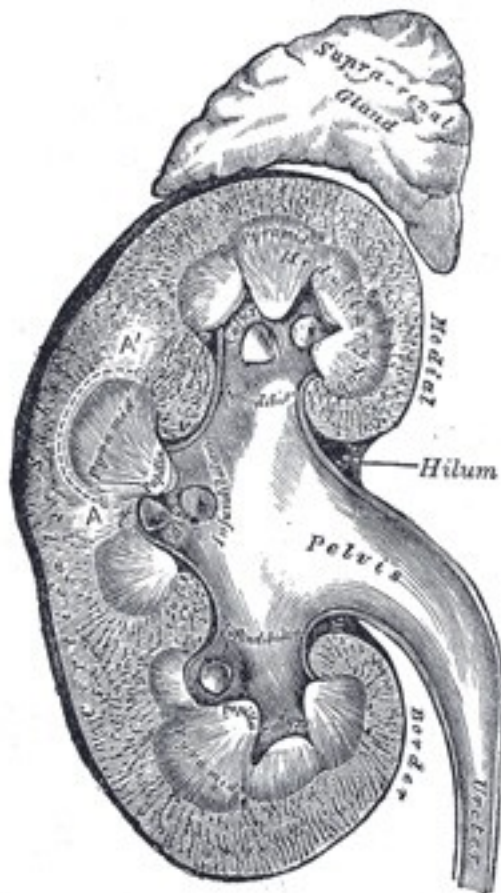
Kidney stones, urinary stones (renal calculi, urolithiasis) = solid concretions (crystal aggregations) of dissolved minerals in urine calculi typically form inside kidneys, ureter, urethra, bladder, prostate

To date over 200 components have been found in calculi; however, the most common constituents of kidney stones are:

- Calcium Oxalate Monohydrate (**Whewellite**); $\text{CaC}_2\text{O}_4 \cdot \text{H}_2\text{O}$
- Calcium Oxalate Dihydrate (**Weddellite**); $\text{CaC}_2\text{O}_4 \cdot 2\text{H}_2\text{O}$
- Magnesium Ammonium Phosphate Hexahydr. (**Struvite**); $\text{MgNH}_4\text{PO}_4 \cdot 2\text{H}_2\text{O}$
- Ca Phosphate & Carbonate (**Carbonate Apatite**); $\text{Ca}_{10}(\text{PO}_4 \cdot \text{CO}_3\text{OH})_6(\text{OH})_2$
- Calcium Phosphate, Hydroxyl Form (**Hydroxyl Apatite**); $\text{Ca}_{10}(\text{PO}_4)_6(\text{OH})_2$
- Calcium Hydrogen Phosphate Dihydrate (**Brushite**); $\text{CaHPO}_4 \cdot 2\text{H}_2\text{O}$
- Uric Acid; $\text{C}_5\text{H}_4\text{N}_4\text{O}_3$
- Cystine; $(\text{SCH}_2\text{CH}(\text{NH}_2) \cdot \text{COOH})_2$
- Sodium Acid Urate; $\text{C}_5\text{H}_3\text{N}_4\text{O}_3\text{Na} \cdot \text{H}_2\text{O}$
- Tricalcium Phosphate (**Whitlockite**); $\text{Ca}_3(\text{PO}_4)_2$
- Ammonium Acid Urate; $\text{NH}_4\text{H} \cdot \text{C}_5\text{H}_2\text{O}_3\text{N}_4 \cdot \text{H}_2\text{O}$
- Magnesium Hydrogen Phosphate Trihydrate (**Newberryite**); $\text{MgHPO}_4 \cdot 3\text{H}_2\text{O}$

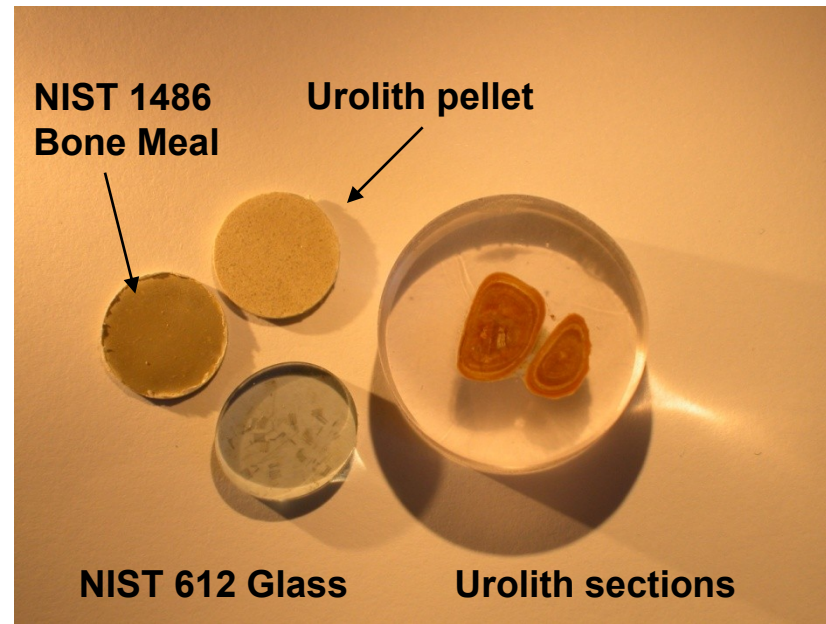


Layered structure: growth of uroliths

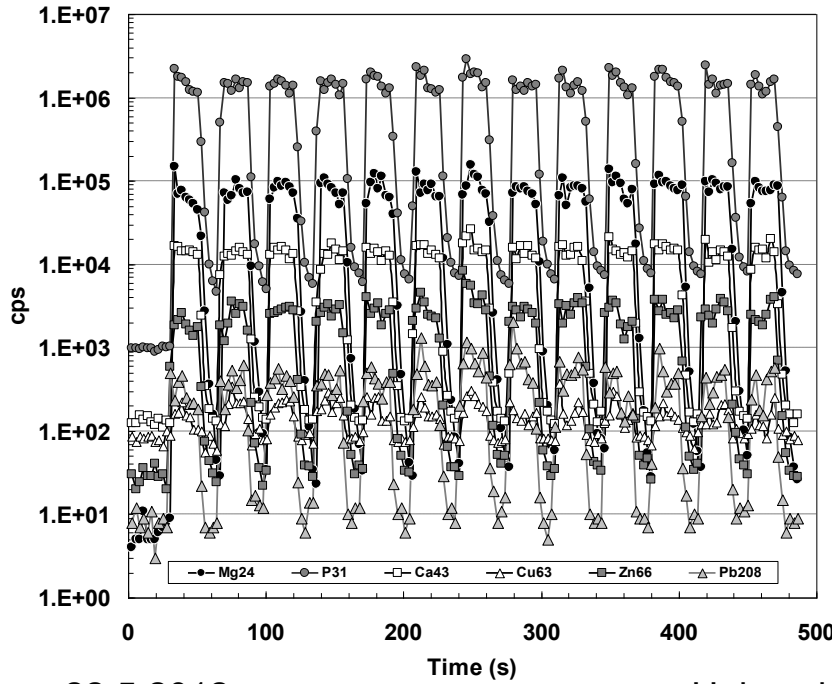
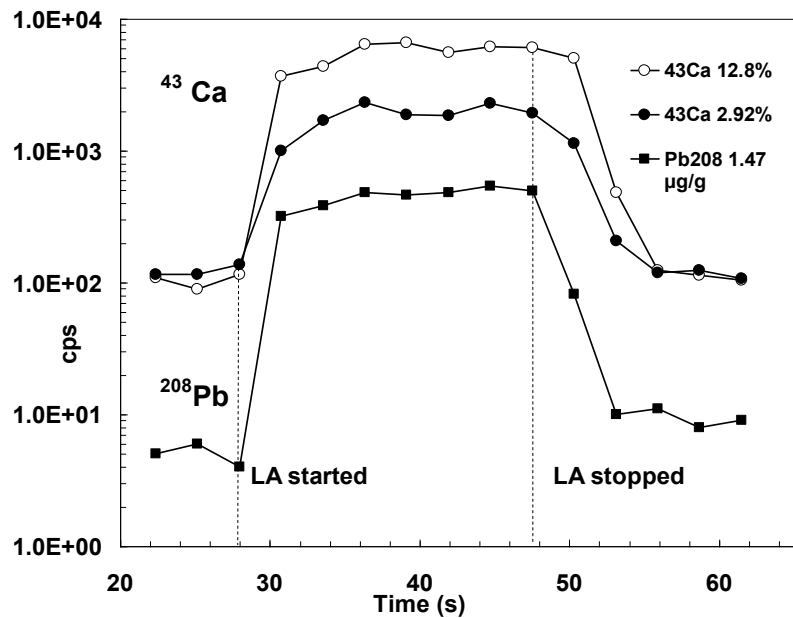


Designed procedure

1. Average elemental contents in uroliths by PN-ICP-MS after acid mixture decomposition
2. LA-ICP-MS calibration with homogenized urolith pellets and assignment of content values found using PN-ICP-MS to the pellets.
3. LA-ICP-MS calibration with pressed pellet of powdered SRM NIST 1486 Bone Meal.

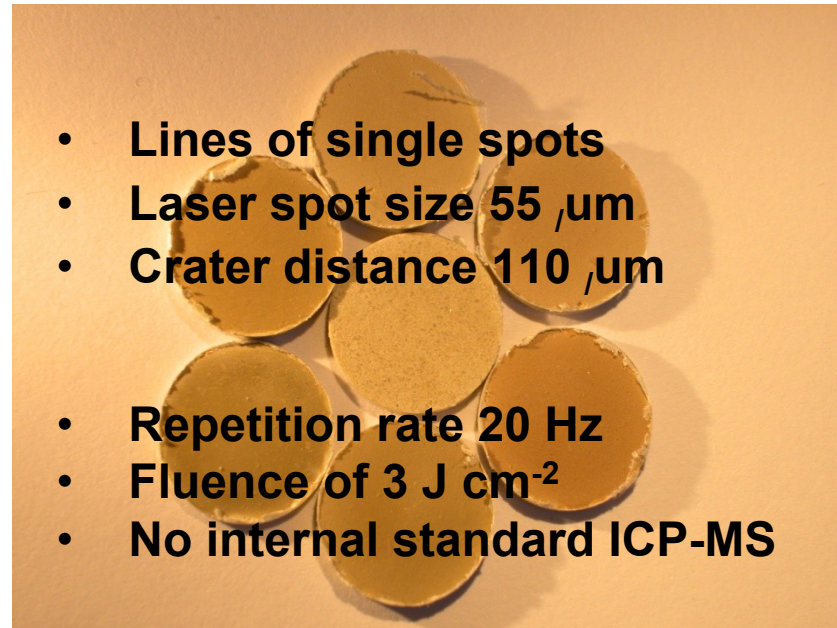


4. LA-ICP-MS elemental distribution recording = line of single-spot ablation events directed perpendicularly to layered structure of urolith section
5. LA-ICP-MS calibration using:
 - NIST 1486 Bone Meal
 - urolith pellets with contents by PN-ICP-MS
 - NIST 612 Glass
6. Calculation of concentration profile of uroliths



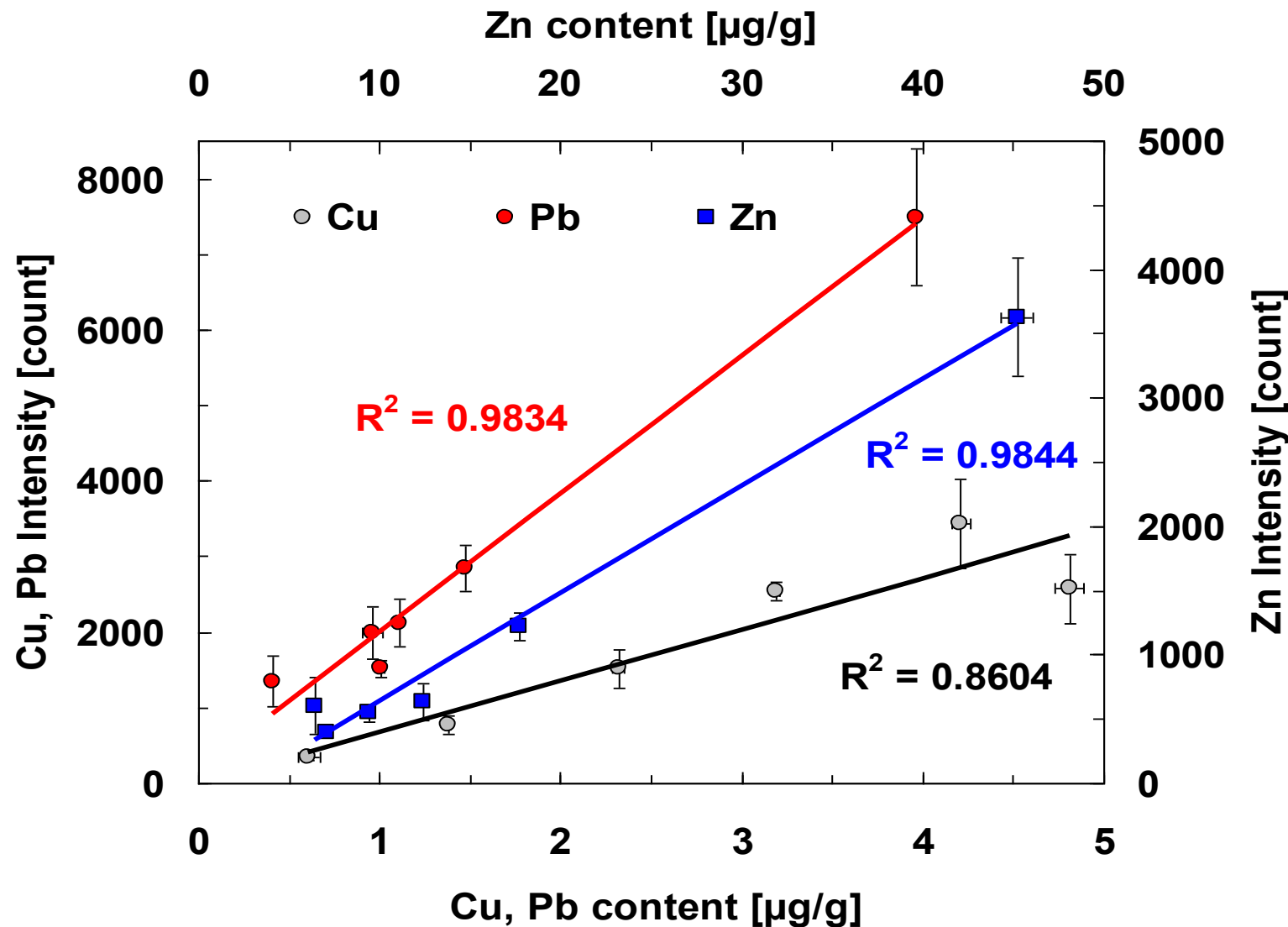
22.5.2012

Universidad de La Laguna

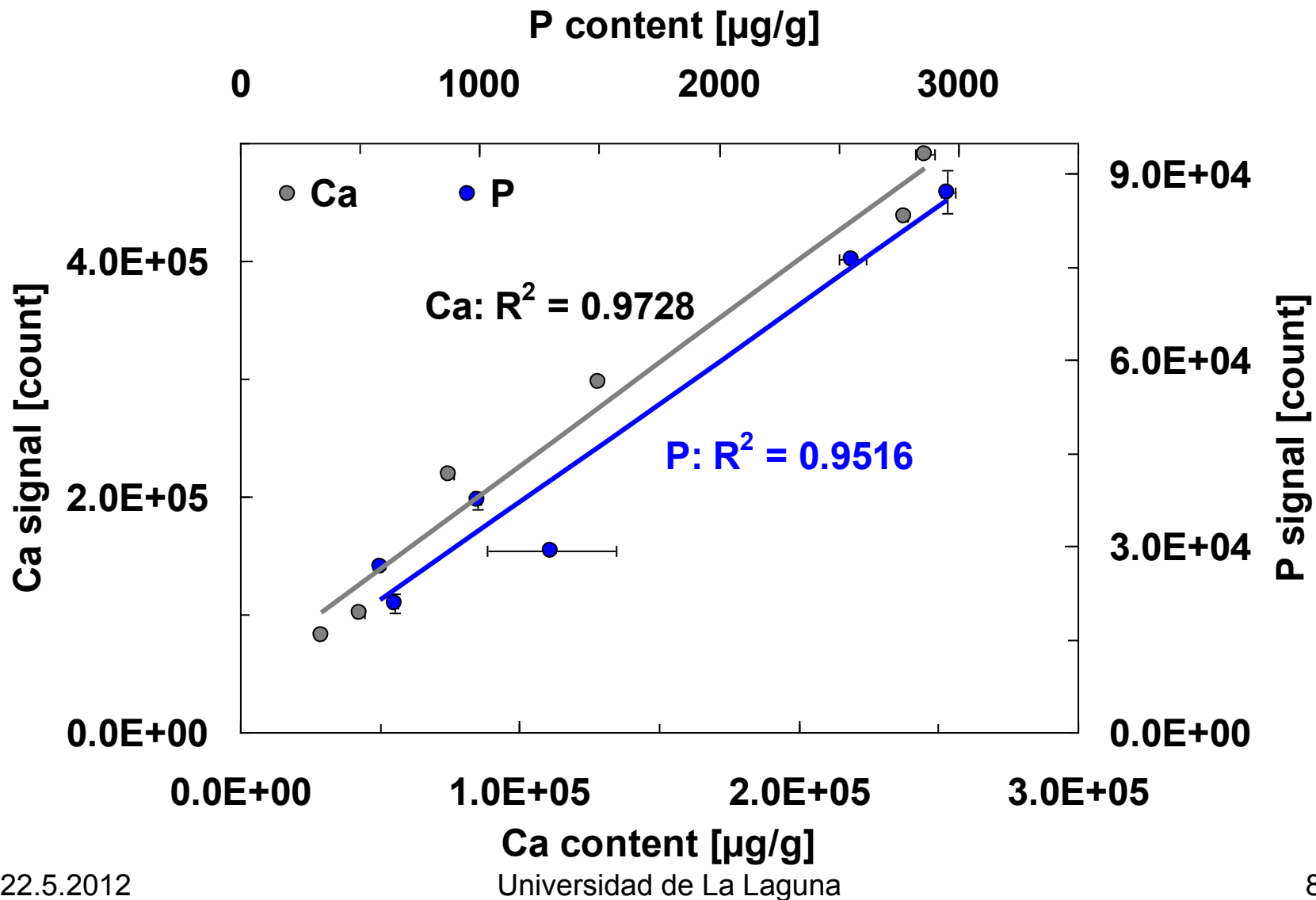


86

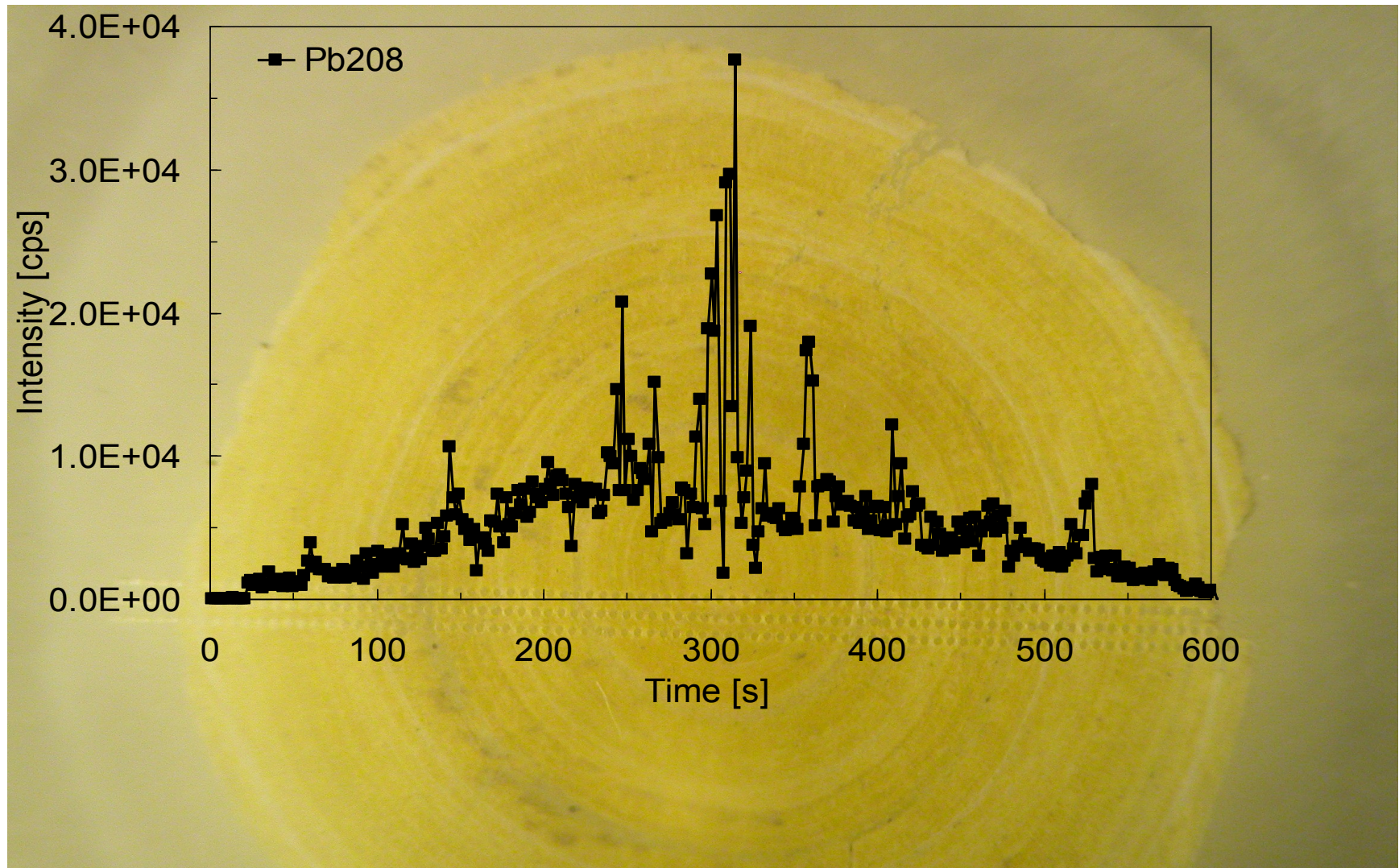
Calibration Zn, Pb, Cu powdered urolith pressed pellets



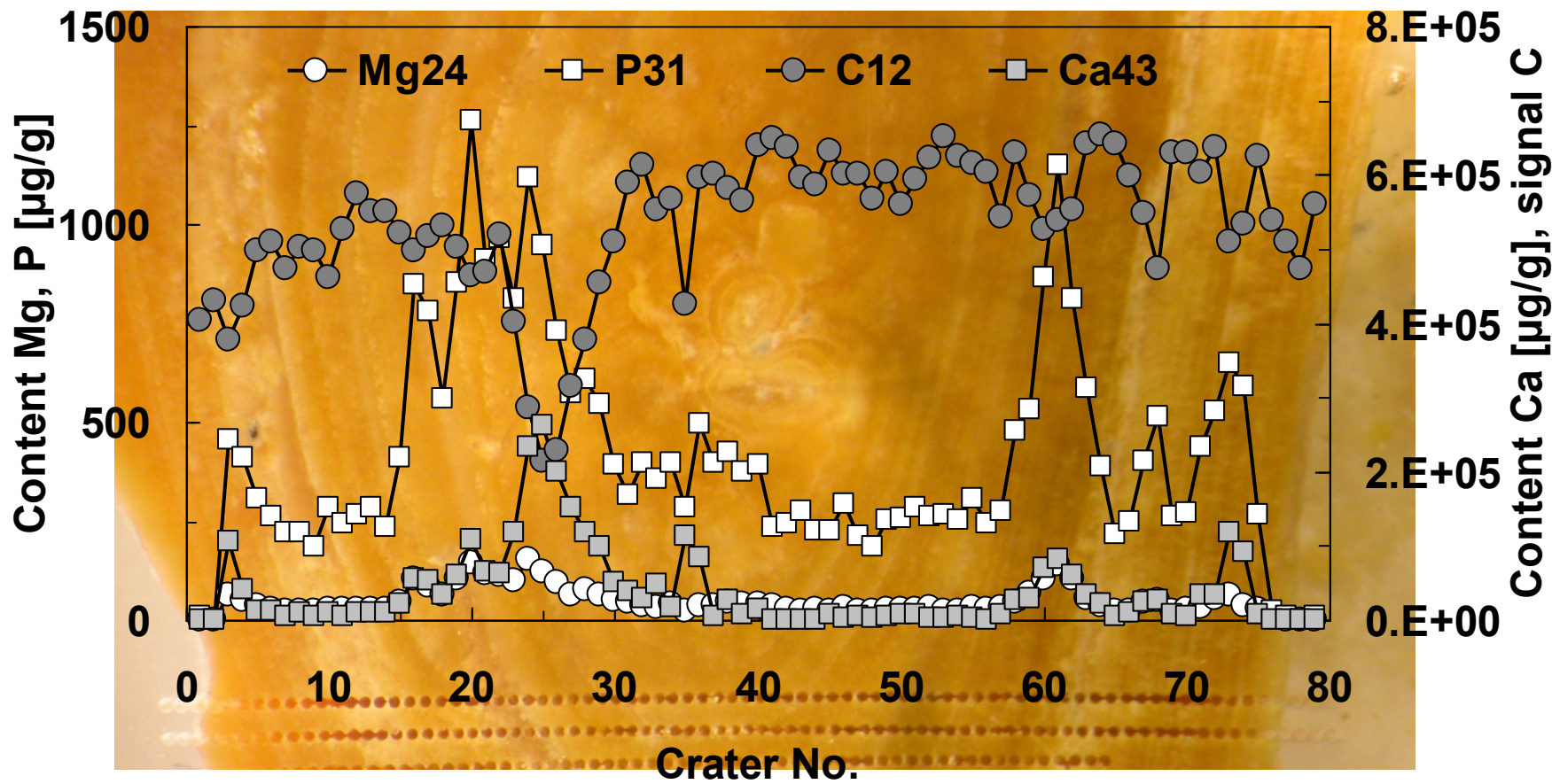
Calibration Ca, P: powdered urolith pressed pellets



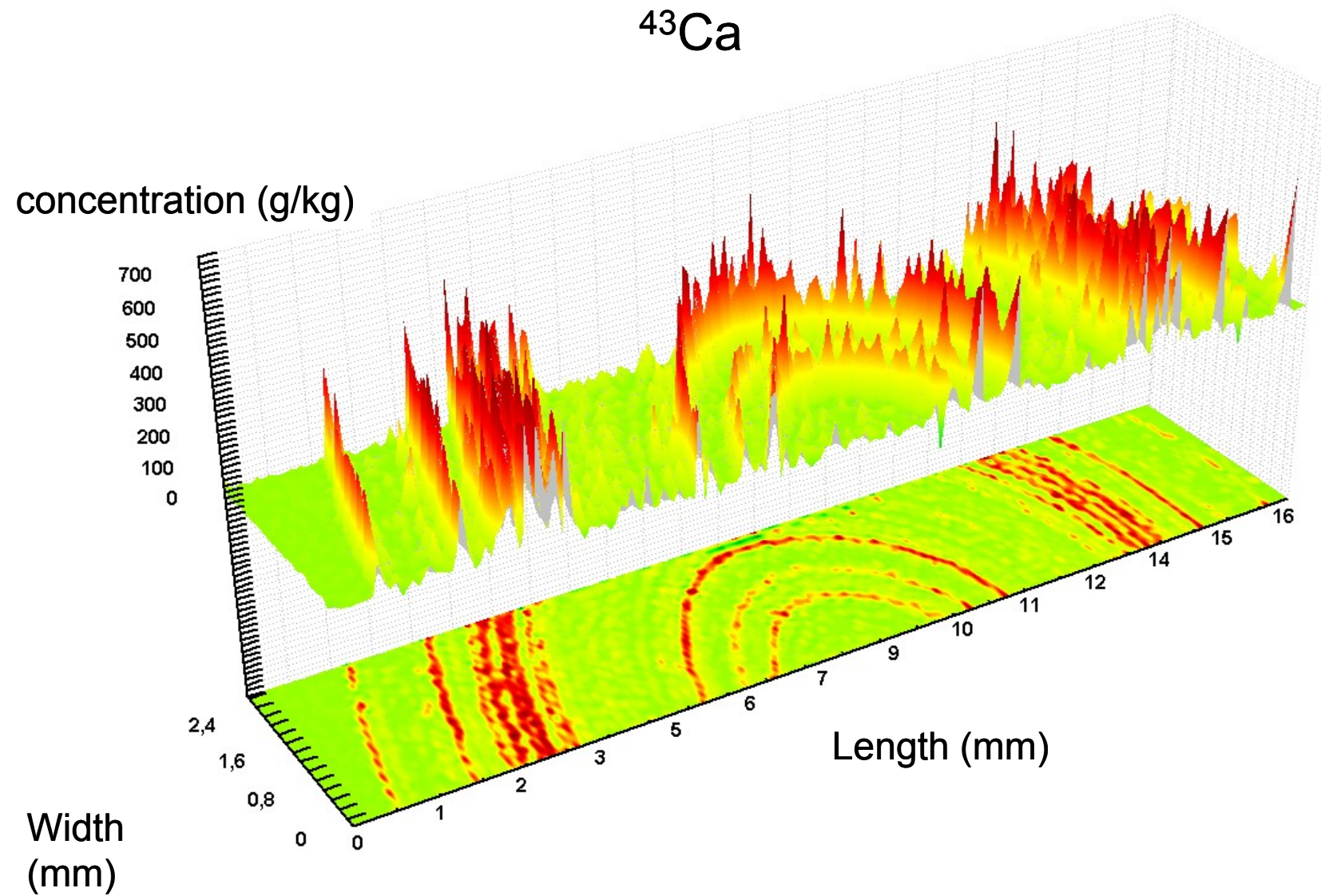
Radial profile of urolith - signal



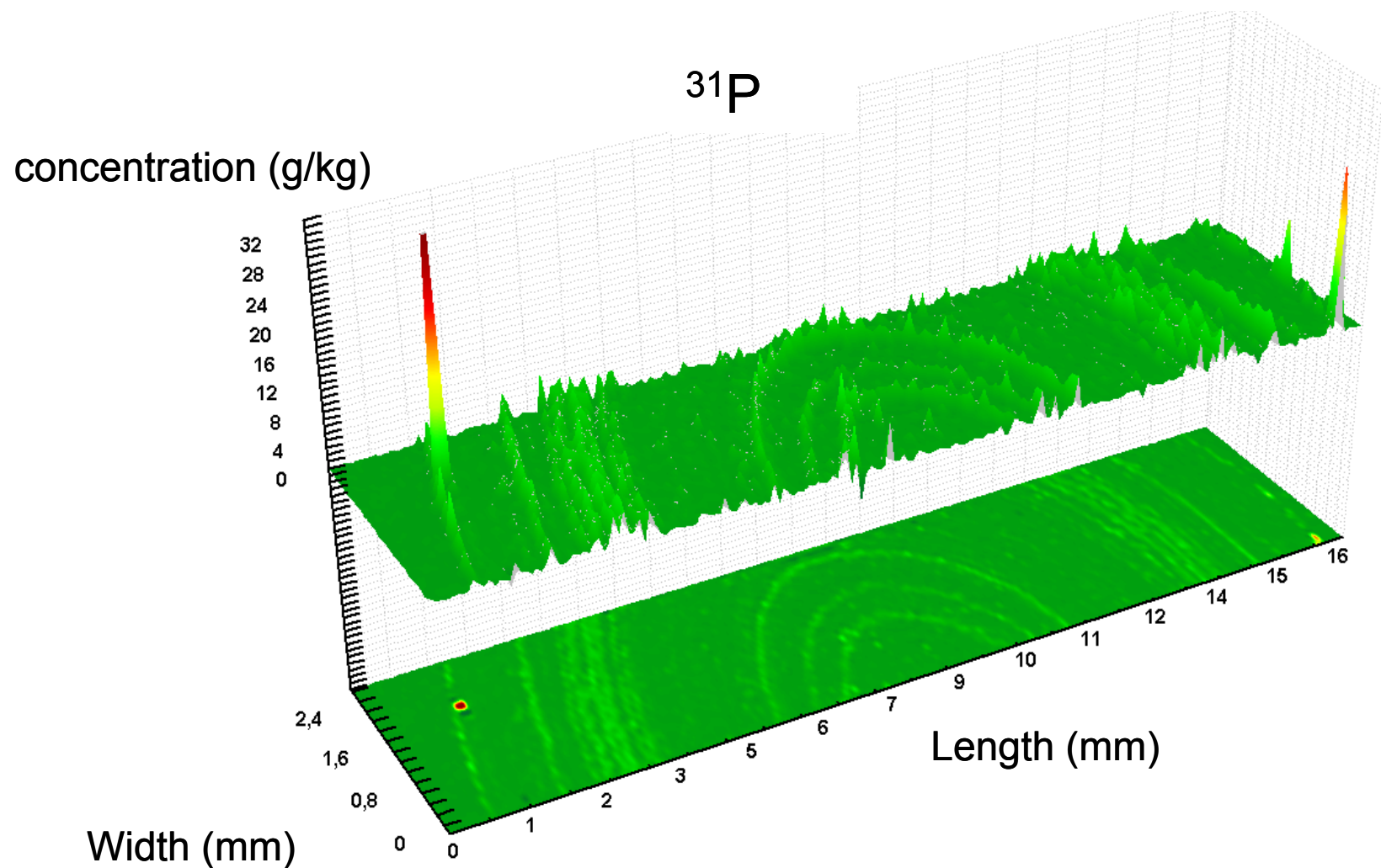
Urolith section, complementarity of apatite and oxalate vs urate, quatification – pressed pellets



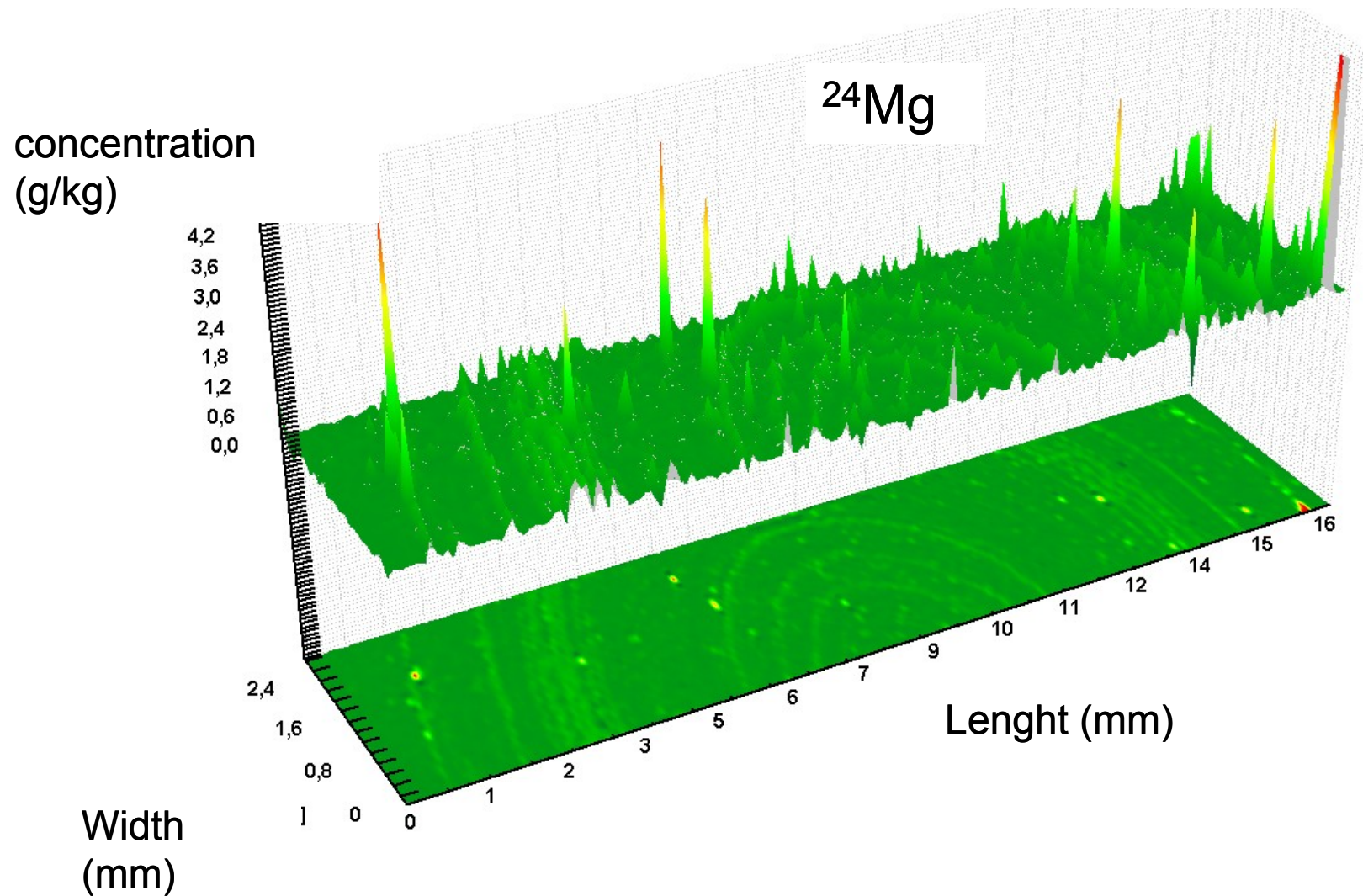
2D graph of distribution of Ca concentration in sample 10806



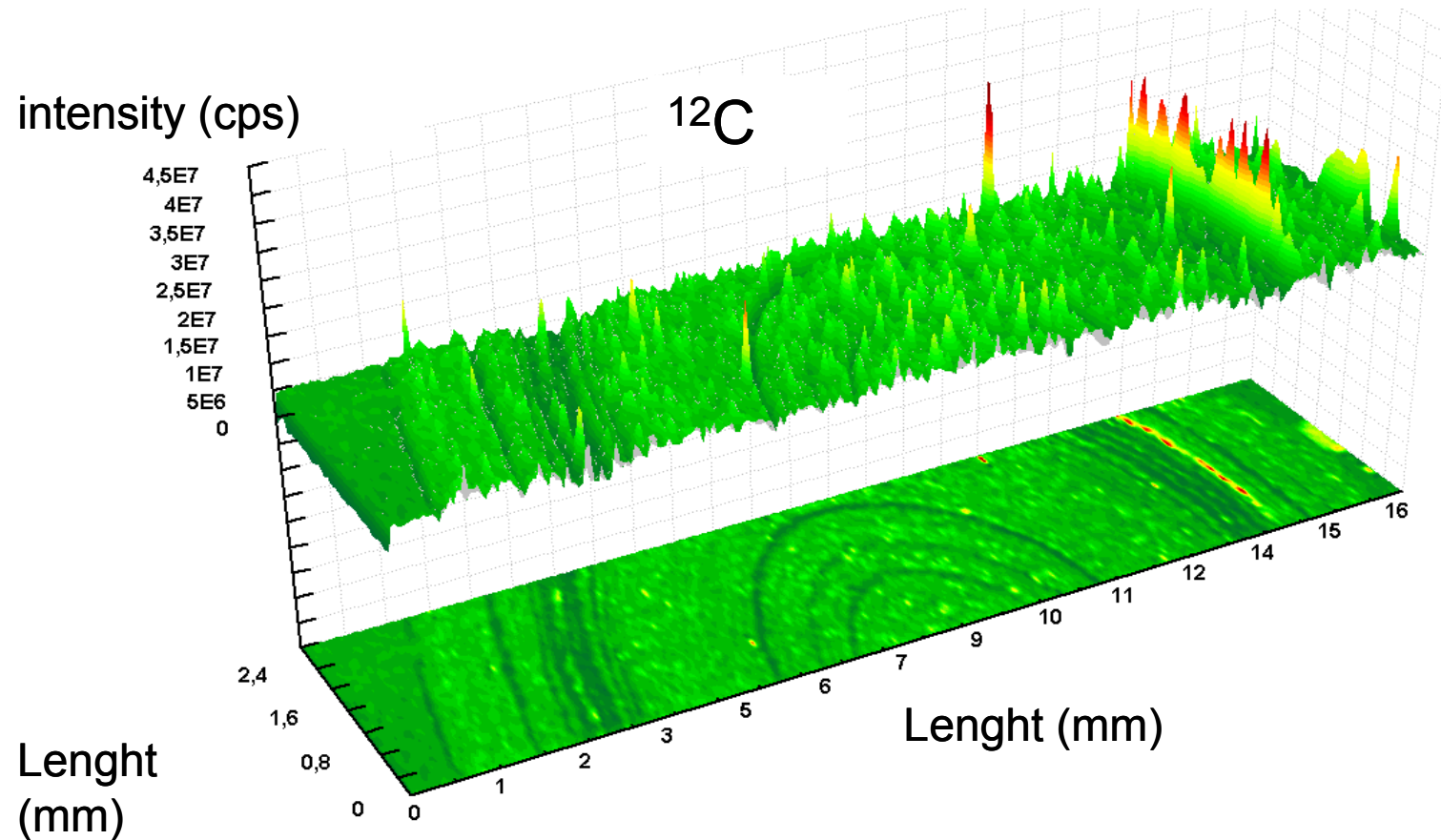
2D graph of distribution of P concentration in sample 10806



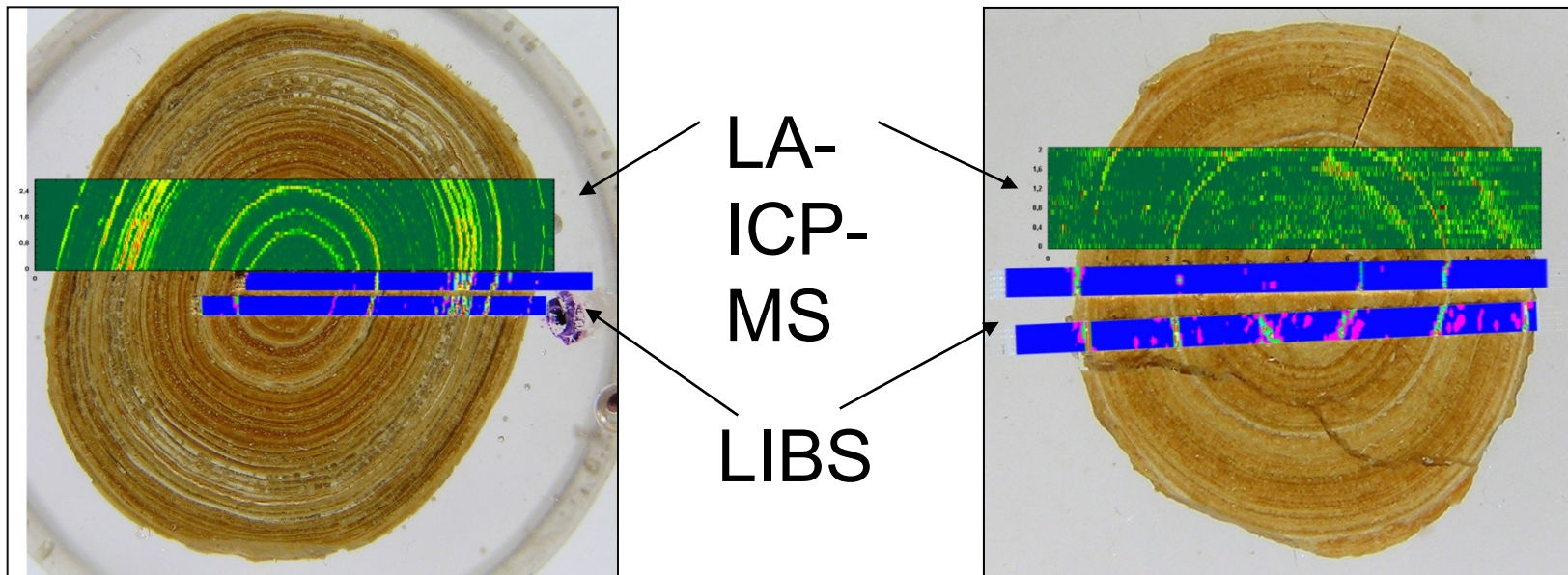
2D graph of distribution of Mg concentration in sample 10806



2D graph of distribution of C presence in sample 10806



Scanned areas of uroliths



Provenance study -Archaeology

- Application of laser ablation–based methods and multivariate statistics to provenance studies of artifacts

OUTLINE

- Archaeometry – study of artifacts
- Application of LA-ICP-MS to study of obsidian artifacts
 - Samples
 - LA-ICP-MS analysis
- Statistical treatment of data

ARCHAEOOMETRY

- **Archaeological science** or Archaeometry consists in the application of techniques of natural sciences to the analysis of archaeological materials.
 - Archaeometry involves dating and studying ancient materials. [1]
1. Killick, D; Young, SMM (1997). *Archaeology and Archaeometry: From Casual Dating to a Meaningful Relationship?*. Antiquity.

Archaeometry

Comprises: [2]

- **physical and chemical dating methods**
- **artifact studies**
- **environmental studies** on past landscapes, climates, flora, fauna; the diet, nutrition and health of beings
- **mathematical methods** for data treatment
- **remote sensing and geophysical survey** for the location and characterization of buried features
- **conservation sciences** for the study of decay processes; development of methods for conservation
- techniques such as lithic analysis, archaeometallurgy, paleoethnobotany, palynology, zooarchaeology

2.Tite, M.S. (1991) Archaeological Science - past achievements and future prospects. *Archaeometry* **31** 139-151.

Artifact studies

- **XRF** X-ray fluorescence spectrometry
- **ICP-MS** inductively coupled plasma mass spectrometry
- **NAA** neutron activation analysis
- **SEM** scanning electron microscopy
- **LIBS** laser induced breakdown spectrometry

Provenance analysis

has the potential to determine the original source of the materials used to make a particular artifact.

APPLICATION OF LA-ICP-MS IN ARCHAEOOMETRY – ANALYSIS OF OBSIDIAN ARTIFACTS

- Obsidian is a naturally occurring volcanic glass formed as an extrusive igneous rock.
- It is produced when felsic lava extruded from a volcano cools rapidly without crystal growth.
- Because of this lack of crystal structure, obsidian blade edges can reach nearly molecular thinness:
 - ancient use as projectile points and blades
 - modern use as surgical scalpel blades

Obsidians: rock and artifact

- a glassy volcanic rock, homogeneous in bulk & surface, reflecting the volcanic environment where it was produced;
- raw material for prehistoric people (paleolith, neolith, 9 000 B.C. Mesopotamia, later Mayas, Aztecs) because of the ability to produce extremely sharp cutting edge;
- study of composition of obsidian tools and material from the original geological source makes it possible to learn about:
 - exchange centers, trade routs;
 - organization of life (hunting, craft)



Viničky, Slovakia

E. Švecová: Bachelor thesis, Sources of obsidian in Central Europe and possibilities of their differentiation, Masaryk University, 2009.



Kašov, Slovakia

Chemical analysis of obsidians

- chemical analysis can yield information on composition of both natural sources and artifacts
- solution analysis can be performed for raw material **✗** artifacts
- non- destructive analysis is required for artifacts: (XRF, NAA, LA-ICP-MS, LIBS)
- LA-ICP-MS: quasi non-destructive, simple sample preparation, applicable to small samples (1 mm), relatively rapid determination

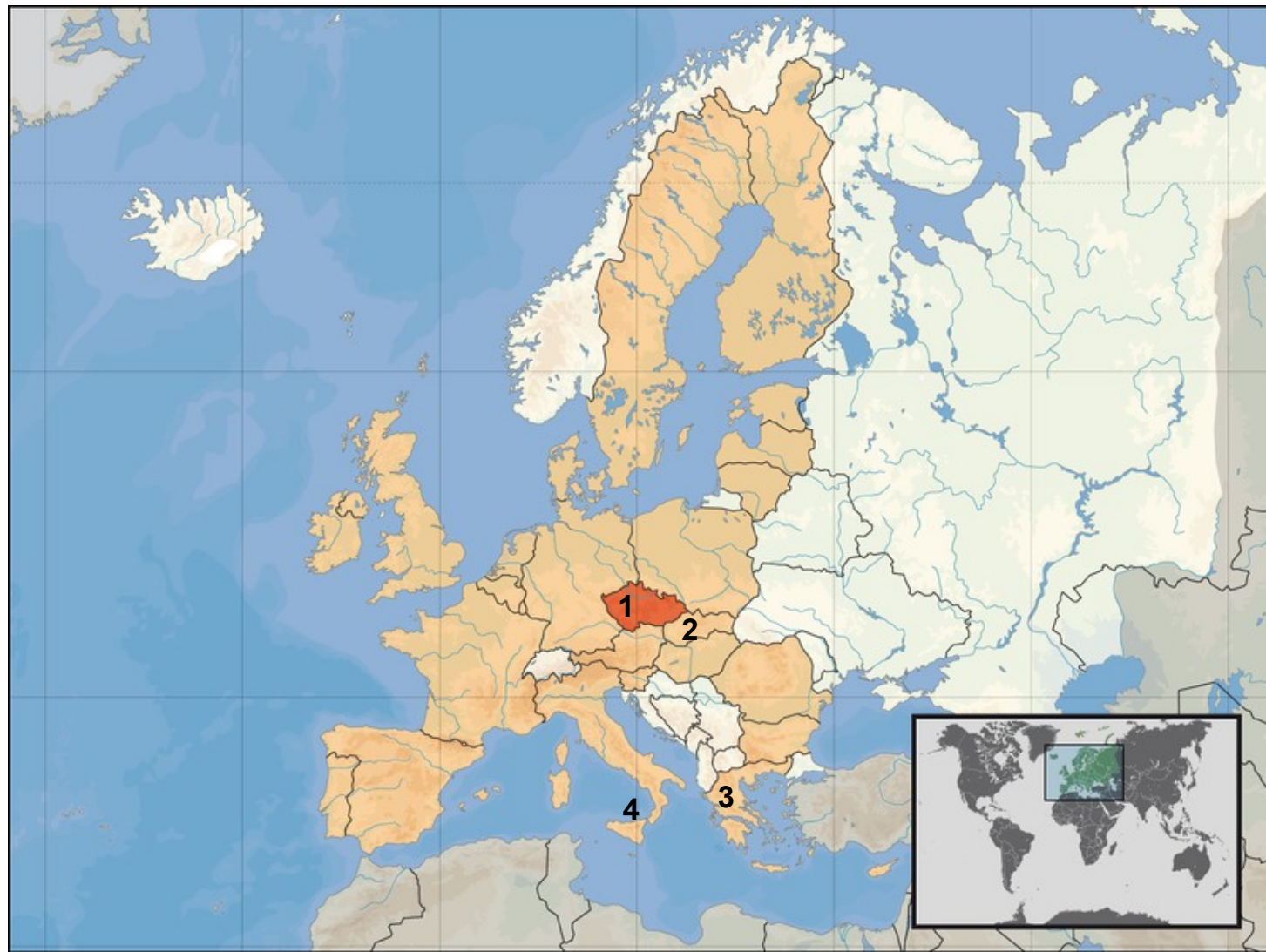
LA-ICP-MS analysis of obsidians

- LA-ICP-MS is used for analysis of obsidians
3. Eerkens J. W., Spurling A. M., Gras M. A., Measuring prehistoric mobility strategies based on obsidian geochemical and technological signatures in the Owens Valley, California, *Journal of Archaeological Science* 35 (2008)668-680.
 4. Whitaker A. R., Eerkens J. W., Spurling A. M., Smith E. L., Gras M. A., Linguistic boundaries as barriers to exchange, *Journal of Archaeological Science* 36 (2007)1-10.
 5. Gratuze B., Obsidian characterization by LA-ICP-MS and its application to prehistoric trade in the Mediterranean and the Near East: Sources and distribution of obsidian within the Aegean and Anatolia, *Journal of Archaeological Science* 26 (1999)869-881.

AIM OF STUDY

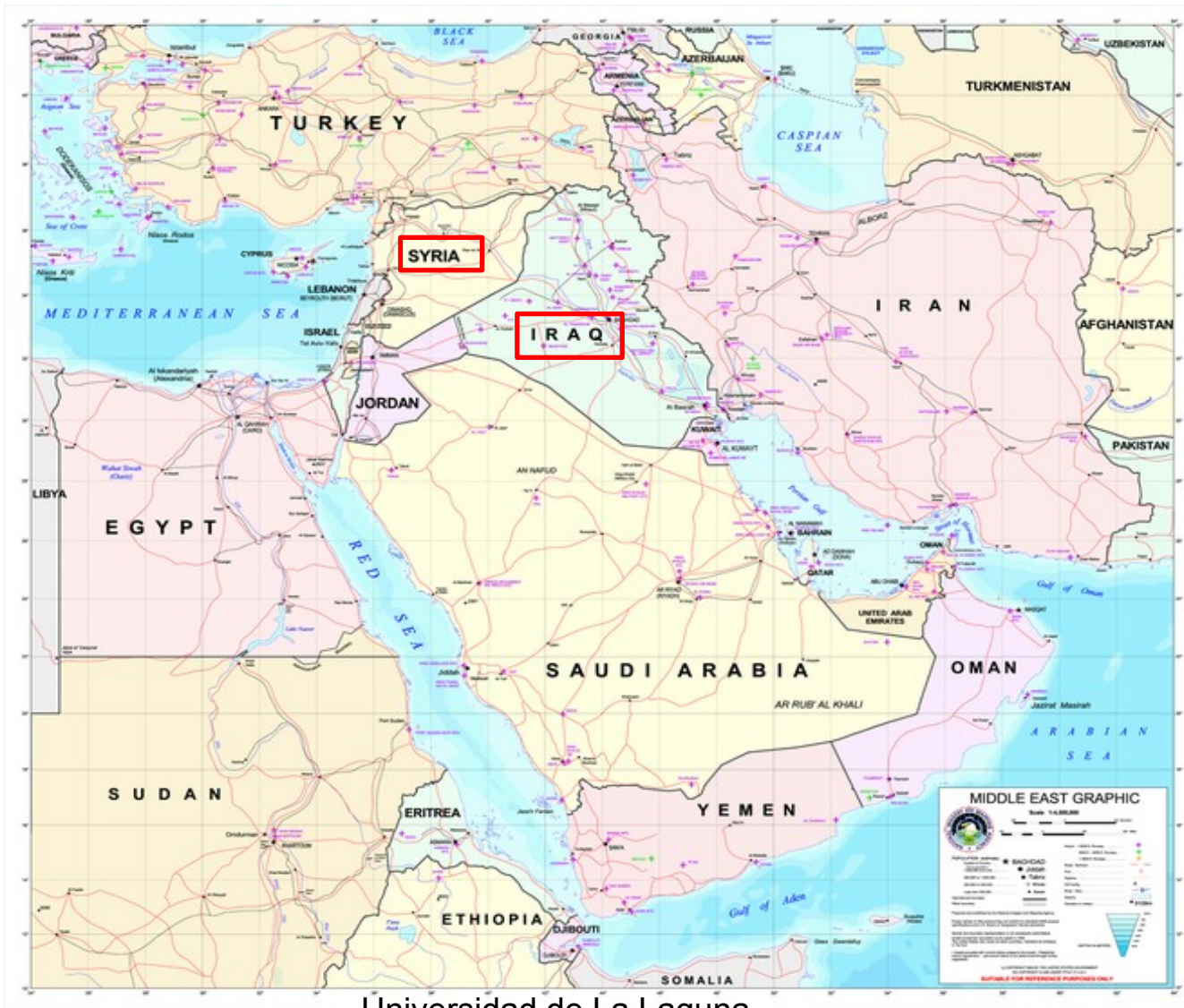
- Development of method LA-ICP-MS
- Analysis of artifacts from various areas
- Selection of elements applicable to distinguish between archaeological sites
- Statistical analysis – distinguishing between areas of archaeological discovery of artifacts

Provenance of samples: 1 – Czech Rep., 2 – Slovakia, 3 – Greece,
4 – Italy, Lipari island





Provenance of samples: Syria, Iraq



List of samples

Czech Republic	Slovakia	Syria	Nicaragua	
artifacts	artifacts	artifacts	artifacts	
Breznik	Kasov I	Tell Arbid I	Sebaco	
Horakov	Kasov II	Tell Arbid II	Somoto I	
Jaromerice	source	Tell Arbid III	Somoto II	
Moravske Branice	Barca			
Nova Dedina	Vinicky			
Popuvky	Mala Bara			
Prstice				
Rozdrojovice				
Sptyihnev	Iraq	Greece	Italy	Mexico
Tesetice I	artifacts	artifact	artifact	source
Tesetice II	Tell Asmar I	Sesklo	La Castagne	
U Kr. Borovice	Tell Asmar II		(Lipari)	
Zebetin				

Composition of obsidians

ACME reference analysis

%	Barca	Lipari	Vinicky
SiO ₂	75.83	73.32	75.89
Al ₂ O ₃	13.17	13.20	13.22
Fe ₂ O ₃	1.05	1.77	0.98
CaO	0.82	0.87	0.82
MgO	0.12	0.05	0.07
Na ₂ O	3.65	4.04	3.66
K ₂ O	4.56	5.27	4.57
TiO ₂	0.05	0.08	0.05
P ₂ O ₅	0.03	0.02	0.03
MnO	0.05	0.07	0.05

**Acme Analytical Laboratories (Vancouver) Ltd., 1020 Cordova St. East
Vancouver BC V6A 4A3 Canada, www.acmelab.com**

mg kg^{-1}	Barca	Lipari	Vinicky
Hf	2.8	6.4	2.8
Nb	9.9	35.0	9.7
Rb	188.2	305.3	191.1
Sr	74.1	19.3	72.9
Ta	1.5	2.4	1.5
Th	16.6	58.7	17
U	10	16.9	9.9
Zr	75.4	178.4	71.2
Y	33.8	41.0	33.7
La	25.6	63.3	25.8
Ce	49.5	127.5	49.1
Pr	6.05	13.04	6.05
Nd	21.9	43.9	21.5
Sm	4.28	8.20	4.27
Eu	0.34	0.14	0.37
Gd	4.04	6.41	4.07
Tb	0.82	1.15	0.81

LA-ICP-(Q)MS

Ablation system – UP 213 Nd:YAG (New Wave, USA)

- ablation chamber – SuperCell 20 cm³ (New Wave, USA)
- diameter of ablation craters – 100 µm;
- laser repetition rate 20 Hz;
- fluence 5 J cm⁻²;
- 1 l/min He carrier through ablation cell
- data acquisition: 120 s (50 s ablation), 10 spots



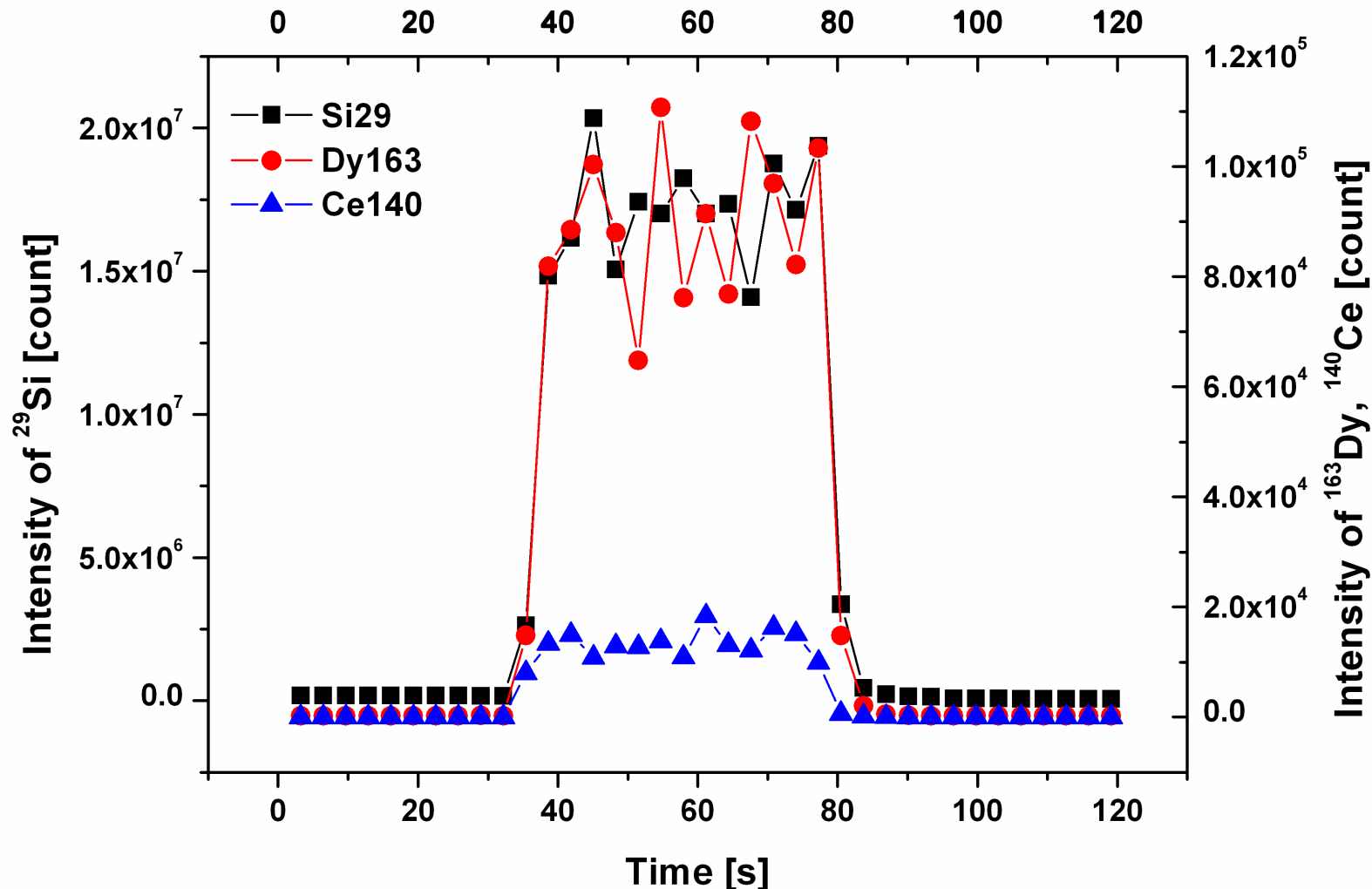
ICP-MS Agilent 7500 CE (Agilent, Japan)

- carrier gas flow 0.6 l/min Ar
- collision-reaction cell: He 5,5 ml/min and H₂ 2,5 ml/min



Calibration
NIST 612
NIST 610

ICP-(Q)MS signal



Vinicky, Slovakia: SiO_2 75.89 %, Dy 4.58 mg kg^{-1} , Ce 49.1 mg kg^{-1} (ACME)

LA-ICP-(TOF)MS

Ablation system – UP 213 Nd:YAG (New Wave, USA),

- ablation chamber – SuperCell 20 cm³ (New Wave, USA);
- diameter of ablation craters – 100 µm;
- laser repetition rate 10 Hz;
- fluence 16 J cm⁻²;
- 300 ml/min He carrier through ablation cell
- data acquisition: after 5 s sample uptake 1 second measurement in 5 spots.

ICP-MS – OptiMass 8000 (GBC Australia)

- plasma gas flow 10 l/min Ar
- auxiliary gas flow 0.5 l/min Ar
- nebulizer gas flow 1.02 l/min Ar
- sampling depth 10 mm

Calibration
NIST 614
NIST 612
NIST 610
NIST GB

22.5.2012

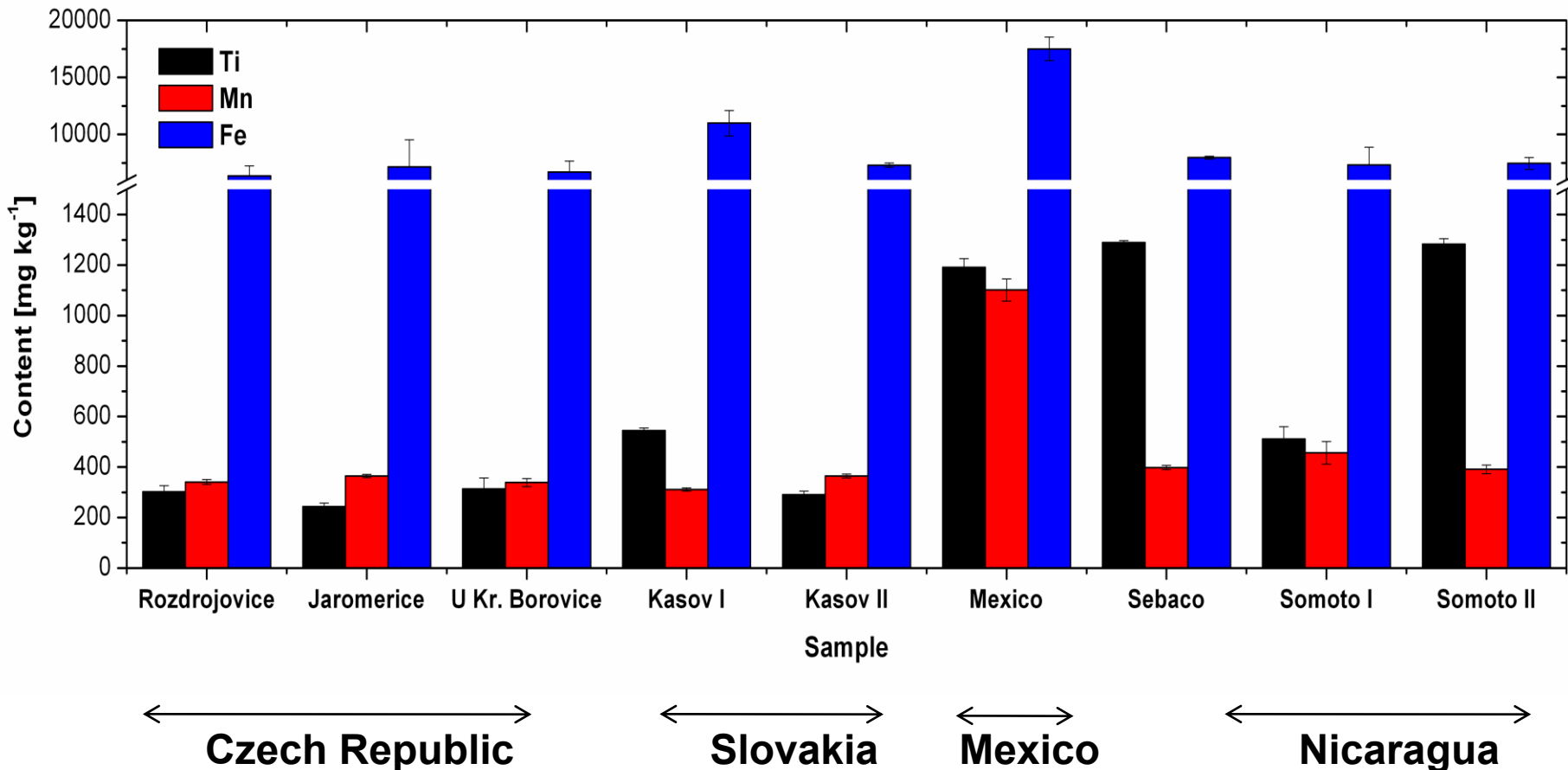


Universidad de La Laguna

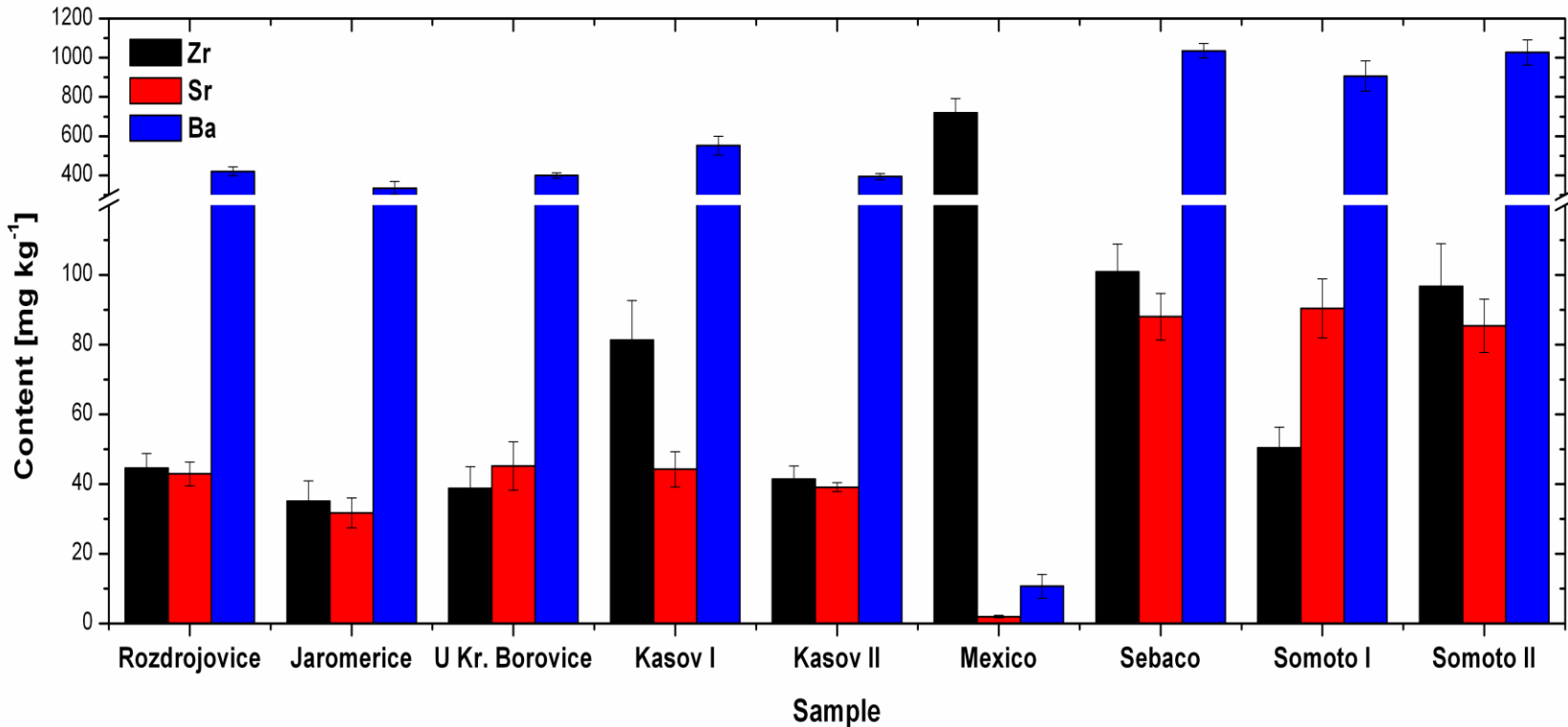


115

Content of Ti, Mn, Fe obtained by LA-ICP-MS



Content of Zr, Sr, Ba obtained by LA-ICP-MS



↔

Czech Republic

↔

Slovakia

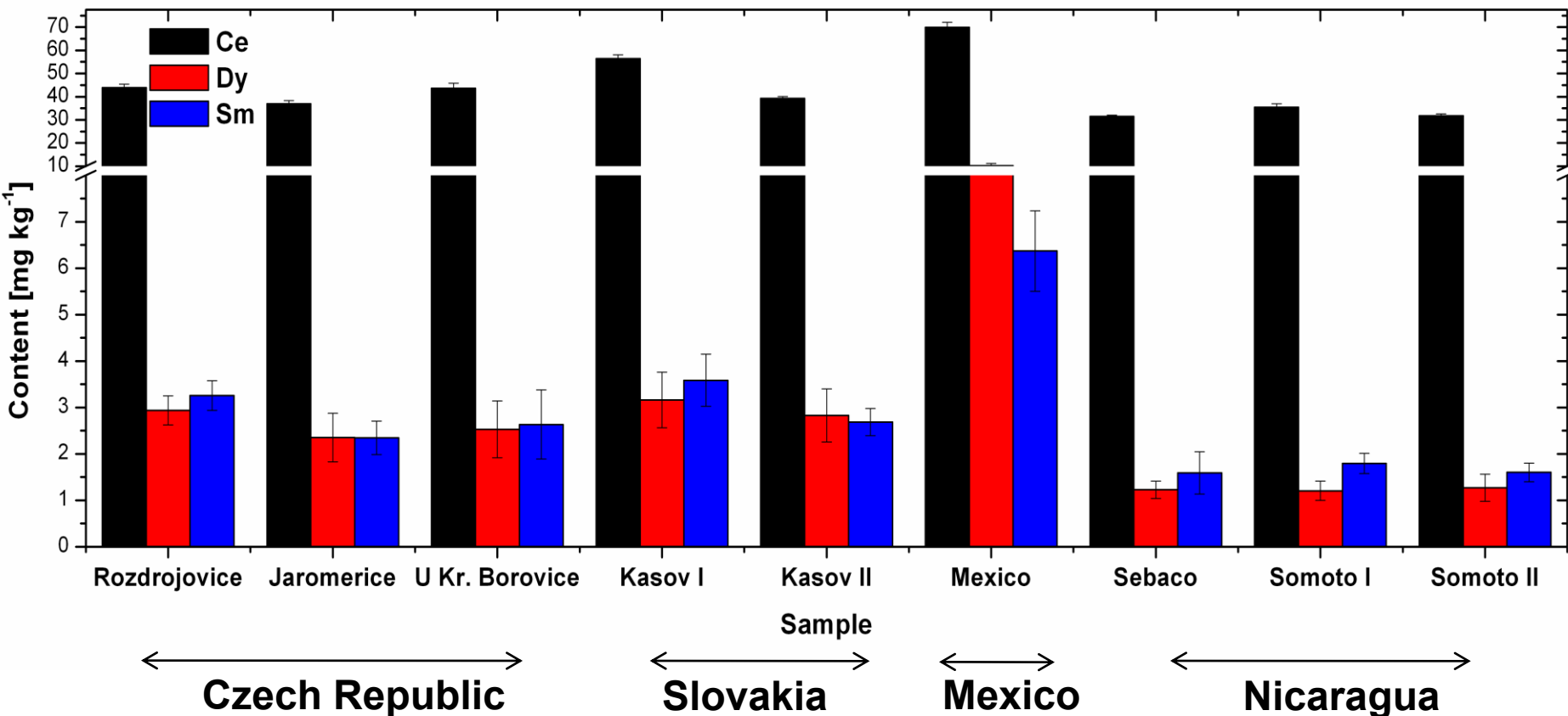
↔

Mexico

↔

Nicaragua

Content of Ce, Dy, Sm obtained by LA-ICP-MS



LA-ICP-MS vs. ACME

Vinicky obsidian sample

Element	Literature	ACME	LA-ICP-MS
	mg kg ⁻¹		
Y	35	33.70	32.71
Zr	66	71.20	60.33
La	24.4-30.4	25.80	25.54
Ce		49.10	55.20
Pr		6.05	5.78
Sm	3.68-4.32	4.27	4.14
Eu	0.41-0.52	0.37	0.38
Gd		4.07	4.27
Tb	0.44-0.84	0.81	0.73
Yb	2.82-3.65	2.96	2.96

STATISTICAL ANALYSIS

R –statistical package (<http://cran.r-project.org/>), released under the GNU General Public License.



Two-way cluster analysis: data matrix is reordered after the results of cluster analysis on objects (samples) and variables (elements). The output of this method is „heat map“.

Principal component analysis: linear transformation of the (correlated) characteristics (elements) of the data matrix into non-correlated principal components. The most information about the variability in original data matrix involved the first PC (see screeplot).

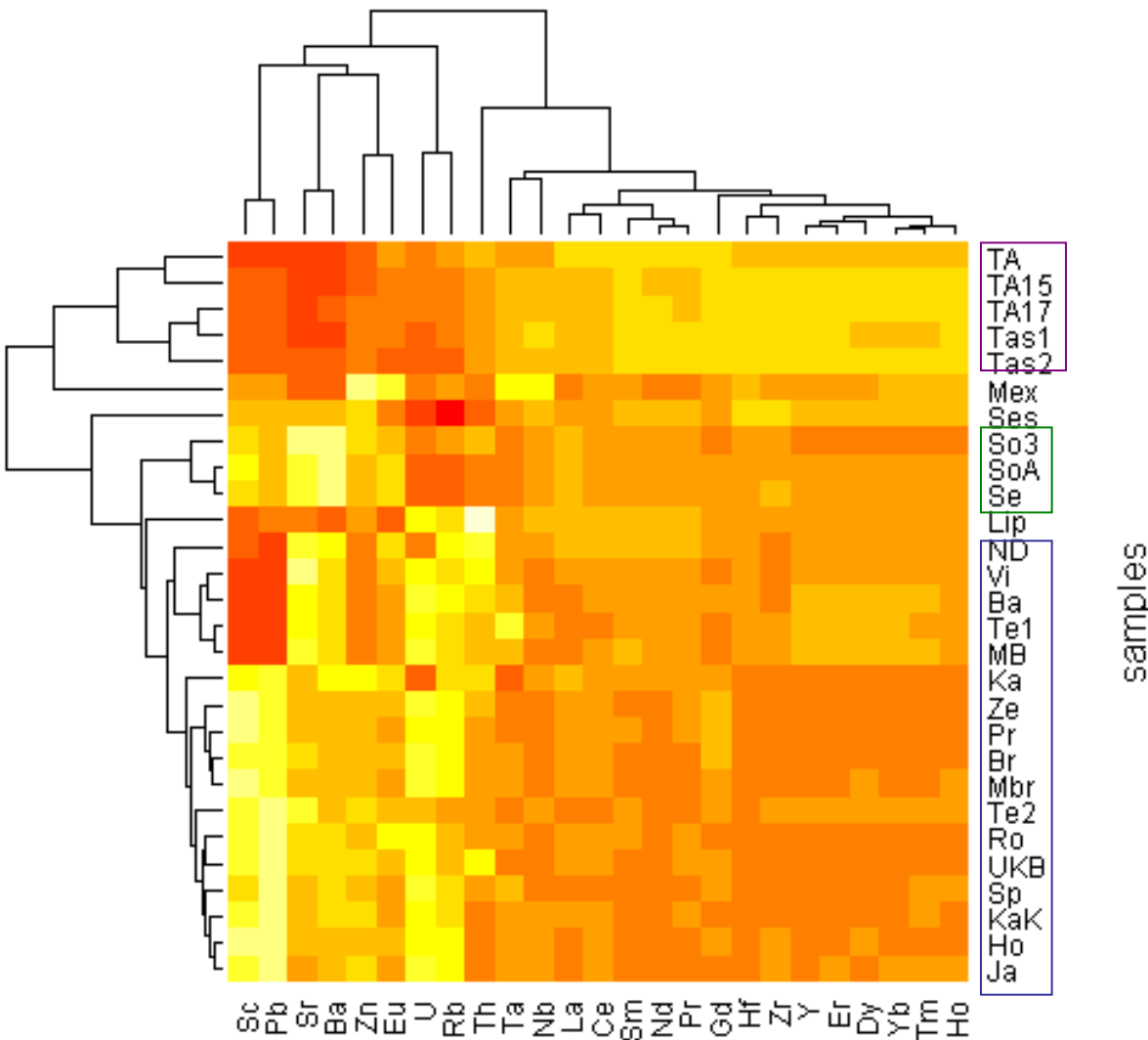
PCA Loadings: reflects the relations between the original variables and between the original variables and principal components. Cosines of the angles in the plot of the PCA loadings are related to the correlation coefficients.

PCA Scores: the coordinates of the objects (samples) in the space of PCs.

Statistical analysis

- **Correspondence analysis (CA):** the method is commonly used for analysis of categorical data, but may be useful as a visualization technique for the analytical data. The method is similar to PCA, but in CA the data are transformed to the „compositional data“ (vectors of proportions describing the relative contributions of each of the categories to the whole) for both rows and columns of the data matrix. The method enables, contrary to PCA, simultaneous depiction of the results for samples and elements in one plot.
- **The results of Principal Component Analysis and Correspondence Analysis were used for the selection of pairs of elements or their ratios for scatterplots.**

Heat map: two-way cluster analysis

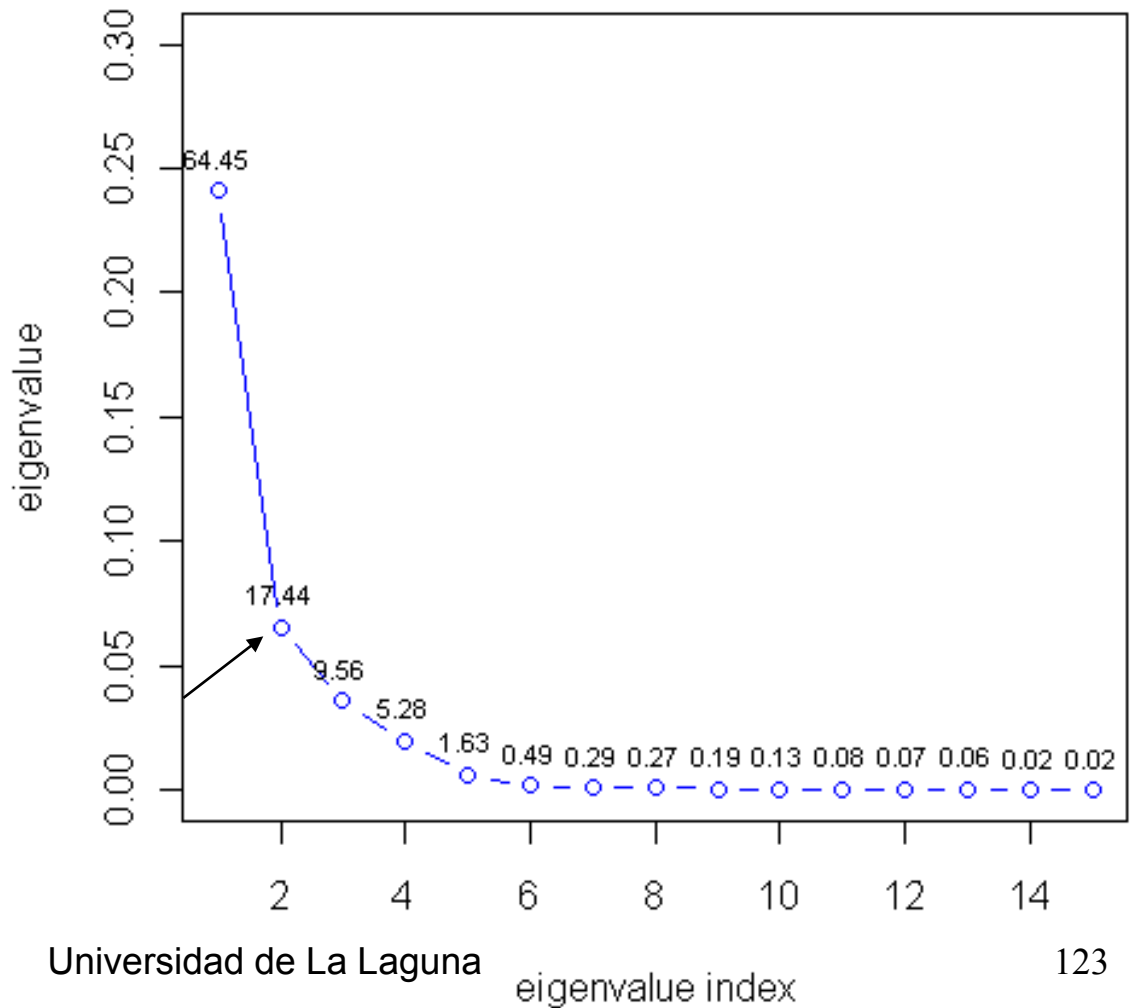


Results of two-way cluster analysis of the autoscaled data (manhattan distances, average linkage clustering). The results of cluster analysis are significantly influenced with correlations in the data.

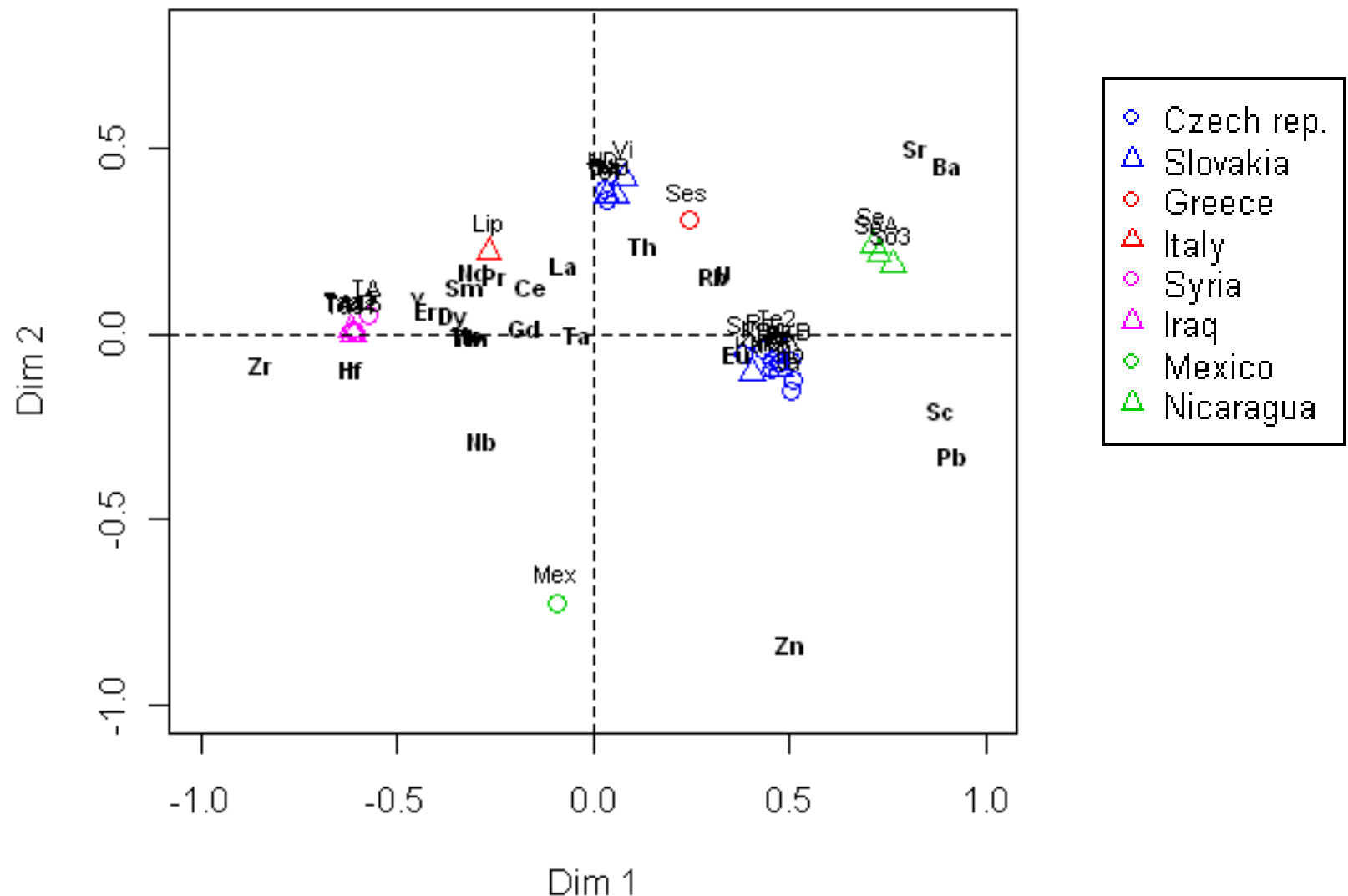
Correspondence analysis (CA)

Correspondence analysis was performed on the mean-normalized data matrix. The breakpoint on the scree plot indicates two important dimensions, involving more than 80 per cent of total inertia of the data.

scree plot (CA)

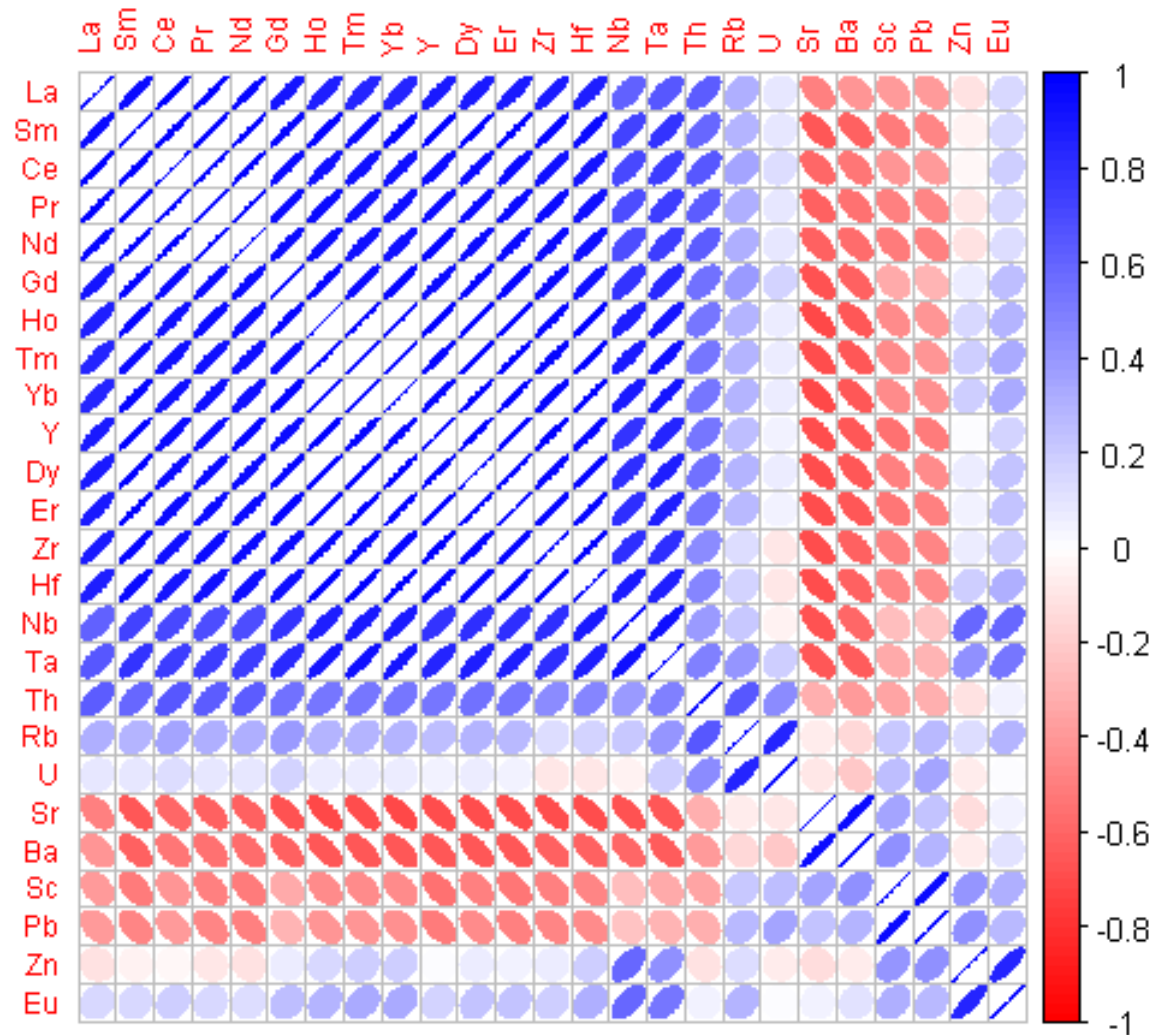


Correspondence analysis (CA)



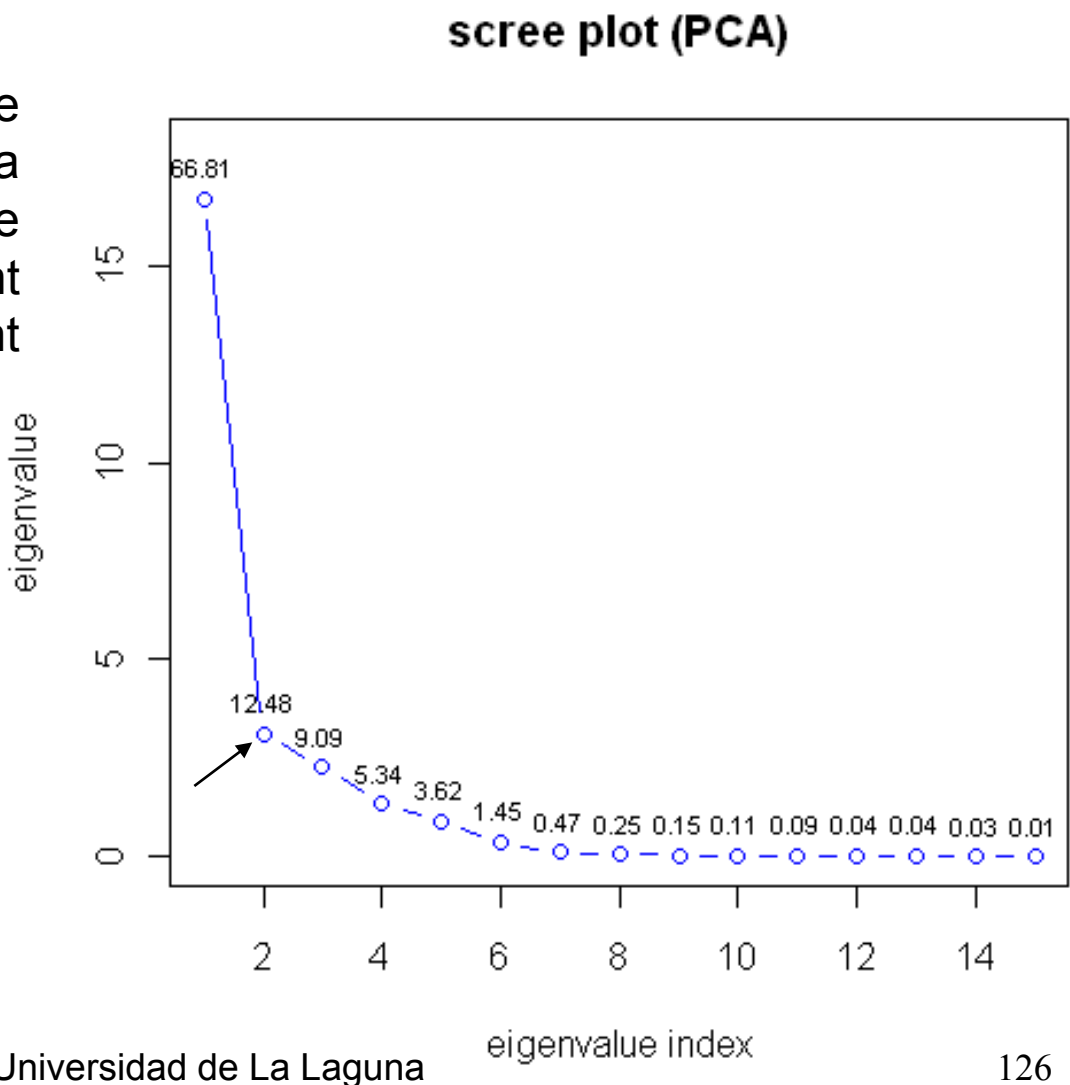
Correlation matrix (Pearson)

Correlation matrix
(Pearson), reordered with
average linkage
clustering.



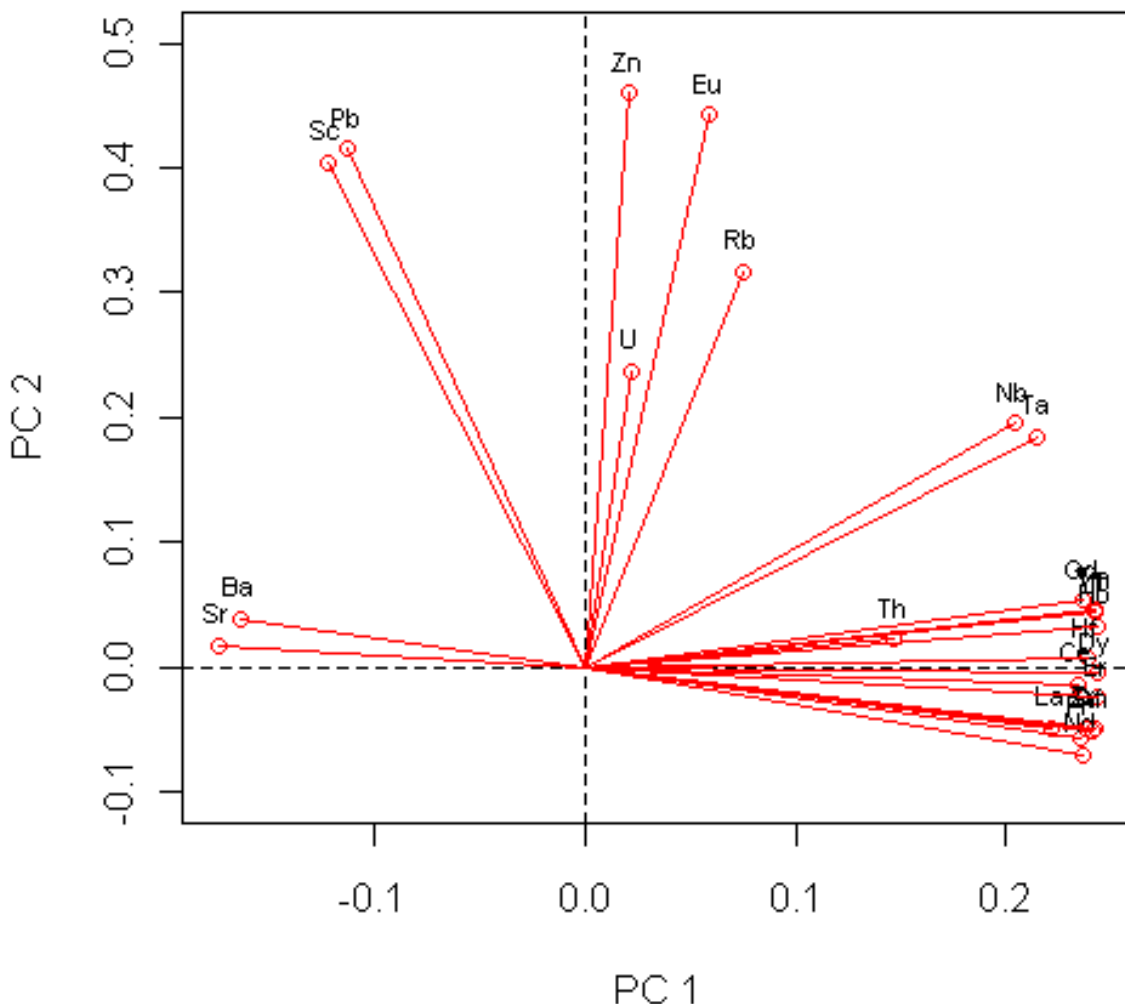
Principal Component Analysis (PCA)

Principal components were calculated from autoscaled data matrix. The breakpoint on the scree plot indicates two important PCs, involving about 80 per cent of total variance of the data.



Principal Component Analysis (PCA)

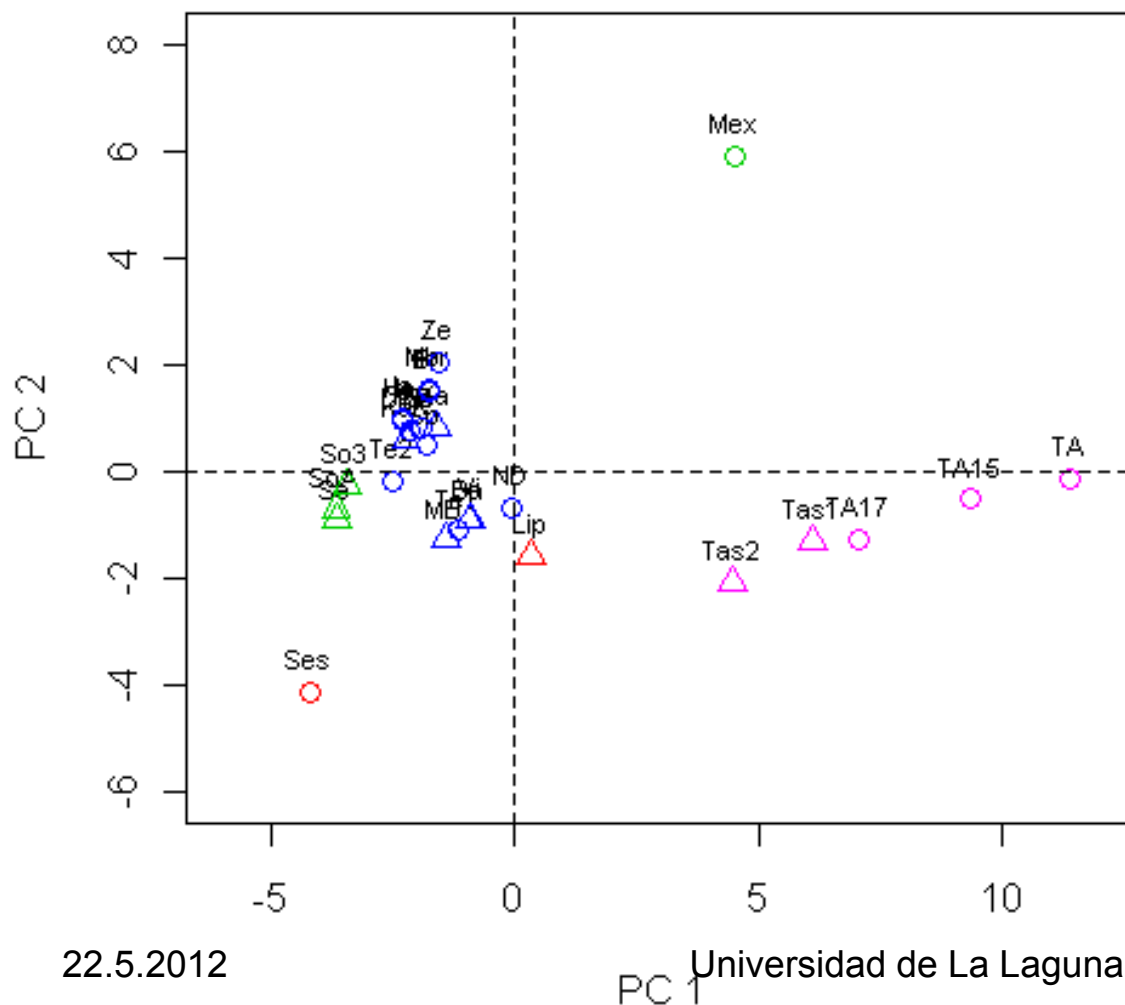
PCA classical (loadings)



PCA loadings reflects correlations of elements in data matrix and contribution of the each element to the each of 2 principal components (cosines of the angles between elements or between elements and axes of PCs, respectively).

Principal Component Analysis (PCA)

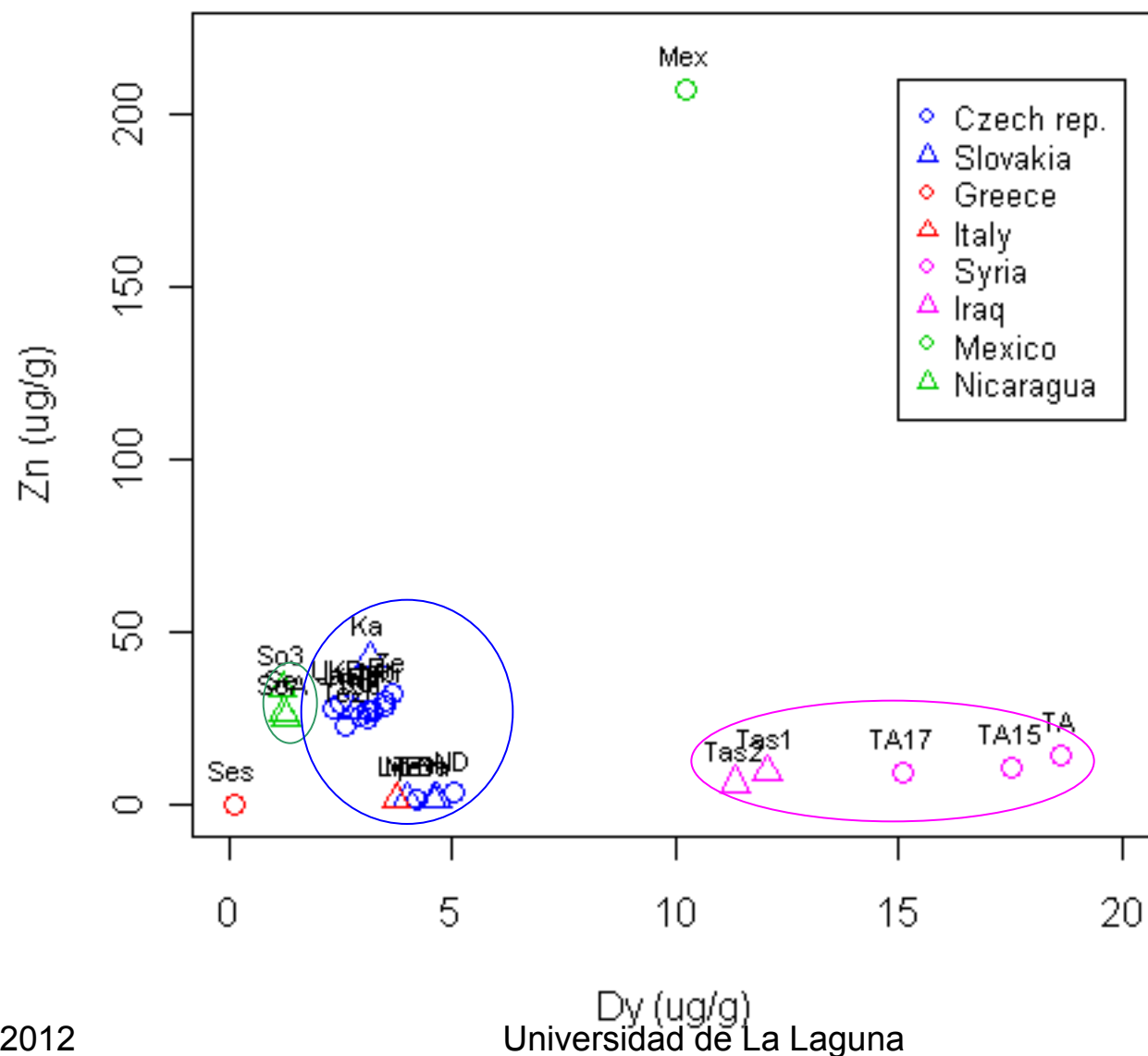
PCA classical (scores)



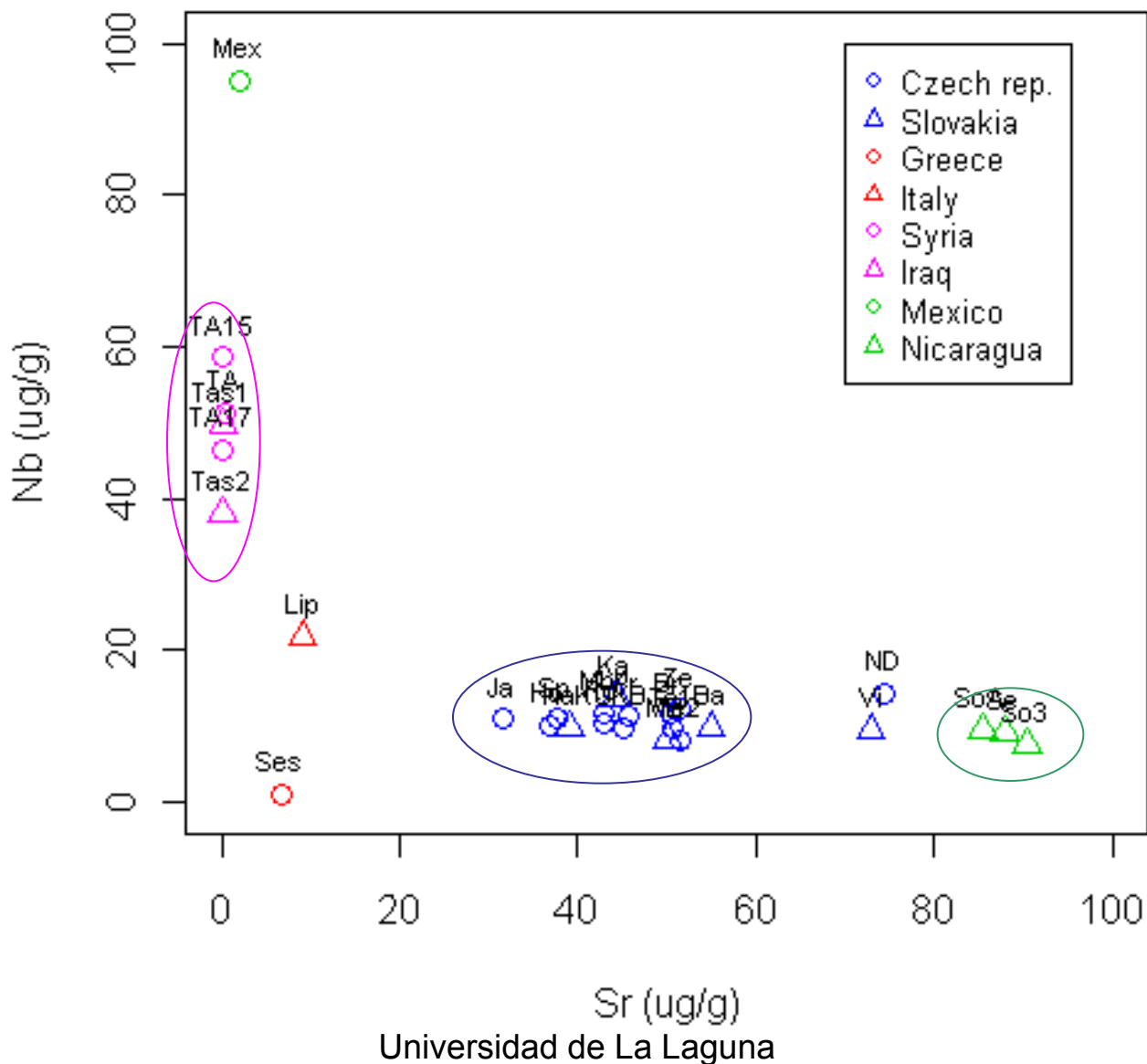
PCA scores are coordinates of the samples in the space of the principal components.

- Czech rep.
 - △ Slovakia
 - Greece
 - △ Italy
 - Syria
 - △ Iraq
 - Mexico
 - △ Nicaragua

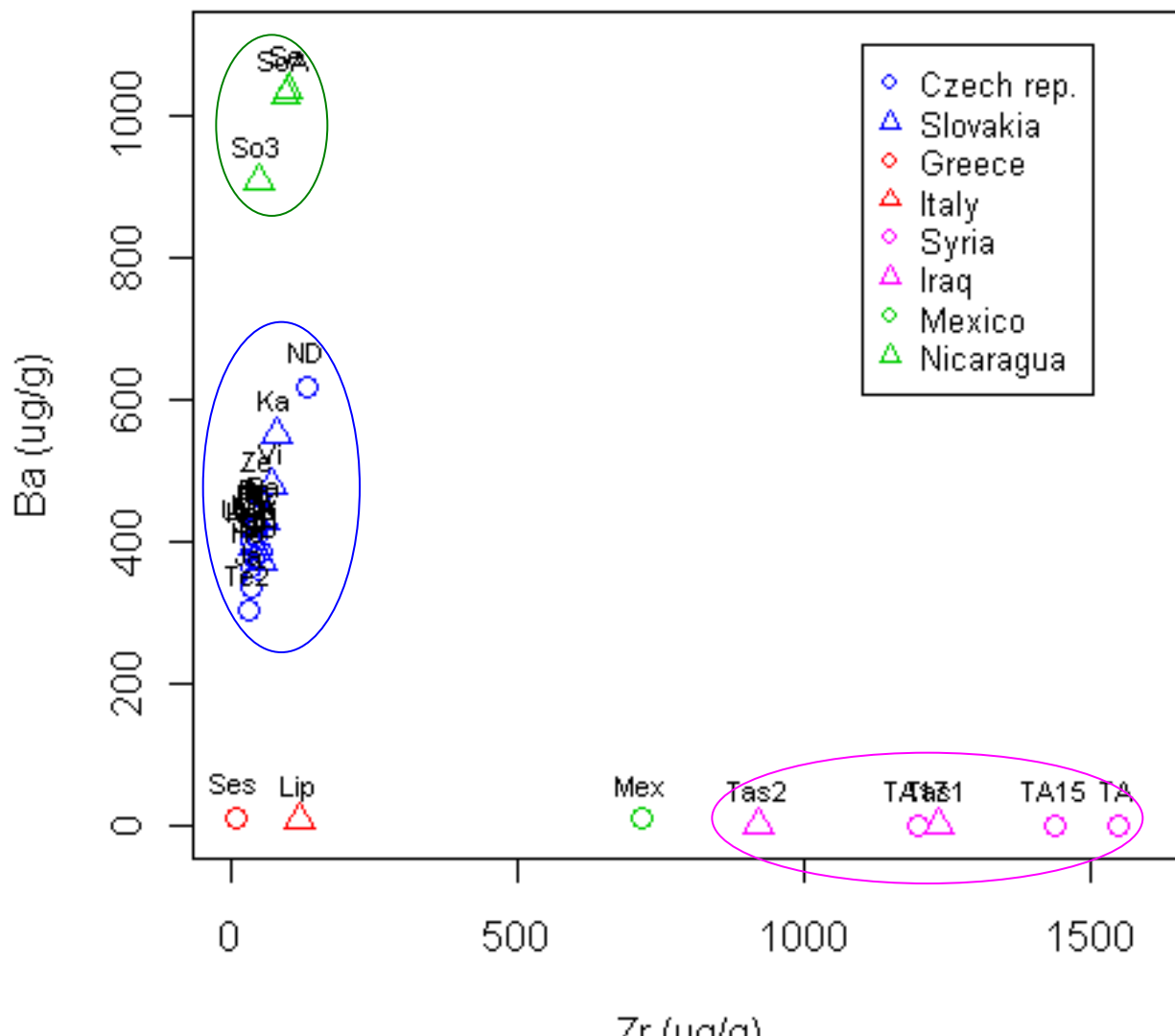
Scatterplot (Dy vs. Zn)



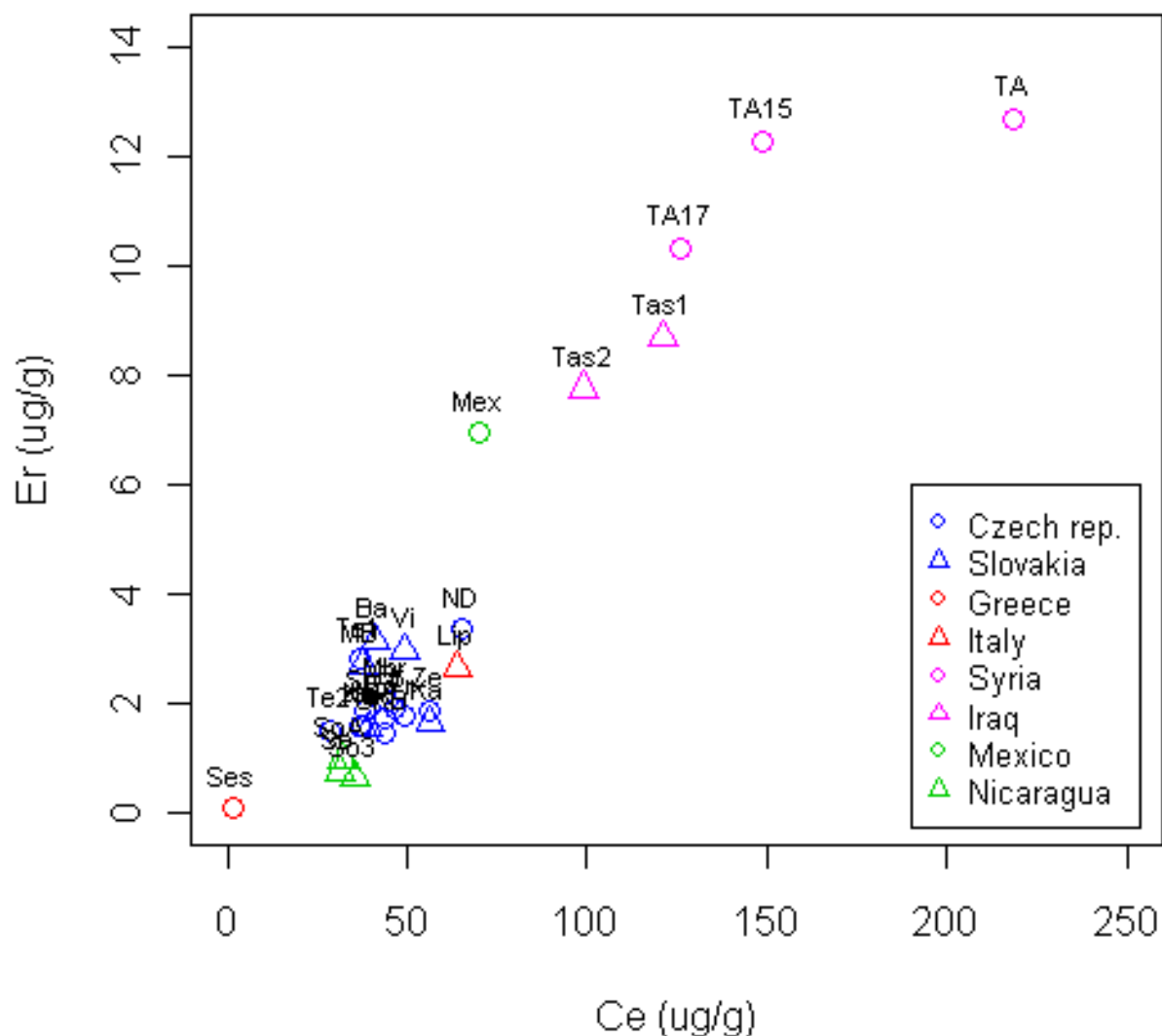
Scatterplot (Sr vs. Nb)



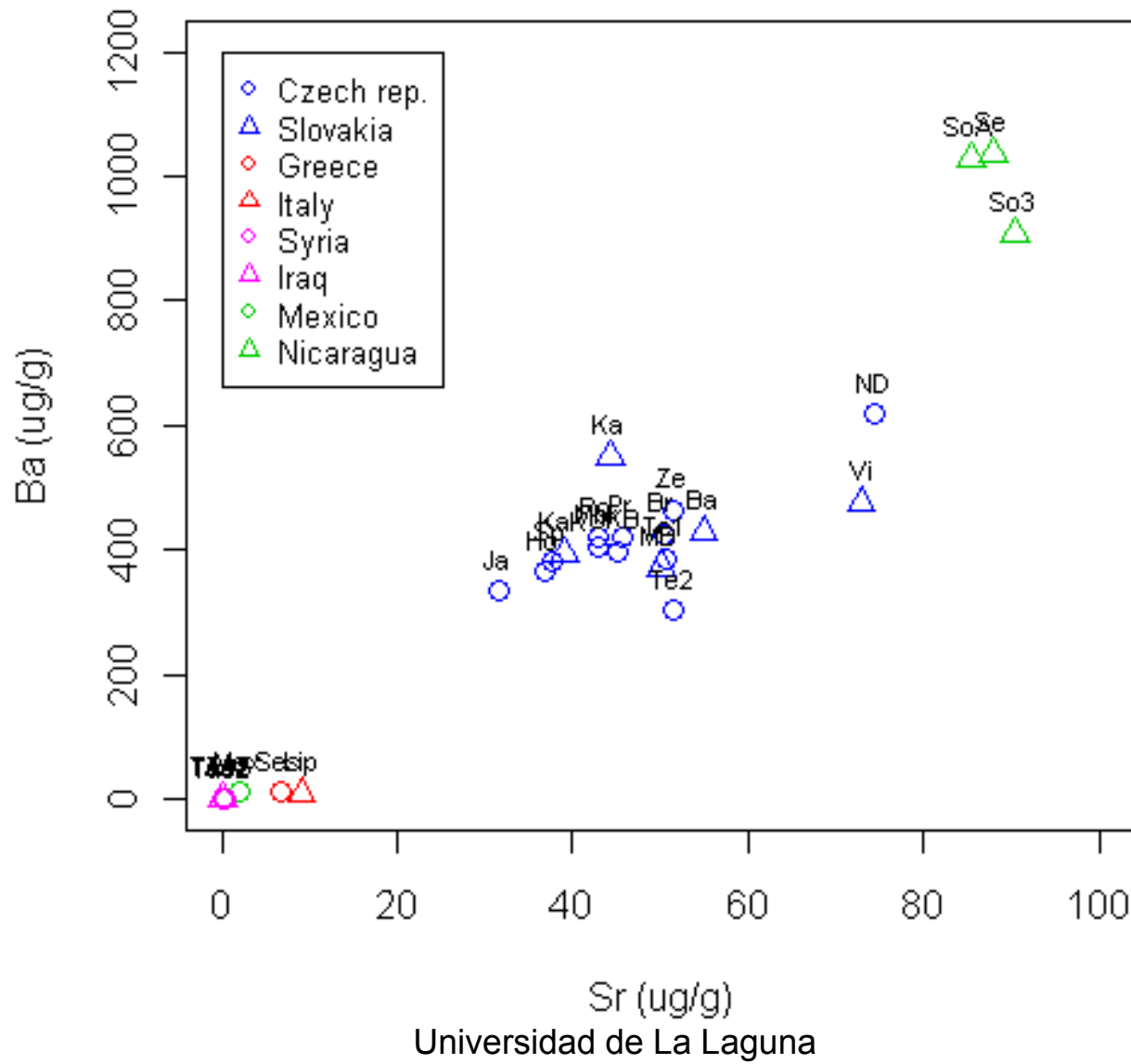
Scatterplot (Zr vs. Ba)



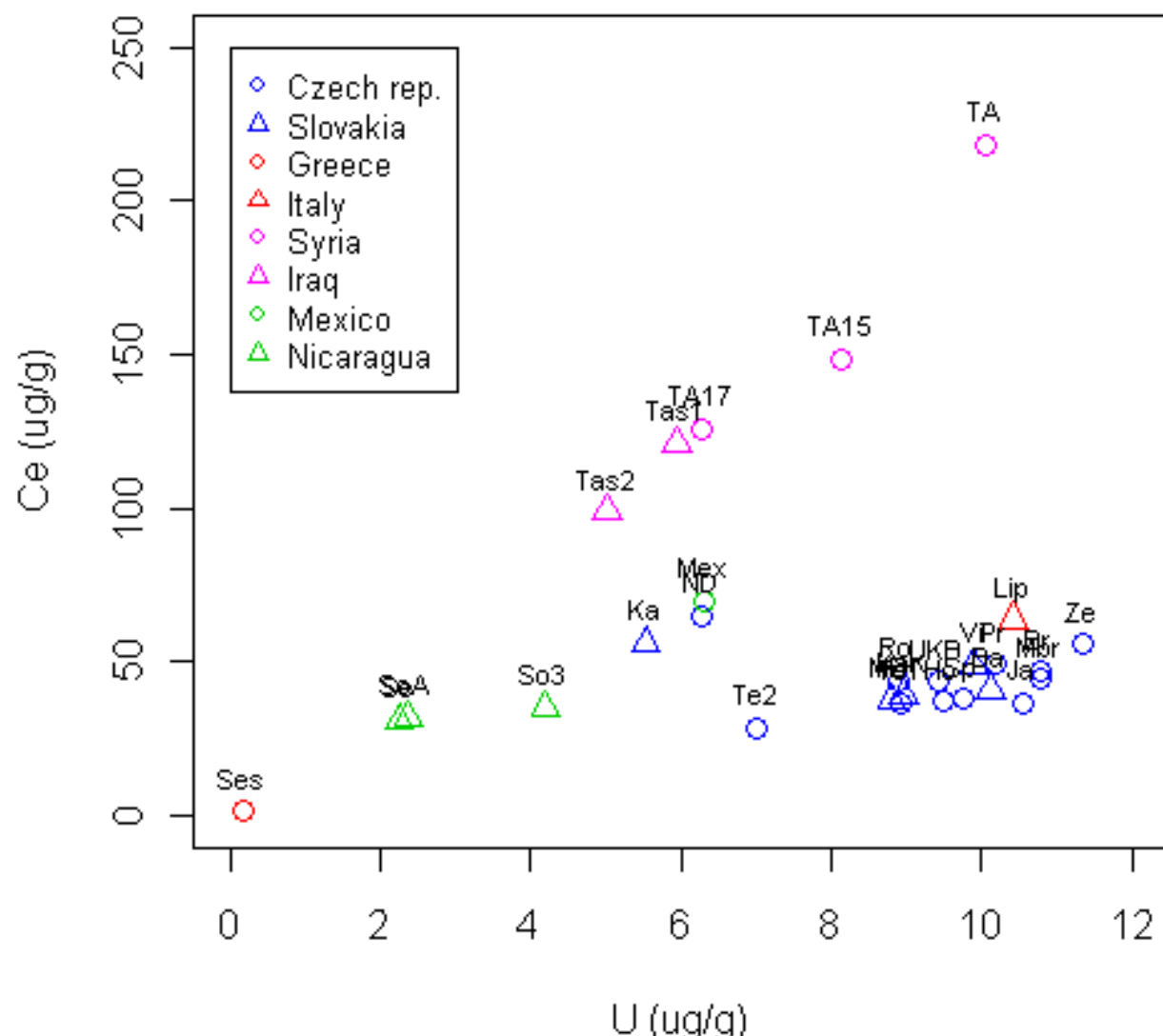
Scatterplot (Ce vs. Er)



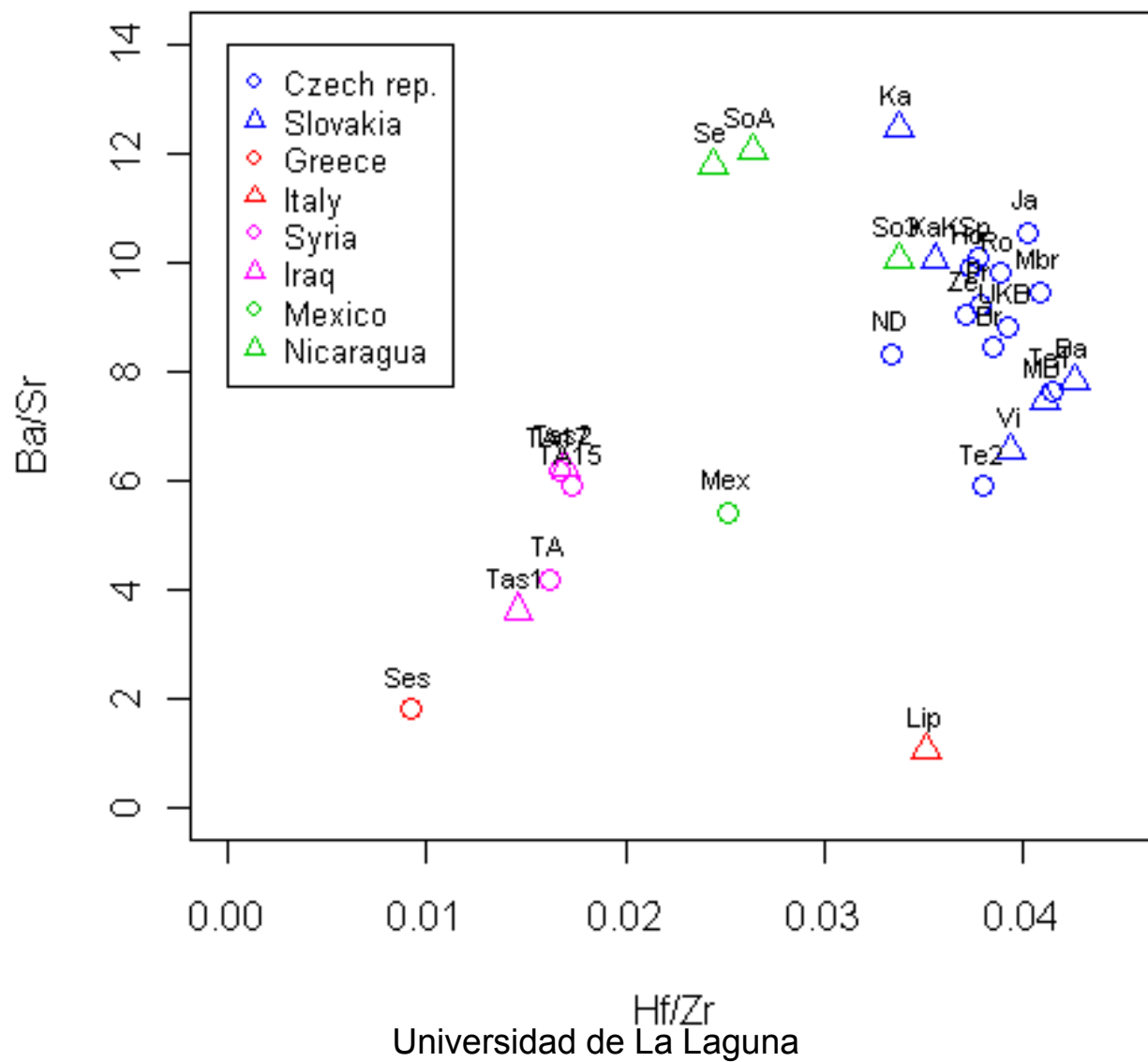
Scatterplot (Sr vs. Ba)



Scatterplot (U vs. Ce)

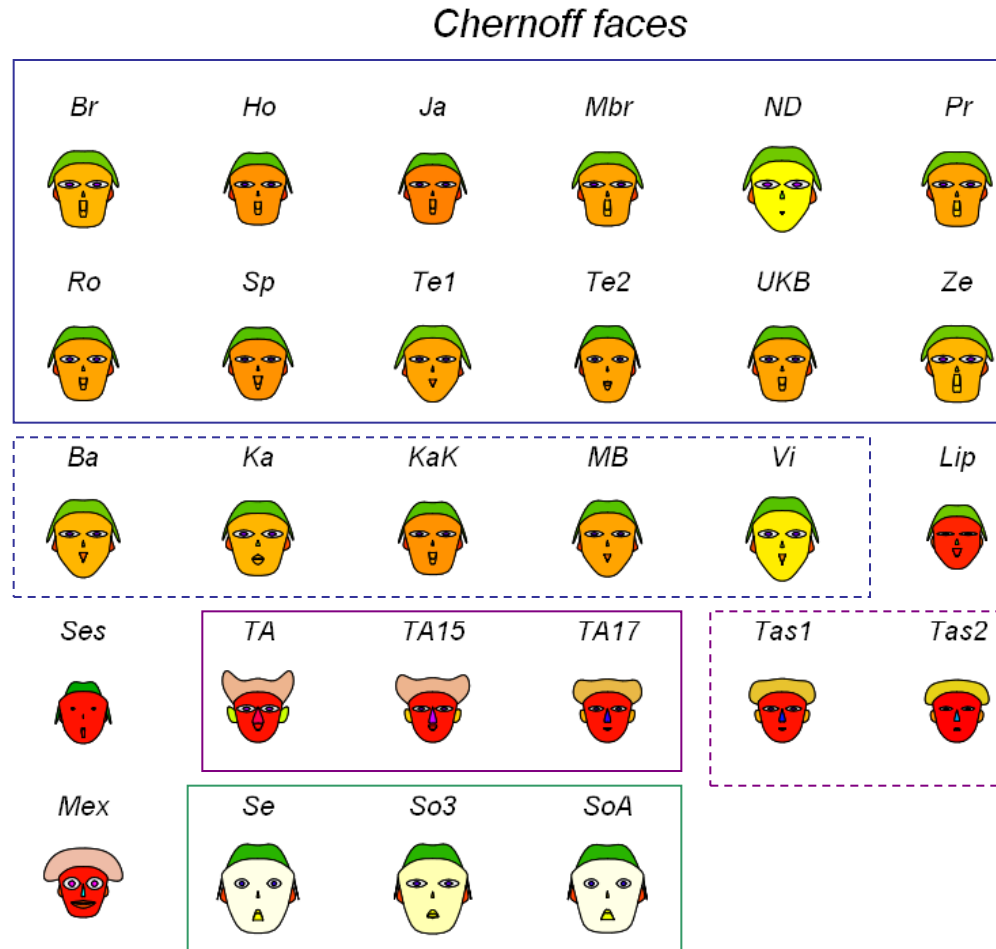


Scatterplot (Hf/Zr vs. Ba/Sr)



Chernoff faces

The elements were chosen and sorted after the increasing value of the PC1 loadings.



modified item var.

height of face Sr

width of face Ba

structure of face Sc

height of mouth Pb

width of mouth Zn

smiling U

height of eyes Eu

width of eyes Rb

height of hair Nb

width of hair Ta

style of hair Gd

height of nose Hf

width of nose Ce

width of ear La

height of ear Nd

CONCLUSION

- Calibration of LA-ICP-MS obsidian analysis using NIST reference materials yields concentration data that are in agreement with solution analysis (ACME)
- Principal Component Analysis (PCA) and Correspondence Analysis (CA) are suitable as exploratory data analysis methods for the purpose of this study.

ONGOING WORK

- Verification of the results of statistical analysis on large-scale data series
- Testing some other multivariate statistical and visualization techniques.

ACKNOWLEDGEMENT



*L. Prokeš, L. Zaorálková, A. Hrdlička, T. Vaculovič, A. Prichystal, M. Galiová, K. Novotný
Dep. of Chemistry and Dep. of Geological Sciences, Faculty of Sciences, Masaryk University, Kotlářská 2, 611 37 Brno, Czech Republic*



*A. Z. Mason, H. Neff
Department of Biological Sciences, Faculty of Sciences, California State University Long Beach, 1250 Bellflower Blvd, Long Beach 90840, USA*

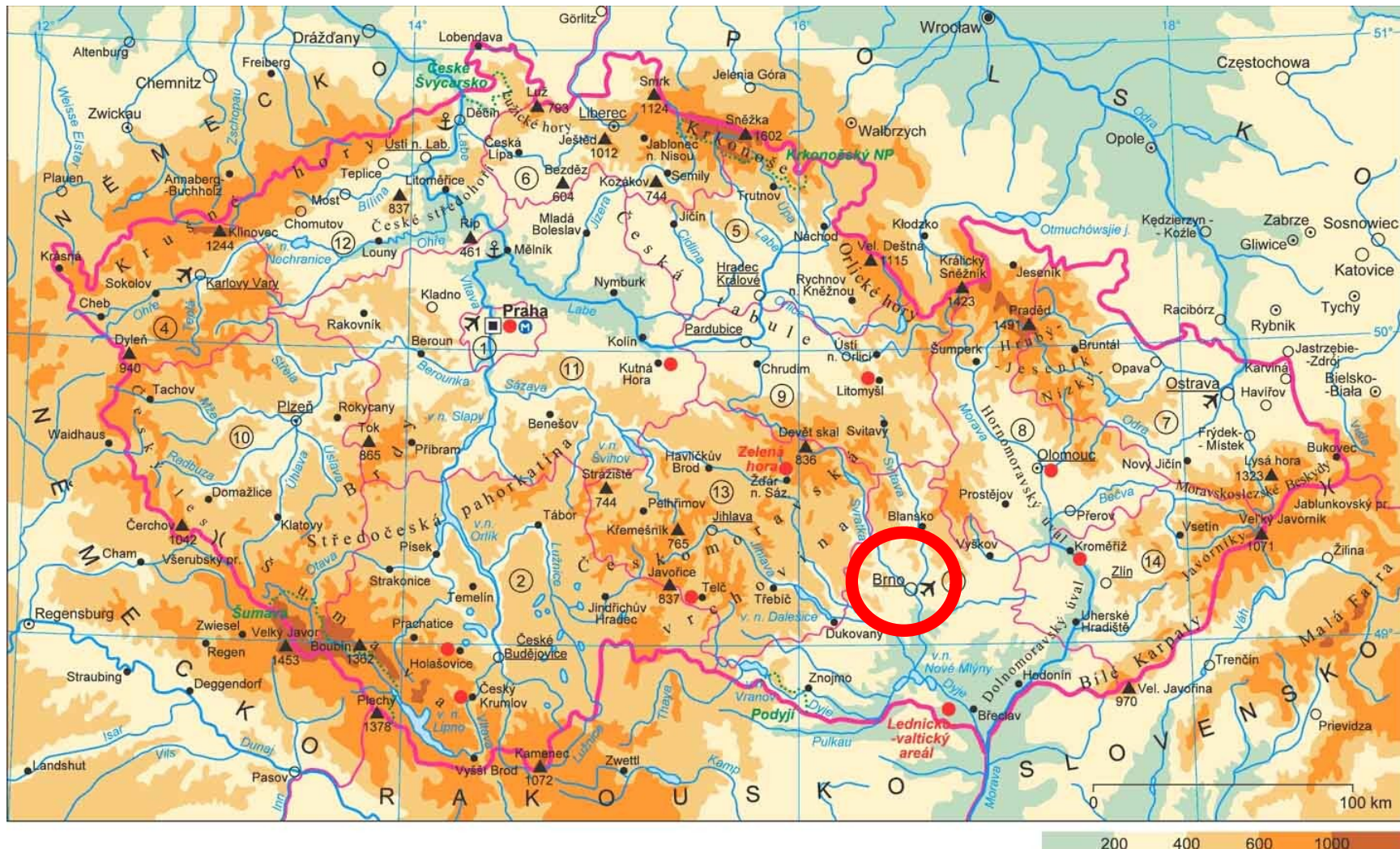
The authors acknowledge support from the Ministry of Education, Youth and Sports of the Czech Republic (projects ME10012, MSM0021622411, MSM0021622412 and MSM0021622427).

Acknowledgements to my collaborators

- Masaryk Univ.
- Karel Novotný
- Markéta Holá
- Tomáš Vaculovič
- Aleš Hrdlička
- Lubomír Prokeš
- Michaela Galiová
- Monika Nováčková
- Veronika Konečná
- Tereza Čtvrtníčková
- Tereza Warchilová
- Tech. Univ. Brno
- Jozef Kaiser
- University of Malaga
- X. Laserna



Czech Republic



22.5.2012 area: 78 864 km², inhabitants: 10.5 millions

142



Brno

inhabitans: 370 000



22.5.2012



Universidad de La Laguna



143

Masaryk University Campus (Brno)

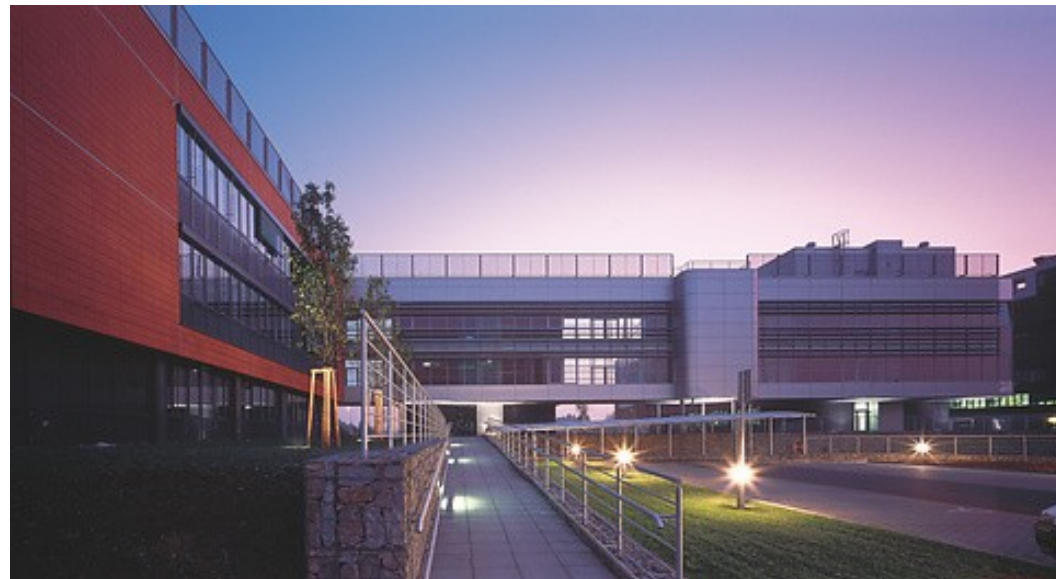


Fac.of Science
Faculty of Medicine
Faculty of Sport Studies

<http://www.muni.cz/general/events/p233332/gallery>



Masaryk University Campus



Masaryk University Campus



Masaryk University Campus



Masaryk University Campus





22.5.2012

Universidad de La Laguna

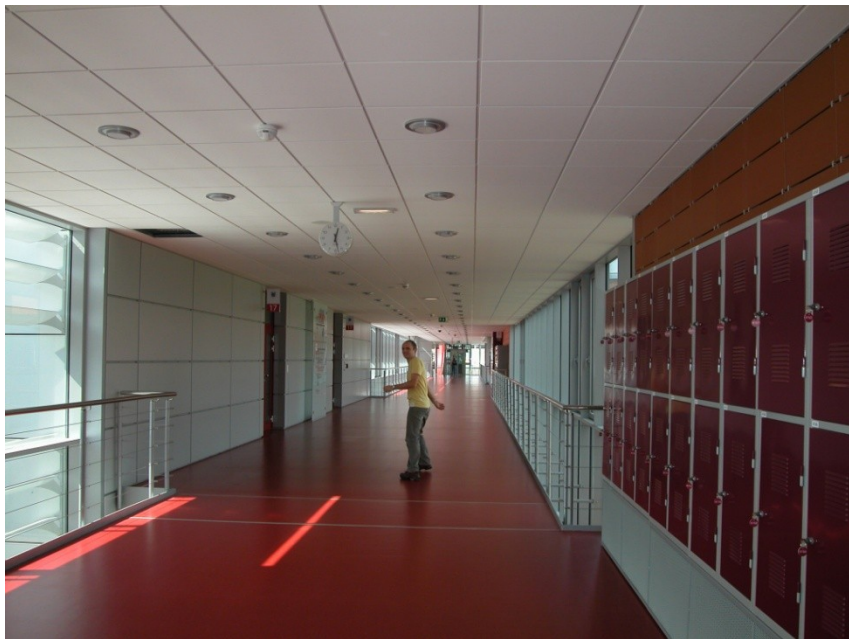
149



22.5.2012

Universidad de La Laguna

150



22.5.2012

Universidad de La Laguna

151





Thank you for your attention

REACTION OF CO₂ WITH SODIUM - NUCLEAR REACTOR COOLING MEDIA

- **Sodium-cooled fast reactor (SFR)** – Generation IV of nuclear reactors; cooling medium – liquid sodium; heat is transferred from sodium circuit in heat exchanger to CO₂. Possible reaction of sodium with CO₂ at elevated temperatures is experimentally studied => determination of carbon in sodium by means of LA-ICP-OES and ICP-OES

T. Vaculovič*, V. Kanický, O.Matal

Molten Na-CO₂ interaction

A new apparatus was designed for sodium melting under CO₂ atmosphere at high temperature.

Apparatus is placed into glove box with CO₂ atmosphere.

Furnace is heated up to 300, 350 and 450 °C, respectively.

180 minutes of melting + 120 min cooling down

Two ways of carbon content determination

1. Laser ablation of solidified sodium with ICP-OES detection (calibration pellets with two types of matrix – NaCl and NaF)
2. Dissolution of solidified sodium with water vapor – nebulization into ICP-OES (calibration solution with NaCl, NaNO₃ and NaOH matrices)

Glove box for:

- 1) Na purity determination by distillation in Ar atmosphere: residual carbonate and oxide dissolved and Na determined ICP-OES
- 2) Reaction of Na with carbon dioxide in CO₂ atmosphere



- 1 – distillation chamber
- 2 – temperature measure.
- 3 – membrane pump
- 4 – two-stage oil pump
- 5 – pressure sensor
(workspace)
- 6 – pressure sensor
(input press. in pump)
- 7 – vent
- 8 – pressure measurement
- 9 – preparation box
- 10 – interface chamber
- 11 – Ar input
- 12 – input vent
- 13 – output vent
- 14 – manometer of interface
- 15 – power meter
- 16 – Ar control

ICP-OES



- **ICP-OES Jobin Yvon**
- **Model Ultrace 170**
- **40.68 MHz, 0.6 – 1.200 kW**
- **Observation lateral**
- **mono.: 1-m Czerny-Turner**
- **poly.: 0.5-m Paschen Runge**
- **SBW: 4-5 pm / 20-25 pmBW**
- **detectors: photomultipliers**
- **PTFE sample introduction system + corundum injector**

Laser ablation system



LA-ICP-OES

conditions of measurement

LA parameters

Laser wavelength/nm	266
Laser spot diameter/ μm	750
Laser power density/(J cm^{-2})	4.7
Laser repetition rate/Hz	10
Carrier gas (argon) flow rate/(L min^{-1})	0.8

ICP-OES parameters

RF power input/W	1200
Observation	Lateral viewing; 15 mm above load coil
Gas (argon) flow rates/(L min^{-1})	outer: 12.0; intermediate: 0.6; sheath: 0.2; carrier: 0.6

LA-ICP-OES results

Matrix	NaF			NaCl								
T/ C	300	450	600	300	450	600						
CC-1L/%	0.81	0.09	1.2	0.1	1.5	0.1	0.84	0.07	1.3 + 0.09	1.6	0.1	
CC-2L/%	0.17	0.03	0.87	0.09	1.2	0.1	0.18	0.02	0.93	0.08	1.3	0.2
CC-3L/%	0.10	0.01	0.47	0.07	1.0	0.1	0.11	0.02	0.50	0.08	1.1	0.1

a) Content of carbon in: first layer – CC-1L, second layer – CC-2L, and third layer – CC-3L.